THE DEVELOPMENT OF A DRI PROCESS FOR SMALL SCALE EAF-BASED STEEL MILLS

by

Hendrikus Mattheus Wessels Delport

Thesis submitted in partial fulfillment
of the requirements for the Degree
of

MASTER OF SCIENCE IN ENGINEERING
(METALLURGICAL ENGINNERING)

In the Department of Process Engineering
At the University of Stellenbosch

Supervised by

Professor Guven Akdogan

STELLENBOSCH

March 2010

DECLARATION

I, the undersigned, hereby declare that the work contained in this thesis is my own original work and that I have not previously, in its entirety or in part, submitted it at any university for a degree.

……..

HMW Delport

…….

Date

ABSTRACT

This thesis deals with the development of a new process for the production of Direct Reduced Iron (DRI), intended for use specifically by small scale Electric Arc Furnace (EAF) based steel mills, who require small volumes of DRI. The term development as used here is taken to include such aspects as conceptual design, theoretical verification and initial practical testing.

The rise of EAF steelmaking brought about the metamorphosis of steel scrap from a waste product into a valuable raw material. Scrap prices rose steeply during the period 1995 to 2009 compelling EAF steelmakers, wishing to have more control over the cost of their input material, to seek for scrap supplements or alternatives. DRI has become an accepted and sought after supplement, or even complete alternative, to steel scrap.

Adding DRI to an EAF charge has a range of advantages, including the dilution of tramp elements and possible cost benefits, but it does have negative effects. These include the lowering of the scrap to liquid metal yield and an increase in power consumed. The effect of charging DRI to a small EAF is quantified. The maximum DRI that may be added to the burden whilst still maintaining the present steelmaking volume, is shown to be as high as 50% if charged continuously, and the maximum price payable for DRI, is shown to be approximately 80% of base grade scrap price. Finally other requirements unique to small scale EAF operators are considered in order to prepare a schedule of requirements for a DRI plant specifically for small scale EAF steel mills.

A review of published information on existing DRI production technology, processes and plants is undertaken is establish the fit of existing processes to the requirements set. Initially the thermodynamics and kinetics of iron ore reduction and coal gasification, specifically downdraft gasification are reviewed. Thereafter existing processes are reviewed. Shaft based processes and rotary kiln based processes are identified as possible suitors to the requirements. Limitations of these processes, specifically heat transfer in rotary kilns and the pressure drop over a reduction shafts are investigated. Finally a typical process in each of the main process classes is adjudicated against the set requirements. None is found to match the set requirements.

A new process is proposed that is claimed to better suit to small scale operation. The uniqueness of the process is embodied in the combination of existing technologies of downdraft gasification and iron ore reduction in a shaft, in a single reactor.

The process consists of two shafts, one placed above the other. Iron ore is charged into the top shaft, called the pre-heat shaft, where it is pre-heated and lightly reduced to wustite with gas from the

bottom shaft, called the reduction shaft. The pre-heated ore is then charged together with coal into the reduction shaft. Gasification air is drawn into the top of the reduction shaft where the coal is gasified in a downdraft gasifier, generating reduction gas which reduces the ore as the gas moves concurrently with the iron ore. The exit gas is cleaned and pumped to the pre-heat shaft where it combusted with air to pre-heat the iron ore in the pre-heat shaft.

The concept is analysed thermodynamically using amongst others, FactSage, and is shown to be thermodynamically viable.

To test the concept process concept practically, an extremely small pilot plant with a production rate of 2kg DRI/h, consisting of only a gasifier/reduction shaft, was designed and constructed using reduction rate data obtained from literature supplemented with data obtained from thermogravimetric analysis of CO reduction of lump Sishen hematite.

Pilot Plant trials were performed using various reductant sources. The degree of metallizaion was analysed using visual inspection of cut and polished samples compared to calibrated standards. Analysis of the results indicate that coal rate and production rate influence the degree of reduction positively and negatively.

The conclusions arrived at include the fact that the process is thermodynamically viable, that it was possible to reduce iron ore in a simplified pilot plant, and that the process was found to be stable and controllable.

It is recommended that a larger scale pilot plant, embodying the full proposed flow sheet be erected to test the process more completely.

OPSOMMING

Die tesis handel oor die the ontwikkeling van ‘n nuwe proses vir die vervaardiging van sponsyster. Die proses is beoog spesifiek vir gebruik deur kleinskaalse Elektriese Boogoond (EBO) gebaseerde staal aanlegte, wat kleiner hoeveelhede sponsyster benodig. Die term ontwikkeling soos hier gebruik word aanvaar om aspekte soos konseptuele ontwerp, teoretiese verifikasie en aanvanklike toetsing te behels.

Die vinnige groei van EBO staalvervaardiging het skroot getransformeer van weggooiproduk tot waardevolle grondstof. Die prys van skroot het skerp gestyg gedurende die periode 1995 to 2009. EBO gebaseerde staal produsente, in ‘n poging om meer beheer te hê oor die koste van hul insetmateriaal, het hul in ‘n toenemende mate tot skrootalternatiewe gewend. Sponsyster het ‘n aanvaarde en gewaardeerde byvoeging, en selfs alternatief tot staalskroot geword.

Die byvoeging van sponsyster by die lading van ‘n tipiese EBO het besliste voordele, maar het dit ook nadelige effekte. Die voordele sluit die verdunning van reselemente en moontlike kostevoordele in, terwyl van die nadele die verlaging van die skroot tot vloeistaal opbrengs, en ‘n verhoging in kragverbruik, is. Die effek van die byvoeging van sponsyster tot ‘n EBO lading word gekwantifiseer. Daar word getoon dat die maksimum hoeveelheid sponsyster wat by ‘n EBO lading gevoeg kan word terwyl die hoeveelheid staal geproduseer konstant gehou word, ongeveer 50% is indien die sponsyster kontinue gelaai word, en die maksimum prys wat vir die sponsyster betaal kan word, word bereken op ongeveer 80% van die prys van basisgraad skroot. Ander vereistes uniek aan kleinskaal EBO bedrywers word oorweeg ten einde ‘n lys van vereistes vir ‘n sponsysteraanleg, uniek aan kleinskaal EBO bedrywers, te kan bepaal.

‘n Oorsig van gepubliseerde inligting oor sponsysterproduksietegnologie word onderneem ten einde die passing van bestaande prosesse met die gestelde vereistes te kan bepaal. Nadat die termodinamika en kinetika van ysterertsreduksie en steenkoolvergassing be-oordeel is, word bestaande sponsysterprosesse beskou. Skag- en Roterende oond gebaseerde prosesse word as moontlik gepaste prosesse identifiseer. Hitte-oordrag en die drukval oor gepakte beddens, synde tipiese beperkings eie aan die twee prosesse, woord beskou. Tipiese prosesse in elk van die hoofklasse van prosesse word ten laaste be-oordeel aan die gestelde kriteria. Daar word bevind dat geeneen van die bestaande prosesse aan die vereistes voldoen nie.

‘n Nuwe proses, wat skynbaar die behoefte van kleinskaalse EBO gebaseerde staalprodusente beter bevredig, word voorgestel. Bestaande tegnolgie word in ‘n unieke opstelling geïntegreer. Reduksie word in ‘n reduksiekag gedoen as gevolg van die ooglopende massa- en hitte-oordragvoordele van ‘n skag. Reduksiegas word verkry van steenkoolvergassing in ‘n afstroomvergasser ten einde teerverwydering in ‘n

naverwerkingsstap oorbodig te maak. Die uniekheid van die proses is beliggaam in die kombinasie van 'n steenkoolvergasser en reduksieskag in 'n enkele reaktor.

Die proses bestaan uit twee skagte, een bo die ander. Ystererts word in die boonste skag, wat die voorverhitskag genoem word, gelaai. Hier word die erts voorverhit en moontlik lig gereduseer tot wustiet met gas van die onderste skag, wat die reduksieskag genoem word. Die voorverhitte erts word saam met steenkool in die reduksieskag gelaai. Vergassingslug, word in die reduksieskag gesuig waar die steenkool in 'n afstroomvergasser vergas word. Hierdeur word reduksiegas gegenereer wat die erts verder reduseer soos dit saamstromend met die erts af beweeg. Die uitlaatgas word gesuiwer en na die voorverhitskag gepomp waar dit verbrand word om die erts te voorverhit.

Die konsep is termodinamies analiseer met gebruikmaking van onder andere FactSage, en werkbaar bevind.

'n Baie klein, vereenvoudigde proefaanleg, met 'n produksievermoë van 2kg DRY/uur, bestaande uit slegs 'n reduksiekag, is ontwerp en gebou met gebruikmaking van kinetika inligting uit die literatuur aangevul met inligting uit termogravimetriese analise van die CO reduksie van Sishen hematiet.

Proefaanleglopies is uitgevoer met 'n reeks reduktantbronne. Die metallisasiegraad is bepaal deur visuele inspeksie van gesnyde, gepoleerde monsters wat vergelyk is met gekalibreerde standaarde. Analise van die resultate toon dat die steenkoolkoers 'n positiewe verband, en die produksiekoers 'n negatiewe verband met die metallisasiegraad het.

Die slotsom waartoe gekom is, is dat die proses termodinamies werkbaar is, dat reduksie van ystererts in 'n vereenvoudigde proefaanleg bewerk kon word, en dat die prose stabiel en beheerbaar voorgekom het.

Die aanbeveling word gemaak dat 'n groter proefaanleg wat die volledige voorgestelde vloeiskema verteenwoordig, opgerig behoort te word, ten einde die proses meer volledig te kan toets.

ACKNOWLEDGEMENTS

I wish to thank the following:

- Murray & Roberts, specifically Messer's Rob Noonan of Murray & Roberts Steel, and James Windt and other colleagues at Cape Town Iron & Steel Works for gratuitously agreeing to fund this study, and for continuous support and encouragement.
- Professor Guven Akdogan for tireless support and assistance.
- Rudolph du Preez and Niklaas Delport for assistance and continued interest shown in the project
- My fellow students for their friendliness.
- My family for putting up with me.
- The Lord for having given me the opportunity to become an engineer, a passion for ironmaking plus a huge amount of opportunities to work in the field.

I wish to offer my humble praise to God, who made all things, including iron, oxygen, carbon and hydrogen, the essentials in ironmaking. After nearly a lifetime of work in the field or ironmaking, the science of which is but one drop in the vast sea of knowledge about His creation, I have come to realise that it would require more than one lifetime of study to begin to understand the subtleties of the field.

TABLE OF CONTENTS

9. Appendices

LIST OF FIGURES

Chapter 1

Chapter 2

Chapter 3

Chapter 4

Chapter 5

LIST OF TABLES

Chapter 4

Chapter 5

GLOSSARY

BF – Blast Furnace.

BOF – Basic Oxygen Furnace.

Coal rate – The mass of coal required to produce 1 ton of product, also called the "coal consumption". The units for this ratio as used in this text is kg coal/t DRI.

DRI – Direct Reduced Iron, a scrap substitute manufactured by reducing iron ore in the solid state.

EAF – Electric Arc Furnace.

Equivalence Ratio – The ratio of air actually supplied to the gasification reaction or process relative to the amount of air required for complete combustion.

FactSage – A computational thermo-chemistry software program.

Hearth Load – The volume of gas produced in a gasifier per square meter of gasifier surface area, units $Nm^3/h/m^2$. It may also be expressed in as m/s, when it is referred to as the Superficial Velocity.

Hematite – A mineral og iron, commonly referred to as iron ore, chemical formula Fe_2O_3.

Magnetite – A mineral of iron, less prevalent than hematite, chemical formula Fe_3O_4, often occurring in combination with titanium, when it is referred to as titaniferous magnetite

Metallization – The process of reducing the iron in iron oxide to iron metal.

Metallization degree – Iron in the metal state as a fraction of the total iron present in the sample.

Minimill – A steel mill based on the EAF process usually employing 100% continuous casting.

Pig Iron – High carbon iron, cast into rectangles with sloping sides, typically 200mm x 100mm x 50mm. It is most commonly produced by a blast furnace but also by various processes treating ilmenite sands. The name refers to the days when molten iron was cast in moulds arranged in sand, fed from a single runner in an arrangement that resembles a sow nursing her piglets.

Rotary hearth furnace – A circular level floor rotating inside a box shaped furnace cavity in which various combustible gases or solids are combusted to supply heat to the reagents on the furnace floor.

Rotary kiln furnace – A horizontal retort mounted at a slight incline, rotating slowly about its axis. In DRI process applications it is used to affect a contact between the iron ore and the reducing agent while heat is supplied by internal combustion of CO and coal volatiles which are products of reactions inside the burden.

SDG – Stratified downdraft gasifier.

Shaft furnace – A vertical retort used to treat iron ore with a reducing gas

Smelting reduction – The practise of reducing iron oxides, followed by, or simultaneous with, the melting of the produced iron and slag. Smelting reduction processes frequently employ two steps. Iron ores are partly reduced in the first step and then final reduction and melting takes place in the second step.

Steel mill – A factory in which steel is produced.

Superficial Velocity – See Hearth Load

Wüstite – An intermediate iron oxide species, also called iron oxide, chemical formula $Fe_{0.957}O$, commonly written as FeO.

DRI PROCESS GLOSSARY

Arex – A natural gas based DRI process employing a shaft furnace but without the characteristic separate gas reformer. Reforming of the natural gas is performed in the shaft employing a process called in-situ catalytic reforming of natural gas.

Ausmelt – A smelting reduction process comprising top-entry submerged lance oxygen smelting in a single vessel, used in copper, lead, tin, nickel, platinum group metals (PGMs), zinc and ferrous metals production units.

CCF – Cyclone Converter Furnace. A coal based smelting reduction process consisting of a melting cyclone for the pre-reduction stage, and a metallurgical vessel for final reduction.

Comet – A rotary hearth based DRI process employing alternative layers of iron ore and a coal/limestone blend to facilitate iron ore reduction whilst removing the sulphur inherent in the coal.

Circofer – A two stage fluidised bed DRI process using coal as reducing agent and employing a circulating and a bubbling fluidised bed.

Circored – A two stage fluidised bed DRI process using hydrogen as reducing agent and employing a circulating and a bubbling fluidised bed. Supplier Outotec

Corex – A high carbon, liquid iron making process consisting of a melter/gasifier in which coal is gasified with oxygen, and the DRI produced in the second step, a reduction shaft, is melted. The gas produced in the melter/gasifier is, after de-dusting, used for reduction in the reduction shaft.

DIOS – Direct Iron Ore Smelting. A bath smelting process in which iron ore is reduced and melted in a bath in which coal and oxygen are blown. The aim is to produce a product with a low carbon content – also referred to as Direct Steelmaking

DRC – A rotary kiln based DRI process

Fastmet – A rotary hearth furnace based DRI process

Fastsmelt – An iron making process consisting of a rotary hearth based DRI process followed by a melting step which could be based on an EAF or a coal based melting furnace.

Finmet – A fluidised bed DRI process employing a reformer to reform natural gas to CO and H_2 and making use of multiple fluidised beds in series to perform reduction.

Finex – A high carbon ironmaking process consisting of a melter/gasifier in which coal is gasified with oxygen and the DRI produced in the second, reduction step, is melted. The gas produced in the melter/gasifier is used for reduction in multiple fluidised beds in series.

Finesmelt – An externally heated rotary kiln based process producing DRI using fine ore.

Fior – The fore-runner of the Finmet process.

Ghaem – A Shaft based DRI process employing in-situ reforming of natural gas in the shaft.

HIB – A natural gas based DRI process employing a two stage fluidised bed. Originally called the Nu-Iron process.

H-Iron – A three stage fluidised bed process for the production of highly reduced iron with hydrogen as reducing agent.

Hlsarna – A project of the Ultra Low Carbon Di-oxide Steelmaking group (ULCOS) using a CCF process to produce steel emitting 70% less CO_2 than conventional steelmaking.

Höganäs – A DRI process producing iron powder by external heating of refractory vessels filled with an iron ore and coke mixture in a tunnel furnace.

HYL III – A shaft based DRI process employing the reforming of natural gas to produce a reduction gas which is fed counter-currently to iron ore in a reduction shaft. HYL III is an improved version of the HYL I process which consisted of multiple batch reactors.

Iron Carbide – A process producing iron carbide, Fe_3C, in a single or dual stage fluidised bed

Iron Dynamcs – A rotary hearth based DRI process.

ITKMk3 – A rotary hearth based process treating composite pellets of iron ore and coal in which the melting point of iron is exceeded creating separate metal and slag droplets called nuggets.

Kinglor Metor – A DRI process employing external heating of an iron ore and coke blend in a vertical retort.

Midrex - A shaft based DRI process employing a reduction shaft and a reformer. Reforming of natural gas is performed with CO_2 in the recycled top gas in an externally heated catalytic reformer. The reduction gas which consists of CO and H_2 flows counter-currently with the iron ore in a reduction shaft.

Oxicup – A process based on a modified cupola charged with carbon rich briquettes of steelplant waste and blown with hot blast. The product is liquid iron and slag and a zinc containing sludge.

Purofer - A shaft based DRI process similar to the Midrex process with some smaller differences in the reforming step.

Redsmelt – A two step smelting reduction process combining a rotary hearth furnace and a submerged arc furnace.

Romelt - A single stage smelting reduction process in which liquid iron is produced in a molten slag/metal bath reactor using non-coking coal and oxygen.

SL/RN – A coal based rotary kiln DRI process.

Spirex – A natural gas based two step fluidised bed DRI Process consisting of a circulating fluidised bed drier followed by a circulating fluidised bed first stage and a bubbling fluidised bed final stage.

Tisco – A coal based rotary kiln DRI process.

Primus – A coal based multiple hearth process for the production of DRI from ore fines or steelplant wastes, either used as DRI or fed directly into an electric arc furnace.

Chapter 1

INTRODUCTION

This chapter deals with the need for and growth in the production of scrap substitutes, specifically DRI. It consists of the following subsections:

- Steel as material of construction
- The rise of EAF steelmaking and minimills
- Advantages of EAF based steelmaking
- Scrap
- Scrap Alternatives

1.1 Steel as material of construction

Life as we know it today is hardly imaginable without steel. Steel is an indispensable material for the technology driven society we live in. Steel is employed in all major industries including the transport, energy, water supply, housing and construction, packaging, agribusiness, automotive and communication industries.

World apparent steel use in 2008 amounted to 1198 million tons, somewhat down from 1215 million tons in 2007 (WSA(1) 2009). Steel has enjoyed a strong growth in consumption during the last decade as mirrored in the world crude steel production.

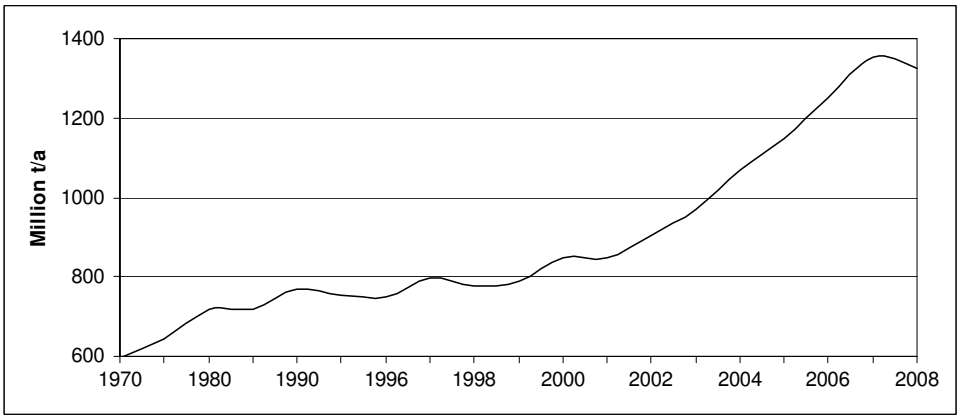

Fig 1 .1.1: World crude steel production 1970 to 2008 in million t/a (WSA 2009)

The two properties of steel which, for almost a century have defined its attractiveness, are its availability and versatility. That attractiveness has in recent years been underpinned by another property namely its

recylability. Contrary to other recycled products like plastic, glass, and others, steel is termed as a 100% recyclable material. The mouthpiece of steelmakers the world over, Worldsteel Association deems this property of steel as so important, it is emphasised above all others in promotional material (WSA(2) 2008).

Two process routes dominate steel production at present, accounting for 97.8% of all steel produced in 2008. These are

- the Blast Furnace - Basic Oxygen Furnace (BF/BOF) process route, also referred to as the integrated route, accounting for 67.2% of steel produced in 2008, and
- the Electric Arc Furnace (EAF) route, also referred to as the minimill route by which 30.6% of all steel was produced in 2008.

A great deal of information about the BF/BOF route, its efficiency and continued dominance in spite of years of predictions of its demise, is covered elsewhere (Lüngen & Yagi, Uhlmanns 2009). This work concentrates on the EAF route and its raw materials, specifically DRI.

1.2 The Rise of EAF Steelmaking and Minimills

1.2.1 History

The industrial application of the EAF process is dependent on the availability of large quantities of reasonably priced electricity. It is therefore not unexpected that much of the pioneering work on the use of the EAF for steelmaking was carried out in the USA.

Early pioneers of the EAF process include Sir Humphrey Davy who discovered the carbon arc, Pinchon who experimented with electric arc welding and Sir William Siemens who patented some aspects of electric arc heating. It is Paul Heroult however, who pioneered the industrial scale application of the electric arc furnace for steelmaking. The first EAF steel production facility was installed in Syracruse New York in 1906 (Fenton 2005).

At first electric steel was considered as applicable to high grade tool steel only, probably due to the low productivity and therefore high cost of the early furnaces. In 1936 Northwestern Steel and Wire became the first US firm to apply the EAF route for carbon steel production only (Berry 1999). If the definition of a minimill is taken to be an operation where 100% of steel is made by the EAF process, and 100% of that steel is cast by continuous casting, then Lake Ontario Steel Co (LASCO) in 1964 became the world's first minimill. (Stubbles 2006).

However, it is Nucor, an innovative and entrepreneurial US steelmaker, who is credited with pioneering the minimill approach to steelmaking with the start of large scale EAF production of long products in 1969 and again for flat products in 1987 (Ahlbrant, Fruehan & Giarratani 1996).

1.2.2 Growth of EAF Steelmaking

The growth of EAF steelmaking over the past 50 years has been astounding. If it is considered that real development of this process route the world over only started in earnest after WWII, it is significant that within 60 years, which is a relatively short time in high investment cost industries, it has become the major steelmaking process route in economies like the USA, Spain, Italy and Turkey, with 58.1% of all steel produced in the USA during 2008 attributed to the EAF route. (WSA 2009).

EAF steel production grew by 143mt/a during the years 2000 to 2007. Outside of China, EAF based steelmaking accounted for 73% of the growth in steelmaking during this time. This fast growth was made possible by a general availability of electricity and scrap and the advantages EAF steelmaking has over the integrated route (see later) (Knopfle and Hunter 2008).

New steelmaking capacity in China and India, where electricity and scrap have not been as generally available, is mostly based on the BF/BOF route. The fast growth in new steelmaking capacity over the last number of years in these two economies explains why the percentage of steel produced by the EAF route world wide has decreased somewhat during the same period. This however does not detract from the fact that EAF steel production grew by approximately 25% during the period 2000 to 2007.

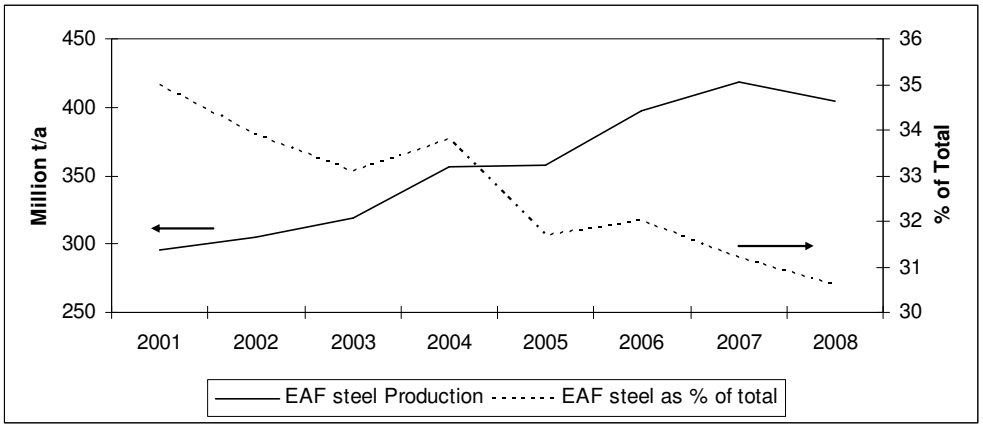

Figure 1.2.1: EAF steel production in million t/a and as a percentage of total world's steel production (WSA 2009)

Worldsteel Association (2009) estimates that 45.5% of steel produced in South Africa in 2008 was produced by the EAF route (WSA 2009).

This fast growth in EAF steelmaking happened due to dramatic and sustained improvements in the EAF process as is evident from the next figure

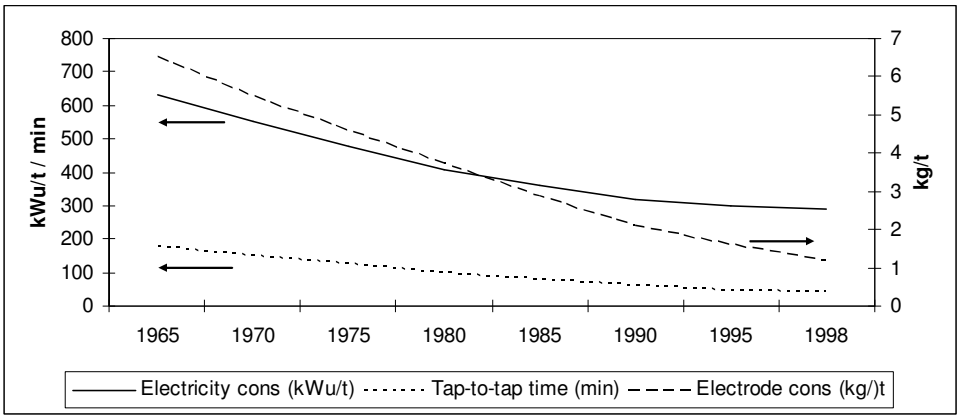

Figure 1.2.2: Technological developments in EAF steelmaking (Janke et al 2000)

The dramatic improvement in consumption rate and productivity is a consequence of major improvements in the technology which include the following (Janke et al 2000)

- Oxygen steelmaking (circa 1968)
- Secondary (ladle) metallurgy (circa 1972)
- Water cooled walls (circa 1976)
- UHP AC furnace (circa 1978)
- Foaming slag (circa 1980)
- Water cooled oxygen/gas burners (circa 1980)
- Ladle furnace (circa 1982)
- Scrap pre-heating (circa 1984)
- Oxygen/carbon lance manipulator (circa 1987)
- DC technology (circa 1988)
- Shaft furnace (circa 1993)

New technology improvements which are not applied on a large scale include

- Higher volume furnaces to reduce the number of baskets charged
- Scrap Pre-heating

- Continuous scrap charging, sometimes combined with scrap pre-heating.

1.3 Advantages of EAF Steelmaking

BF/BOF steelmaking is generally regarded as more suited to high volume and clean steel production than EAF based steelmaking whereas EAF based steelmaking is regarded as having cost and environmental advantages to BF/BOF steelmaking, specifically:

- Capital cost

  Investment cost for an EAF based steel mill is reported to be somewhere in the order of 320 -350 US$/t/a (140 – 170 for steelmaking + 180 for casting and rolling) vs. 1200 – 1800 US$/t/a for a similar sized BF/BOF plant (900 – 1500 for steelmaking + 300 for casting and rolling. (Ahlbrandt et al 1996, Fenton 2005)

- Environmental Impact

  If the environmental impact of the total facility is considered, EAF based plants are regarded as having a substantially smaller negative impact on the environment than BF/BOF plants of similar size due to lower energy requirements 5.7 vs 14.9GJ/t, a lower waste burden (Janke et al 2000) and reduced CO_2 emission of 500 vs 2000kg/t (Gojic 2004) (Knopfle and Hunter 2008)

- Cost structure

  The pricing structure of an EAF based steel mill differs fundamentally from that of an integrated plant. Where an integrated plant would generally have a high fixed cost with a lower variable cost, EAF based plants generally have the opposite, namely a lower fixed cost but a higher variable cost. (Ahlbrandt et al 1996, Brunner 2002, Burns 2009, Bianchi Ferri & Memoli 2007)

  A simplified cost structure is shown in Figure 1.3.1. From the figure it is clear that in spite of the fact that the total value of the fixed and variable cost in both instances are approximately similar ($238/t BF/BOF and $239/t EAF process routes), the make-up is vastly different

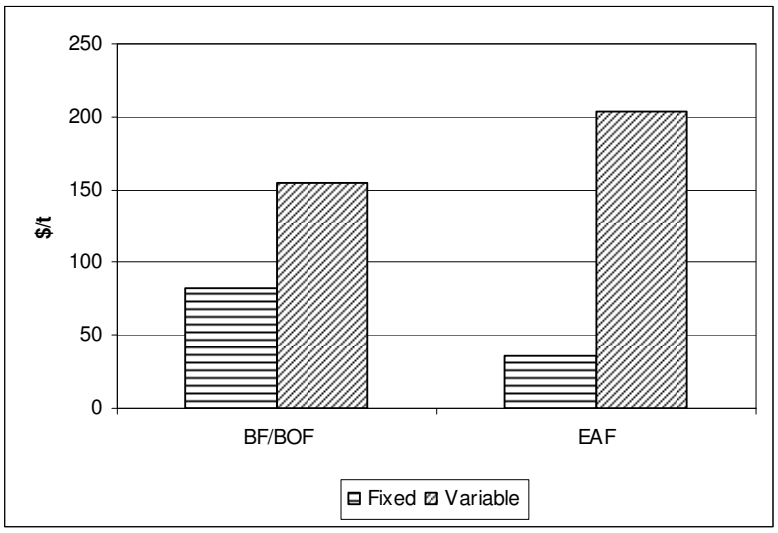

Figure 1.3.1: The cost structure of BF/BOF and EAF steelmaking . (After Ahlbrandt et al 1996)

1.4 Scrap

1.4.1 The Raw Material for EAF Steelmaking

Scrap fundamentally, is obsolete steel articles which have reached the end of their useful life. This period is generally 20 years (Janke et al 2000). However some 30% of the steel manufactured into end products 20 years ago is lost to amongst other reasons, corrosion. This main type of scrap is generally termed obsolete scrap.

There are two other types of scrap as well, namely Home scrap (In plant scrap) which is scrap generated within the steel plant, and Process scrap (Prompt scrap) which is scrap generated during manufacturing processes. The arising of the last two types of scrap as a fraction of the raw steel produced, has dropped over the last number of years due to improved manufacturing techniques.

It is possible to estimate the scrap available for steelmaking by using past steel production and manufacturing trends. (Janke et al 2000). From Figure 1.4.1 it is possible to estimate that world scrap availability will remain at present levels for the next 15 years as world steel production was essentially flat between 1990 and 2005 and present trends of reduction in Home and Process scrap will continue.

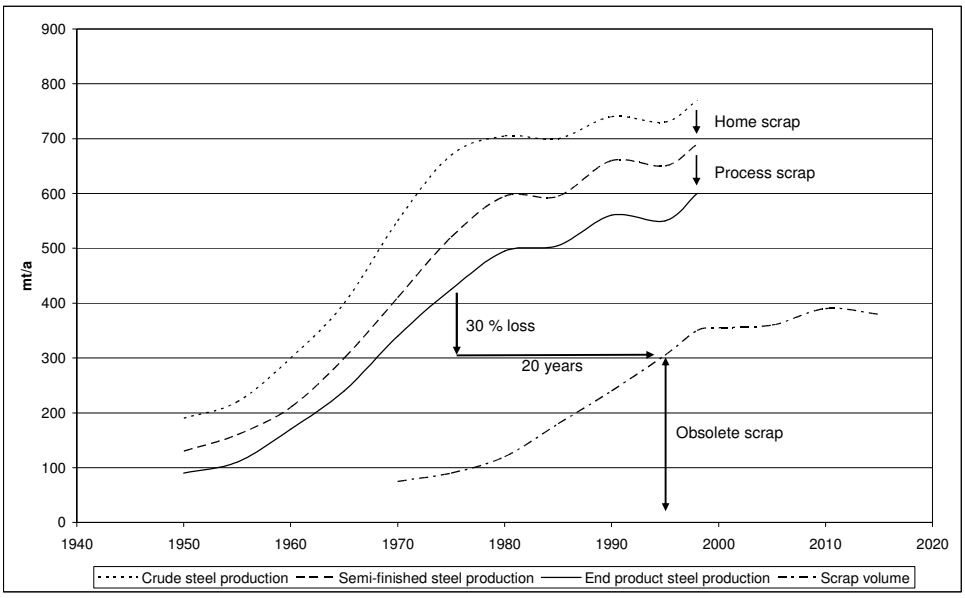

Figure 1.4.1 Interrelation between world steel production, steel consumption and scrap generation (Janke et al 2000)

1.4.2 Scrap Industry

The development of the EAF process is mirrored in the metamorphoses of the scrap industry as well. The collection, processing and trade of steel scrap is a global industry which has developed on the basis of profit incentives described as an outstanding example of recycling via the market. It is also the world's oldest recycling sector (Aylen & Albertson 2006)

A total of 475.5million ton of scrap was consumed worldwide during 2008 to produce 30.6% of the world's steel of 1326.5million ton. (WSA 2009). Since most types of scrap is readily transported, with few inherent risks such as decay, theft, fire in ships holds etc, it is traded extensively around the world. This is evident from the fact that 126.8million ton was imported while 96.4million ton of scrap was exported worldwide in 2008. This trade happens mostly from developed economies to developing economies as is evident from the following table.

Country	**Nett Exports million t/a**	**Country**	**Nett Imports million t/a**
USA	21.7	Turkey	17.4
UK	6.6	S Korea	7.3
France	5.7	Spain	6.7
Japan	5.3	Italy	5.8
Canada	4.1	Taiwan	5.6

Table 1.4.1 Top 5 scrap in- and exporting countries during 2008 (WSA 2009)

Considering the fact that scrap traded at some $250/t c&f in 2007 (I&ST 2009), the value of scrap consumed during 2007 amounted to $108bn. If it is assumed that iron ore sold for $65/t in 2007, the value of all iron ore consumed in 2007 amounted to only $75bn.

In most countries the scrap industry has a pyramid shape structure. Material is collected, consolidated, processed and graded as it passes up a tier of firms. Many small scrap collectors collect scrap from various sources and deliver it to fewer scrap dealers. Scrap dealers perform a necessary cutting and sorting function and separate ferrous scrap from non-ferrous scrap types. Scrap dealers as a rule deliver their product to fewer still scrap merchants who perform further processing which might include shredding of auto bodies and other obsolete equipment. Scrap merchants supply the final processed scrap to steel mills locally and overseas.

All aspects of the recycling cycle have improved tremendously over the years. Not only has the specification of scrap been improved on, clarified and communicated, but the whole collection chain has been optimised and streamlined. This includes processes for cutting and sorting of the scrap (e.g. plasma cutters, shredders, sorters) as well as identifying scrap types (e.g. handheld spectrometers). (Aylen & Albertson 2003)

1.4.2 Scrap Quality

Unwanted elements in scrap, generally called tramp elements, can best be defined as elements not added purposely to steel but which cannot be removed by standard metallurgical processes. Tramp elements include Cu, Ni, Sn, As, Cr, Mo, Pb and others. Most of these elements have a deleterious effect on steel quality. As a rule the maximum allowable level of these elements are lower in flat products than in long products.

It is also apparent that continued recirculation of scrap will increase the level of these elements in the steel. Although processes exist whereby some of these elements may be removed to an extent from steel, the only viable method at present is to dilute the level down to below the maximum allowable level.

1.4.3 Scrap price

Scrap prices are determined by demand and supply on world markets and are set in the USA, the world's largest open scrap market. Aylen & Albertson (2003) suggests that scrap prices in turn, influence the prices of other steelmaking raw materials either directly, e.g. scrap substitutes like pig iron and DRI, or indirectly, e.g. iron ore.

Scrap prices have risen steeply from 2001 to 2008 with a rise of more than 500% during this time. Some authors have described the rise as astronomical. (Knopfle and Hunter 2008). However, 2009 saw a sharp

fall in prices as the impact of the worldwide economic recession impacted severely on steel production, and demand fell sharply.

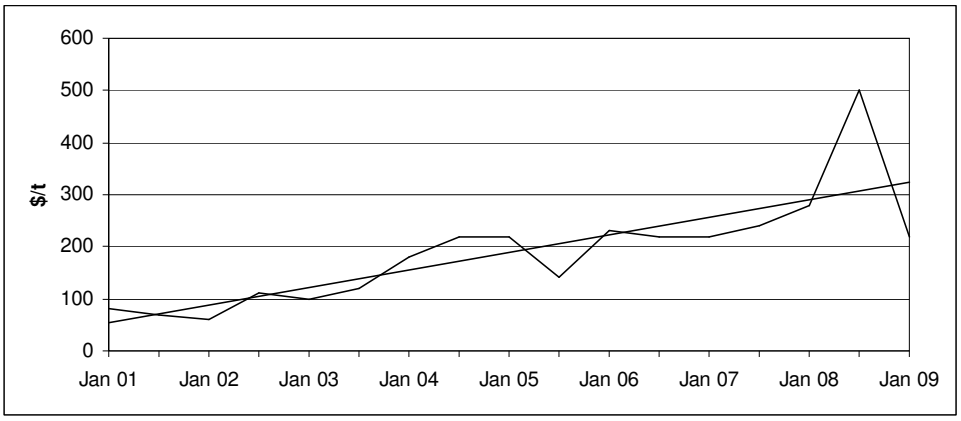

Fig 1.4.2: Scrap price in $/t HMS#1 grade scrap (I&ST 2009)

The steep rise in the price of the main raw material of the EAF steelmaking route raises the question of whether this route has become less competitive when compared to the integrated steelmaking route. This does not seem to be so, as the steep rise in world steel production from 2002 onwards (Figure 1.1-.) exerted strain on the supplies of all iron and steelmaking raw materials, including iron ore, coking coal and coke. (Knopfle and Hunter 2008). This in turn put upward pressure on the prices for these materials. Scrap prices merely followed the upward trend. It is significant that prices of all steelmaking raw materials have followed the same trend, confirming the statement of Aylen & Albertson (2006).

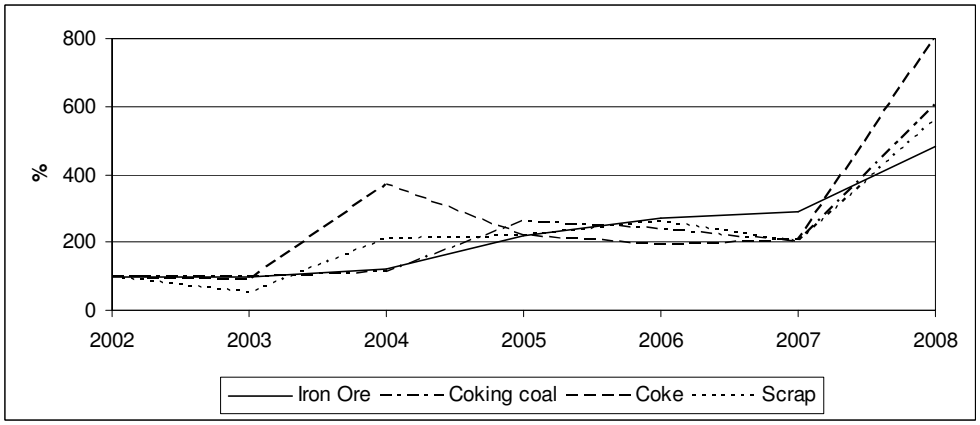

Figure 1.4.3: Index of steelmaking Raw Material Prices. (Hamilton 2009)

1.5 Scrap Alternatives

Steeply rising and volatile scrap prices and high and rising tramp element levels have possibly contributed more than many other factors in compelling EAF producers to consider alternatives to scrap.

Some requirements for scrap alternatives include the following

- High ferrous content

  The aim of the EAF operation is to produce steel, therefore any charged raw material should not introduce unnecessary non ferrous elements. These non ferrous elements typically include materials such as gangue (sand, concrete, ash etc.), tramp elements or combustibles such as wood or oils.

- Chemical stability

  The chemical analysis of scrap substitute should not fluctuate unnecessarily

- Physical requirements

  The scrap substitute should not be too large (>1m) or too small (<1mm). Too large pieces or clusters may cause damage to refractories during charging, may cause arching to panels, or may break electrodes. Fine materials, or the fine fraction of coarse materials, may be sucked from the furnace by the off-gas system.

Scrap alternatives include pig iron, direct reduced iron and iron carbide.

1.5.1 Pig Iron

Pig iron is liquid high carbon iron, cast into convenient shapes, generally rectangles with sloping sides, typically 200mm x 100mm x 50mm. It is most commonly produced by a blast furnace but also by various processes treating ilmeniet sands. The name refers to the days when molten iron was cast in moulds arranged in sand fed from a single runner in an arrangement that resembles a sow nursing her piglets.

Pig iron is a long-established supplement to scrap. It is almost never viewed as a replacement for scrap, since if sufficient pig iron is available to make the full complement of steel, utilising a BOF to decarburise the iron would be much more economical than using an EAF. Even if the pig iron is produced distant from the EAF, it may be more economical to produce the semi-finished steel profile e.g. billet bloom or slab at the location where the pig iron is produced and ship this semi to the mill to be rolled. Pig iron typically trades for a premium of 5 – 10% above normal scrap prices. This put pig iron out of the reach of many EAF operators, especially those not producing high grade steel.

Pig iron also has some disadvantages to scrap which is often overlooked. These disadvantages relate to the high level of Carbon and Silicon typically in pig iron. The Carbon content of pig iron is typically between 4 and 5% and the Silicon level normally ranges between 0.5 – 1%. This implicates that the purchaser paid a 5 – 10% premium also for the 5% of the pig iron which is not Fe. This non-Fe part also has some consequences.

The Carbon and Silicon is typically oxidised from the melt by injecting oxygen into the melt yielding additional chemical energy to the melt. However, often the injection rate of Oxygen is limited whilst the evolved CO may lead to a higher volume of hotter off-gas, overloading the furnace evacuation system leading to forced power-off time. Therefore excessive levels of Pig iron in the charge may lead to increased heat times. Furthermore since the additional SiO_2 formed, lowers the slag basicity, which has to be countered by the addition of additional CaO, not only increases the cost of the input further, but also increases the slag volume and thereby further reduces the yield.

1.5.2 Direct Reduced Iron (DRI)

DRI may be defined as the product created when iron ore is reduced at temperatures below its melting point. The structure of the product may be porous or spongy due to the loss of as much as 30% of its mass, and is therefore also referred to as sponge iron.

In its search for low residual Fe units to complement or replace expensive scrap, the Electric Arc Furnace Industry has turned increasingly to Direct Reduced Iron (DRI). (Manning & Fruehan 2001; Grobler & Minnitt 1999). DRI offered many EAF operators a solution to all three reasons compelling them to seek for an alternative in the first place, namely security of supply, cost and quality. Therefore many EAF operators have invested in DRI facilities for more than one reason.

This has led to a rapid increase in DRI production during the last decade, with production totalling 65.8Mt during 2008, (WSA 2009). Perhaps more significant than the rise in DRI production is the rise of DRI expressed as a percentage of EAF charge if it is assumed that EAF's globally have a yield of 90%.

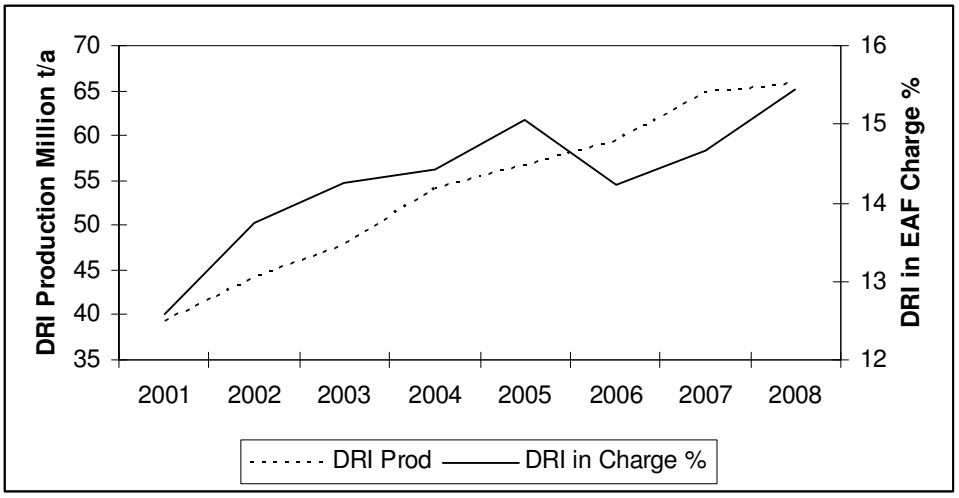

Figure 1.5.1: DRI production and DRI % in global scrap (WSA 2009)

However, as is the case with pig iron, charging DRI to an EAF is not without penalties when compared to charging pure clean scrap. These include, but may not be limited to, an increase in power consumption and a reduction in yield. This will be explained in more detail in Chapter 2.

For this reason existing EAF operations can normally tolerate only a certain portion of DRI before the production level would reduce. This portion is determined by mostly cost reasons since the disadvantage of the increase in power consumption and the reduction in scrap to steel yield has to be made good by the reduction in price of the input material.

Chapter 2

SMALL SCALE EAF OPERATORS AND THEIR UNIQUE REQUIREMENTS FOR A DRI PROCESS

This chapter aims to identify the unique requirements that small scale EAF based steel mills have for a DRI process. It covers the following

- DRI as scrap substitute
- DRI quality and its effect on EAF operation
- DRI Price
- Environmental considerations
- Capital cost
- Oxygen use
- Requirements of small scale EAF operators for a DRI Process

2.1 DRI as Scrap Substitute

One of the advantages of the EAF based steelmaking route is the fact that it is less dependant on economy of scale for viability than is the integrated steelmaking route. (Ahlbrandt et al 1996). This is evident from the South African primary carbon steelmaking scenario where primary steelmaking facilities with an annual capacity of less than 1million t/a all use the scrap based route.

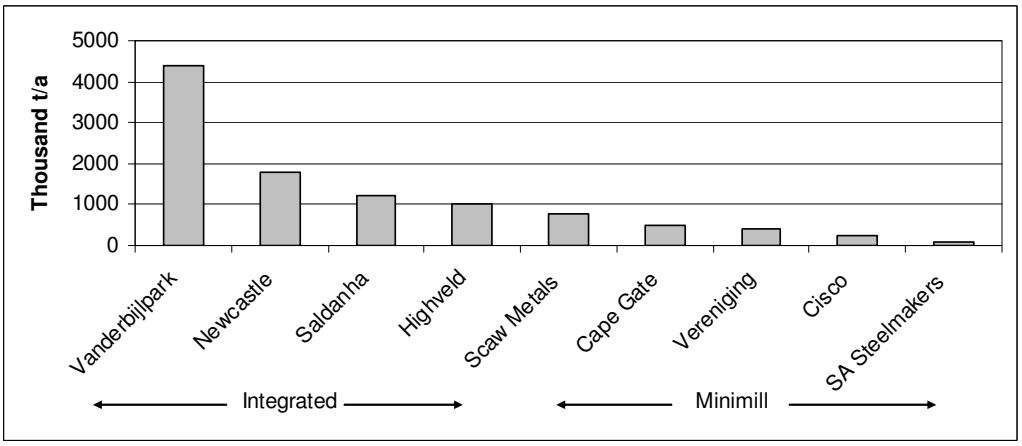

Figure 2.1.1: Approximate steelmaking capacities of South African Steelmakers (Source: SAISI, Arcelor-Mittal Annual Report 2008, Anglo Annual report 2008, Highveld Steel annual report 2007, SAISI 2009)

As a rule most EAF plants start off using 100% scrap as input material. As is the situation in many industries, steelmakers generally strive to continuously improve on productivity. This frequently leads to an increase in production, and consequently, an increased raw material demand.

However, scrap, unlike traditional raw materials which are mined or produced and where production may be increased by expanding on operations, cannot be manufactured or produced. Rather scrap production depends on the collection of obsolete items which were produced as long as 20 years ago. Scrap production in a region therefore is influenced by the economic activity of the region some 20 years earlier.

When the scrap consumption of an EAF based mill operating in a region has reached the scrap collection rate in that area, and the mill desires to expand on throughput, its options therefore are limited to:

- Using a scrap alternative if available in that area
- Importing scrap or scrap alternatives from another area
- Producing an alternative to scrap

DRI has been shown to be the alternative of choice for many steelplants. It is significant to note that Scaw Metals, Cape Gate & Arcelor-Mittal's Vereniging plant supplement their scrap supply with DRI that they produce themselves.

However, in deciding how much DRI may be added, the implications of adding DRI to the charge needs be considered, since as mentioned in Chapter 1, replacing good quality scrap with DRI in an EAF charge increases power consumption and reduces the scrap to liquid steel yield, which in most cases also translates into a reduction in steel throughput.

2.2 DRI Quality

A number of aspects of DRI quality effect EAF performance directly. These include but may not be limited to metallization degree, gangue, carbon and sulphur content.

2.2.1 Metallisation Degree of DRI

The terms **Degree of Reduction** and **Degree of Metallisation** are unfortunately often used synonymously in industry. It is evident from Figure 2.2.1 that the two concepts, although related are different. The degree of reduction is defined as the mass of oxygen removed during reduction expressed as a fraction of the total oxygen removable during reduction, while the degree of metallisation is defined as the mass of metallic iron expressed as a ratio of the total iron present in the ore.

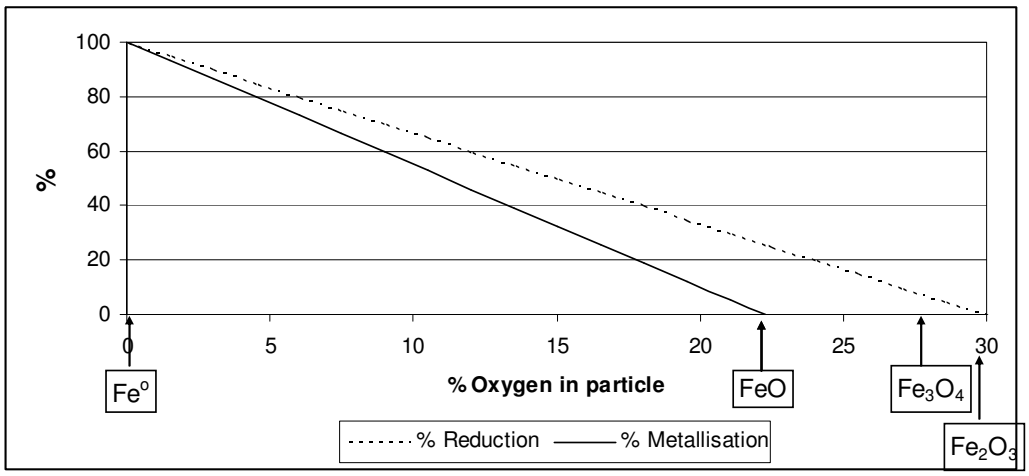

Figure 2.2.1: Mass of oxygen in DRI as a function of metallization degree of the DRI

DRI is very rarely 100% metallised, but rather somewhere between 88 and 95%. The un-metallised iron is typically still present as Wüstite (FeO). (Battell 1973). This remaining FeO has two impacts on the furnace operation.

- The oxygen associated with the FeO represents a waste to the purchaser, as full DRI price was paid for it and no useful product is obtained. It might be argued that oxygen is used in most EAF steelmaking operations and that the oxygen in the DRI may perform some decarburising or other oxidation function. Although this might the true, the fact still remains that the same amount of oxygen could have been purchased at tonnage oxygen supply price and used as and when it suited the operation. See figure 2.2.1.
- The remaining FeO may be melted and taken up in the slag as (FeO), representing a further loss of iron units to the steelmaker. Also when high amounts of well metallised, or lower amounts of low metallized DRI is used, the slag FeO content may be excessively high leading to very low carbon levels in the steel which has to be recarburised with expensive Carbon subsequent to the EAF.

Rather most EAF operators prefer to either have carbon in the DRI, or add cheaper Carbon to the charge thereby performing reduction of the remaining FeO in the EAF. This however requires additional power input since reduction of FeO with carbon is an endothermic reaction.

2.2.2 DRI gangue content

Gangue originally present in the iron ore from which DRI is produced, (mostly SiO_2 and Al_2O_3), remains in the DRI after reduction, since no melting takes place during DRI production. Compared

to clean scrap, heating the SiO_2 and Al_2O_3 to 1630ºC, a typical tapping temperature of an EAF process, represents an additional heat demand.

This increased energy demand is not the only effect though. When the SiO_2 and Al_2O_3 are taken up in the EAF slag, it reduces the basicity of the slag, which, left unremedied, would lead to an increase in the sulphur content in the steel as the sulphur distribution ratio typically exhibits a strong positive correlation to slag basicity (Fruehan 1998). The reduction in slag basicity has to be countered by adding additional lime to adjust the basicity of the slag to achieve the required sulphur level in the liquid steel. This increases the slag volume in the furnace. Pre-heating, calcination of the $CaCO_3$ remaining in the lime, and melting of the lime represents an additional heat demand compared to scrap. This heat demand is negated to some degree by the negative heat of mixing of SiO_2 and CaO. (Peacey & Davenport 1979)

2.2.3 Carbon content

The carbon content of DRI is somewhat of a bone of contention. Reduction of the remaining FeO requires carbon for the reduction reaction. This carbon may be in the DRI or added to the charge in the form of anthracite. Approximately 1% of carbon in DRI is required to balance 6% of FeO in the DRI (Jones et al 1998). The advantage of having carbon present in the reduced part of the DRI and therefore intimately mixed with the unreduced Fe (FeO), and immediately available to effect the rest reduction when the particle heats up and finally melts, it not disputed.

What is disputed is the price that is paid for this carbon. Since DRI is sold on a $/t basis, the carbon in the DRI is purchased at the same price as the Fe. It is argued that the advantage this internal carbon may have above carbon from anthracite charged with the DRI, is not worth the price difference.

2.2.4 Sulphur content

A high level of sulphur in DRI is unwanted since any sulphur entering the EAF which is above the specification of the specific steel grade being produced, has to be removed, either in the EAF as explained above, or in subsequent steelmaking operations. Sulphur removal with Ca-wire injection or similar techniques in the ladle furnace is normally fast and predictable, but represents an additional expense.

2.3 Power consumption

Heating and melting additional gangue and lime as well as reduction of the remaining FeO requires additional power input into the furnace. EAF's as a rule operate at their maximum power supply rate.

This limit may be due to electricity availability, or distribution equipment (switch gear & transformer/s) capacity or furnace power input equipment limitations (electrode mast and/or arms, electrodes). Any additional power requirements would therefore increase the tap-to-tap time and ultimately reduce steel production.

2.4 Yield

To ensure that carbon levels in the steel as tapped remain at the required levels, higher slag volume resulting from the SiO_2 and Al_2O_3 in the DRI plus the additional lime charged, has to be oxidised to the same level as before. This may lead to a higher Fe loss in the slag due to the fact that a higher slag volume now contains the same level of (FeO) than previously.

This means that adding DRI to the charge mix tends to increase the power consumption and reduce the scrap to liquid steel yield. To illustrate the effect of the fraction of DRI in the charge on the power consumption and scrap to liquid metal yield, a mass balance was constructed for a typical EAF. See Appendix 1. The increase in power consumption of 100kWh/t increase for a 100% DRI charge as compared to a 100% scrap charge is in good correlation with figures obtained in actual practice (Dressel, 1999).

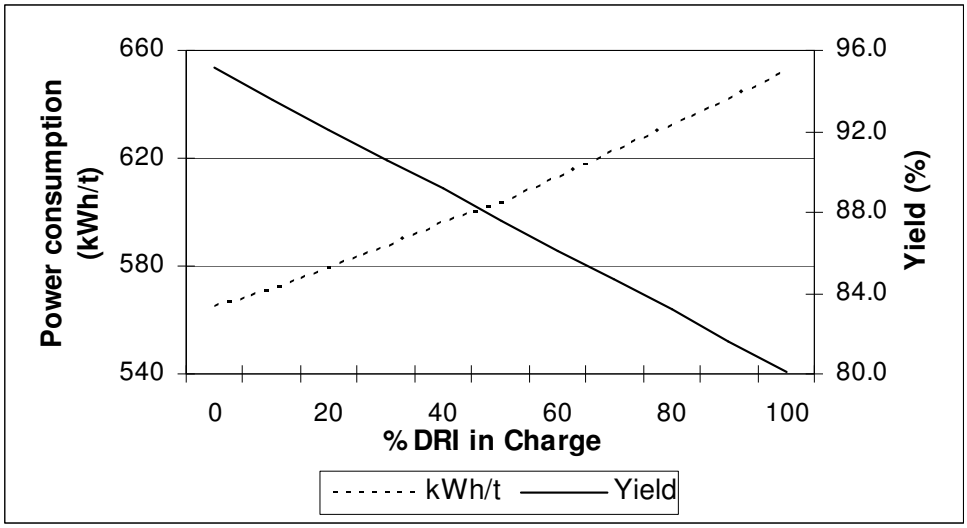

Figure 2.3.1. Calculated power consumption and scrap to liquid steel yield vs. DRI in the charge. (Assumptions: 40t EAF, 24MW Transformer, Slag basicity, $(CaO)/(SiO_2) = 3$)

2.5 Tap-to-tap time

DRI may be charged into the furnace in two ways. The first is using the scrap basket charging procedure as before. When using this practice it has been found that DRI tends to stick to furnace walls when charging more than 35% of the charge. (Dressel 199) However, some EAF shops charge the DRI

continuously through the roof of the furnace. By charging only one basket and making up the rest of charge with DRI, a saving of time and energy is realised by not opening the roof. This compensates to a certain degree for the increase in power consumption.

In order to investigate the impact of charging DRI through the roof on an existing EAF on the tap-to-tap time, a simulation was performed. The following two tables compare three charging scenarios for a 40t EAF.

- Scenario 1 is the base case. Only good quality scrap of a high enough density to allow all scrap necessary to produce 40t of steel to be charged with three baskets. Time for furnace preparation and charging of a baskets is defined as in the table
- Scenario 2 is the situation where scrap density is too low to allow charging only 3 baskets, and a fourth basket has to be charged.
- Scenario 3 is the scrap + DRI case. The maximum scrap is charged in the first basket, thereafter all the DRI necessary to produce 40t of steel, is charged continuously through the roof of the EAF.

Assumptions for liquid steel yield and power consumption calculation are indicated in table 2.5.1

Item	**Units**	**Scrap**	**DRI**
Electricity Consumption			
Total	kWu/t	520	650
% used during melting	%	80	80
% used during refining	%	20	20
Yield	%	90	85
Transformer size	MW	24	24

Table 2.5.1: Assumptions for EAF loading simulation

Scenario		1		2		3	
Description		3 Scrap Baskets		4 Scrap Baskets		1 basket, rest DRI continuous	
	Units	t or kJ	Mins	t or kJ	Mins	t or kJ	Mins
Preparation			7		7		7
Charging Basket 1	t	22	3	18	3	22	3
Melting	kJ	3E+07	20.6	2E+07	16.8	3E+07	20.6
Charging Basket 2	t	14	3	12	3	26	
Melt	kJ	2E+07	13.1	2E+07	11.2	4E+07	28.7
Charging Basket 3	t	10	3	8	3		
Melt	kJ	1E+07	9.4	1E+07	7.5		
Charging Basket 4	t	0	0	8	3		
Melt	kJ	0	0.0	1E+07	7.5		
Refining	kJ	2E+07	10.8	2E+07	10.8	2E+07	10.9
Tapping			5		5		5
Total time			74.8		77.8		75.2
Total scrap loaded	t/h		46		46		48
Average Yield	%		90		90		87.3
Steel made	t/h		41.4		41.4		41.9
Steelmaking rate	t/h		33.2		31.9		33.4
Power consumption	kWu/t		520		520		575
Availability	%		95		95		95
Steel production	t/d		757		728		762
	t/a		253579		243804		255291
Scrap Consumption	t/a		281755		270893	46%	134043
DRI Consumption	t/a					54%	158414
Total Input	t/a		281755		270893		292457

Table2.5.2: EAF loading simulation

From the simulation it would seem that the saving in time of not opening the roof to load a scrap basket, more than compensates for the increased power consumption as well as the decreased yield. It is quite unexpected that as much as 50% of the scrap may be replaced with DRI fed through the roof without affecting throughput.

2.6 DRI Price

A small scale EAF plant producing reinforcing steel, where the addition of DRI to the burden would not necessarily yield a quality advantage due to the dilution of tramp elements, has to offset the disadvantages of charging DRI as explained above by the price discount of the DRI. Comparing a heat with 50% DRI to a 100% scrap heat using typical cost figures for a mill in the Western Cape yields a typical cost of DRI to achieve the same cost of steel. Assumptions include

- Power consumption and scrap to liquid steel figures are as indicated in Figure 2.3.1.
- Electrode consumption increases in relation to power consumption increase, starting with 2kg/t liquid steel for a 100% scrap charge.
- Slag basicity is maintained at $(\%CaO)/(\%SiO_2) = 3$,
- Slag $(\%FeO) = 25\%$.

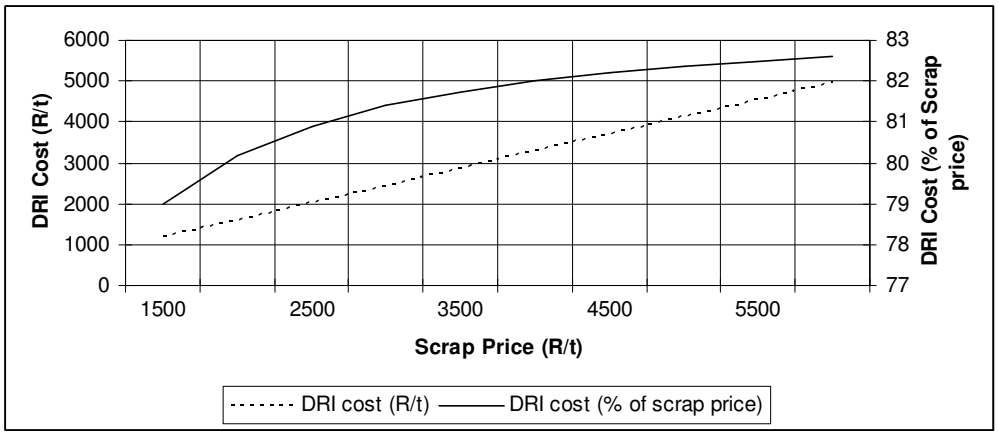

Figure 2.6.1: Calculated DRI cost compared to scrap cost in R/t and % of scrap cost.

Assumptions: Electrode consumption increases in relation to power consumption increase. Slag basicity $(\%CaO)/(\%SiO_2) = 3$, Slag $(\%FeO) = 25\%$.

From the figure it is clear that the maximum cost of DRI is dependent on the cost of scrap but it is approximately 80% of the scrap price.

2.7 Environmental considerations

Present environmental legislation in South Africa is in general conformity with similar legislation in other parts of the world. In essence environmental legislation stipulates that no process may be operated unless its emissions are within set limits. Environmental authorities, including national, provincial and municipal may set limits to emissions in a variety of domains. Emissions that may relevant to DRI processes, including the following:

- Air emissions
- Water emissions
- Noise emissions

- Solid waste emissions
- Flicker and radiation emissions

Any prospective plant owner needs to ensure that emissions from the intended process falls well within the set limits, since history has shown that the limits set tend to become more strict as time progresses.

2.8 Capital cost of a DRI Plant

Capital cost estimates are site specific and therefore not readily available in literature. A typical capital cost estimate for a DRI plant of 500kt/a production capacity is $250/annual ton (Energiron 2009). When this is extrapolated with the so called 2/3 rule to compute the specific capital cost of a 100 000t/a plant, it estimates to

$$C_{p,v} = C_{p,u} (v/u)^{2/3}$$

$$500000*250 = 100000.C_{pu}.(5/1)^{2/3}$$

$$C_{pu} = \$427.50/\text{annual ton}$$

For a 100 000t/a DRI production facility this would equate to a capital investment of R342 million. If this capital investment is approached as a loan which has to be paid back over 20 years at 10% interest rate by a capital cost charged to the product, R401.72/t has to be charged to the product.

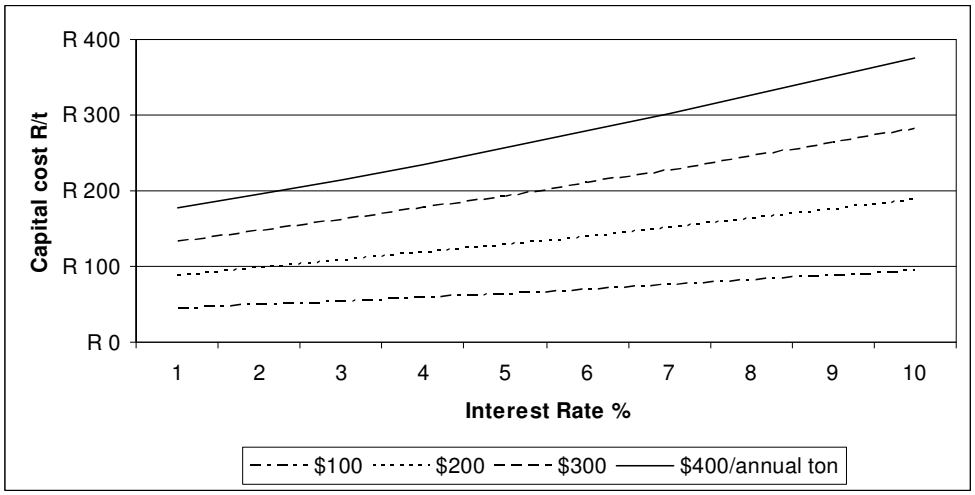

Figure 2.8.1: Capital cost in R/t for varying investment costs. (Amortization period = 20 years, R/$ = 8.)

2.9 Oxygen use.

Oxygen suppliers will as a rule be prepared to erect a dedicated Air Separation Unit (cryogenic or PSA/VPSA) to supply oxygen on a contractual basis to any consumer. This type of contractual

arrangement is generally referred to as an "over the fence" supply scheme or as a tonnage oxygen scheme to differentiate it from bottled oxygen.

However, more often than not, oxygen supply companies require the inclusion of a so-called "take-or-pay" clause in the supply contract. This clause simply requires that the customer will take a minimum stipulated volume of oxygen daily, and in the event that the volume is not taken, pay the oxygen company as if that amount of oxygen was taken. This is understandable in the light of a number of reasons, including but not limited to:

- Oxygen plants have high capital costs and the oxygen supply company does not have any control over the activities of the consumer therefore cannot be held liable for market collapse, negligence etc. on the side of the consumer.
- Especially cryogenic oxygen plants take hours or even days to reach steady state conditions at the required product specification, (generally referred to as reaching purity), so cannot easily be turned up or down.

Companies listed on the JSE Sequrities Exchange have to comply with King II, (King Report on Corporate Governance for South Africa) (Kneale 2009) which requires compliance with Global Reporting Initiative guidelines. These guidelines require companies to disclose the full liability of long term off-take contracts on their balance sheets. This would require oxygen consumers to disclose the full possible impact of oxygen take-or-pay clauses on their balance sheets. In effect the capital cost of the oxygen plant then becomes a liability on the balance sheet of the oxygen consumer.

2.9 Requirements of small scale EAF Operators

On basis of the foregoing, the following requirements of small scale EAF operators (<250 000t/a liquid steel) for a DRI process may be summarised. The requirements include:

- DRI quality: (Paragraph #2)
  - Metallization: As high as possible, Met > 90%
  - Gangue content: As low as possible, Gangue <5%
  - Sulphur: As low as possible S < 0.05
- Volume: (Paragraphs #3, 4, 5)
  - Maximum 50% of present scrap input

- DRI cost: (Paragraph #6)
    - Delivered cost < 80% of HMS#1 scrap price
- Environmental (Paragraph #7)
    - Comply with environmental regulations without incurring excessive cost
- Capital cost (Paragraph #8)
    - Capital cost: As low as possible Capital Cost < $100/annual ton
- Oxygen use (Paragraph #9)
    - Preferably no oxygen use

Chapter 3

LITERATURE REVIEW

This chapter covers a review of research done in the field of DRI production, as well as the practical implication there-of. It entails the following aspects

- Principles involved in the reduction of iron oxides, particularly
    - Thermodynamics
    - Kinetics
- Principles involved with the gasification of coals
- Physical processes involved with the production of DRI
- Existing DRI Processes

3.1 Introduction

The reduction of iron oxides is fundamental to all ironmaking processes, including the Blast Furnace and all Direct Reduced Iron processes. It is therefore not unexpected that it has been the subject of much research and debate over many years. Whereas the thermodynamics of iron oxide reduction is well researched and covered in literature and reference works, the kinetics of iron oxide reduction is less so. It is also a complex topic which, in spite of the volume of work performed, still possesses some uncertainties. These are probably not as much as one commentator put it: "still beset with uncertainties, inconsistent experimental data, and with conflicting theories" (Prakash 1996)

Since reduction of iron ore in the Blast Furnace and most DRI processes (shaft, fluid bed and rotary kiln based) occurs primarily by means of the gaseous reductants CO and/or H_2, this type of reduction has been the subject of most of the early research work starting in 1960 with the work of McEwan. (McEwan 1960).

Reduction of iron oxides with solid carbon in fine iron oxide/carbon blends often in the form of composite pellets, has however, come under intensive study in recent years coinciding with the increase in interest in the Rotary Hearth and Smelting Reduction type processes. (Fruehan 1977, Prakash 1996, Sun 1997, Coetsee et al 2002)

3.2 Thermodynamics and equilibria of Iron Oxide reduction

Excellent assessments on the thermodynamics of iron oxide reduction have been published in reference books and reviews (Oeters & Ottow 2009, Peacey & Davenport 1979, Batelle 1973, Rosenquist 1974), and only relevant aspects are discussed.

The following table indicates some important properties of the oxides of Iron relevant to this work: Note. For the sake of simplicity, the term notation FeO is used to designate $Fe_{0.947}O$ throughout this thesis.

Specie	O:Fe ratio	H^f_{298} (kJ/kmole)	H^f_{298} (kJ/kmole Fe)	ΔH^f_{298} (kJ/kmole Fe)
Fe_2O_3	1½	-826 000	-413 000	-39 333
Fe_3O_4	1⅓	-1 121 000	-373 667	-107 766
FeO	0.947	-266 000	-266 000	-266 000
Fe	0	0	0	0

Table 3.2.1: Some Properties of selected Oxides of Iron (Peacey & Davenport 1979)

The last column indicates the enthalpy of formation, in this case heat emitted, per kmole of Fe when that species of Fe is oxidised to the next higher species, i.e. Fe to FeO, FeO to Fe_3O_4 and Fe_3O_4 to Fe_2O_3. Reducing a species to the next lower species would require the same enthalpy of formation, but in this case heat has to be supplied. From this it would seem that about 2½ times the amount of energy is required to reduce Fe_3O_4 to FeO than Fe_2O_3 to Fe_3O_4, and about 2½ times the amount of energy is required to reduce FeO to Fe than Fe_3O_4 to FeO, indicating the relative increase in difficulty to reduce lower Fe species.

The generalised form of the carbothermic reduction reaction of Iron Oxide contains two reactions, namely the reduction of an iron oxide FeO_n and the oxidation of a suitable reductant (C,H_2, CO). (Oeters & Ottow 2009)

$$FeO_n \Leftrightarrow Fe + nO \quad \text{..... [1]}$$

$$nO + n(C,H_2,CO) \Leftrightarrow n(C,H_2,CO)O \quad \text{..... [2]}$$

$$FeO_n + n(C,H_2,CO) \Leftrightarrow Fe + n(C,H_2,CO)O \quad \text{..... [3]}$$

The formula for describing iron oxides as FeO_n, is not well known in the practical ironmaking milieu, rather the form Fe_xO_y is used more often. Re-writing [3] using this form yields

$$Fe_nO_m + m(C,H_2,CO) \Leftrightarrow nFe + m(C,H_2,CO)O \quad \text{..... [4]}$$

The overall carbothermic reduction reaction of hematite occurs via the different species of Iron according to the following component reactions: (only reduction with CO is shown)

$3Fe_2O_3 + CO \Leftrightarrow 2Fe_3O_4 + CO_2$ ..... [5]

$2Fe_3O_4 + 2CO \Leftrightarrow 6FeO + 2CO_2$ ..... [6]

$\underline{6FeO + 6CO \Leftrightarrow 6Fe + 6CO_2}$ ..... [7]

$3Fe_2O_3 + 9CO \Leftrightarrow 6Fe + 9CO_2$ ..... [8]

Which may be simplified to

$Fe_2O_3 + 3CO \Leftrightarrow 2Fe + 3CO_2$ ..... [9]

3.3 Thermodynamics and equilibria of Gasification

Table 3.3.1 indicates some important properties of the reductants (C,H_2,CO) as used in reaction [4]. The following are pertinent aspects

- C is solid carbon ($C_{(s)}$), in most processes char from devolatilised, charred (pyrolised) coal
- CO and H_2 are gaseous Hydrogen ($H_{2(g)}$) and Carbon Monoxide ($CO_{(g)}$), obtained mostly from gasification of some hydrocarbon. When the hydrocarbon is natural gas, the gasification is normally performed with CO_2 or H_2O in which case it is generally referred to as reforming.
- Higher oxides of $C_{(s)}$ may serve as further reductants for more reduction as indicated in table 3.1.2.

C		H_2		CO	
Specie	H^f_{298} (kJ/kmole)	Specie	H^f_{298} (kJ/kmole)	Specie	H^f_{298} (kJ/kmole)
C	0	H_2	0	CO	0
CO	-111 000	H_2O	-242 000	CO_2	-394 000
CO_2	-394 000				

Table 3.3.1: Some Properties of selected Reductants (Peacey & Davenport 1979)

Reactions involved with reductants, generally referred to as gasification reactions, are too numerous to list, and only some pertinent reactions are indicated. These include the following (Reactions are listed in groups with their universally given names)

Combustion reactions

$$C_{(s)} + O_{2(g)} + \Leftrightarrow CO_{2(g)} \quad \text{..... [10]}$$

$$H_{2(g)} + ½O_{2(g)} \Leftrightarrow H_2O_{(g)} \quad \text{..... [11]}$$

$$CO_{(g)} + ½O_{2(g)} \Leftrightarrow CO_{2(g)} \quad \text{..... [12]}$$

Gasification reaction

$$C_{(s)} + ½O_{2(g)} \Leftrightarrow CO_{(g)} \quad \text{..... [13]}$$

Bouduard reaction (also called the soot formation reaction when it happens in reverse)

$$CO_{2(g)} + C_{(s)} \Leftrightarrow 2CO_{(g)} \quad \text{..... [14]}$$

Water gas reaction

$$H_2O_{(g)} + C_{(s)} \Leftrightarrow CO_{(g)} + H2_{(g)} \quad \text{..... [15]}$$

Reforming reactions

$$CH_{4(g)} + CO_{2(g)} \Leftrightarrow 2CO_{(g)} + 2H_{2(g)} \quad \text{..... [16]}$$

$$CH_{4(g)} + H_2O_{(g)} \Leftrightarrow CO_{(g)} + 3H_{2(g)} \quad \text{..... [17]}$$

Shift reaction (Also called the CO_2 or Water shift reaction)

$$CO_{(g)} + H_2O_{(g)} \Leftrightarrow CO_{2(g)} + H2_{(g)} \quad \text{..... [18]}$$

Pyrolysis reaction

$$C_nH_{m(s)} \text{ (Coal)} + \text{Heat} \Leftrightarrow C_{(s)}\text{(Char)} + H_{2(g)}, CH_{4(g)}, H_2, CO_{(g)}, CO_{2(g)},$$

$$C_nH_{m(g)}\text{(Higher alkanes, alkenes, alkynes, aromatics etc)} \quad \text{..... [19]}$$

The principal components of a typical gasification reaction, namely CO, H_2, CO_2, H_2O and CH_4 are thought to be the product of a sequence of reactions. (Lowry 1963) These are:

- Oxidation of carbon and hydrogen and other combustibles in the coal volatiles to CO_2 and H_2O according to reactions [10] and [11]
- Gasification of carbon with the products from these reactions, specifically CO_2 and H_2O according to reactions [14] and [15]
- Approach of shift reaction [18] equilibrium.

The equilibrium gas composition is dependent on molar rations of carbon, oxygen and hydrogen, temperature and pressure. The equilibrium gas composition for a 1:.5:5 $C:O_2:H_2$ molar ratio at 1 atmosphere is indicated in Figure 3.3.1

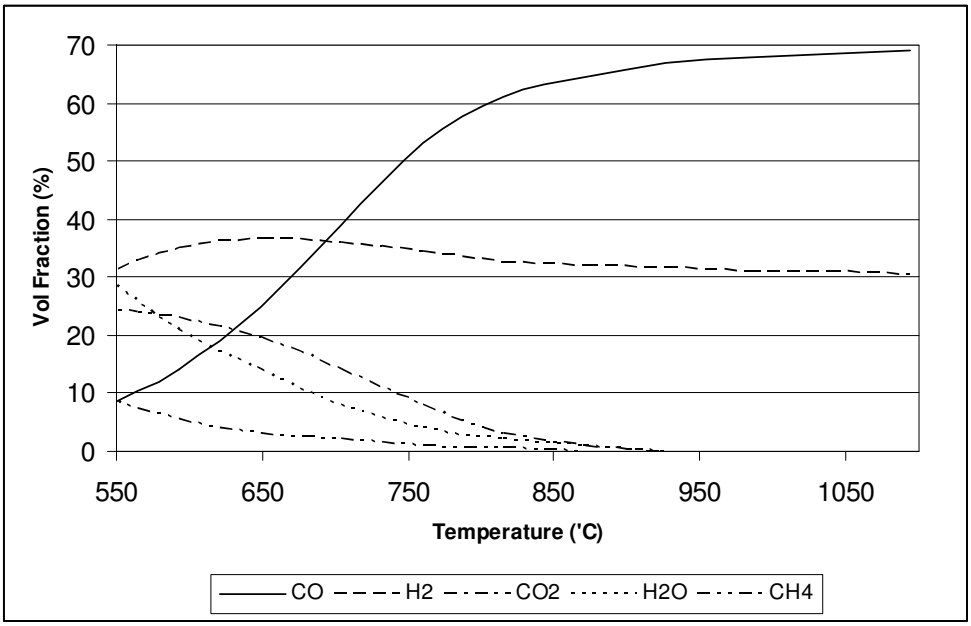

Figure 3.3.1: Equilibrium gas composition for the C-O-H_2 system at 1 atmosphere (Lowry 1963)

Analysis

The Gibbs Free Energy for the generalised carbothermic reduction reaction may be defined as:

$Fe_nO_m + m(C,H_2,CO) \Leftrightarrow nFe + m(C,H_2,CO)O$ ..... [4]

$\Delta G^o = -RTlnK$

$K = a^n_{Fe} \cdot p^m_{(C,H2,CO)O} \ / \ a_{FenOm} \cdot p^m_{(C,H2,CO)}$

If (C,H_2,CO) is solid carbon, and the activities of all the pure solids are taken at unity, then:

$K = p^m_{CO}$

From Tables 3.2.1 and 3.3.1 it is seen that H^f_{298} of FeO is about twice that of CO, therefore the reaction is strongly endothermic, and needs heat to be supplied to proceed. Analising the volume fraction of CO and CO_2 in the gas as a function of varying heat inputs using FactSage, yields the following diagram.

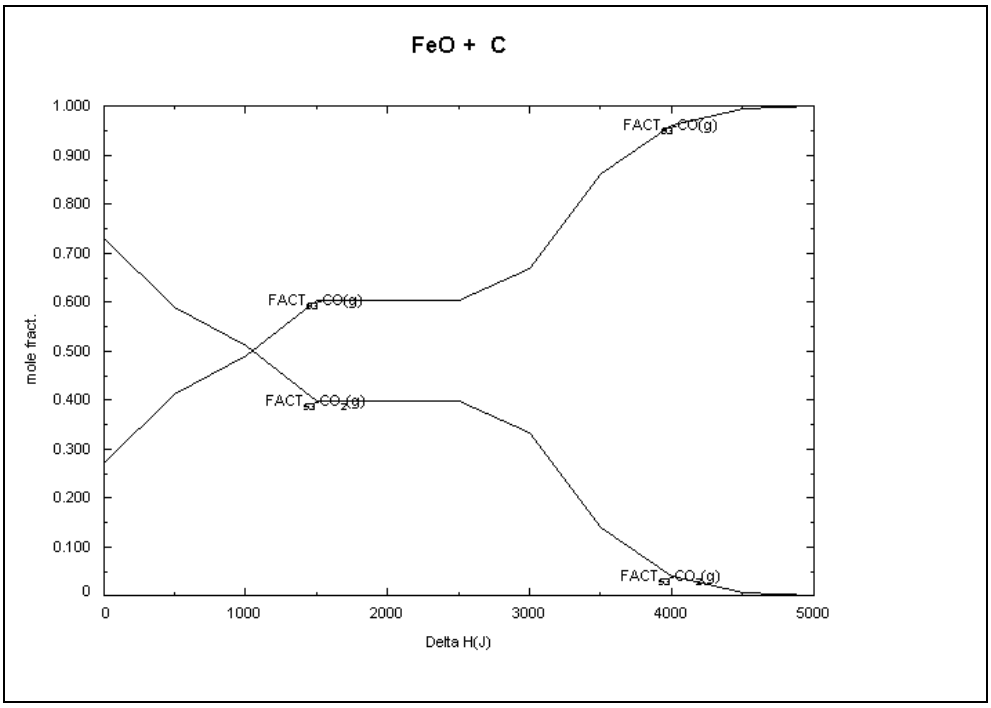

Figure 3.3.2: CO and CO_2 mole fraction vs. heat input for the reduction of FeO with Carbon

However, it is uncertain what the contribution of the solid carbon reduction reaction is to the overall reduction reaction in practical applications, since "Only during the very beginning of the reduction does a solid-phase reaction take place at the interface of the oxide and carbon. This reaction, however, triggers the gaseous reduction which is responsible for the further reduction." [Batelle 1973] Therefore the study of the reduction of Fe_nO_m with CO or H_2 has received more attention in past research work.

Thus if (C,H_2,CO) is CO, then the equilibrium coefficient K, is denoted by

$$K = p^m_{CO2} / p^m_{CO}$$

Equilibrium gas compositions may be calculated at a range of temperatures and displayed on a variety of types of diagrams. The first being $\ln(p_{CO2}/p_{CO})$ vs. the inverse of temperature ($10^4/T$) (Figure 3.3.3). A more common diagram is to construct a plot of $CO/(CO+CO_2)$ vs. Temperature. This is sometimes referred to as the Bauer/Glaesner diagram (Uhlman 2009) or the Chaudron curve (Pichler & Merkel 1949) It is customary to also indicate the $CO/(CO+CO_2)$ ratio for the Bouduard reaction [14] on the same graph. (Figure 3.3.4)

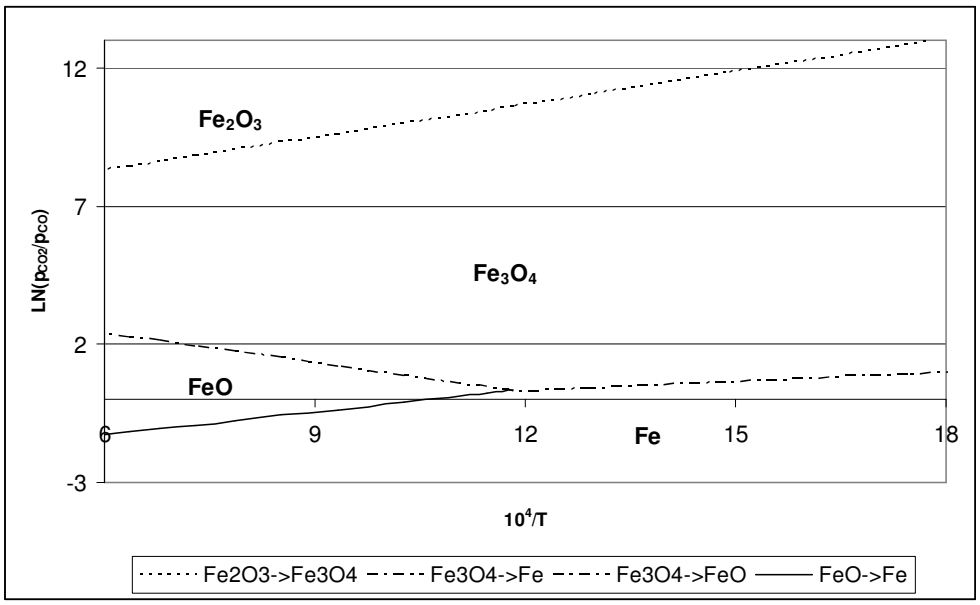

Figure 3.3.3: Natural logarithm of the ratio of CO_2 to CO partial pressures vs. Reciprocal of the Temperature for various reduction reactions of Fe_nO_m with mixtures of CO and CO_2

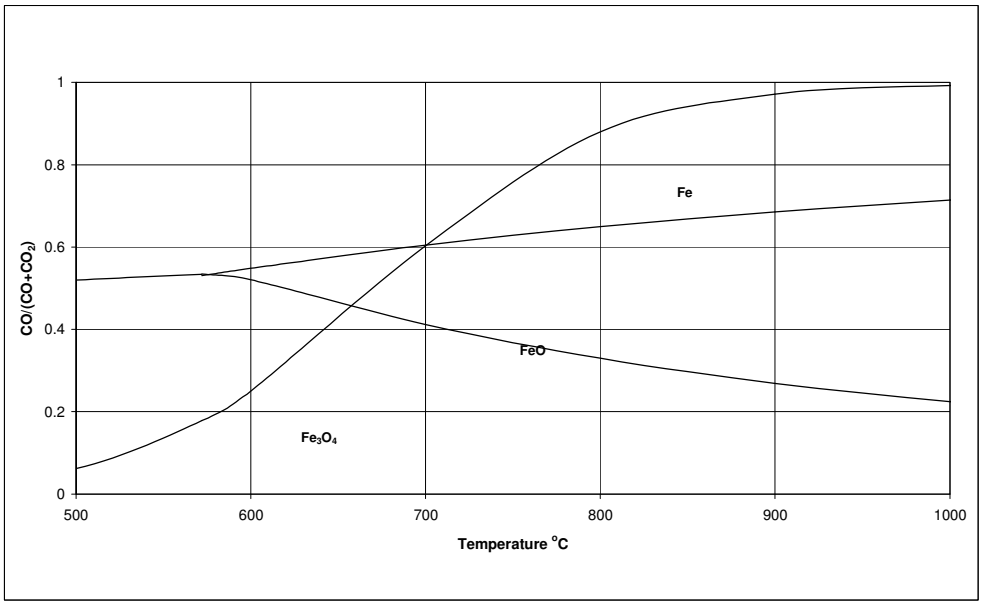

Figure 3.3.4: Equilibrium gas composition for the reduction of Fe_nO_m mixtures of CO and CO_2 and for the Bouduard reaction

The same may be done for reduction by H_2, when K is denoted by

$$K = p^m_{H2O} / p^m_{H2}$$

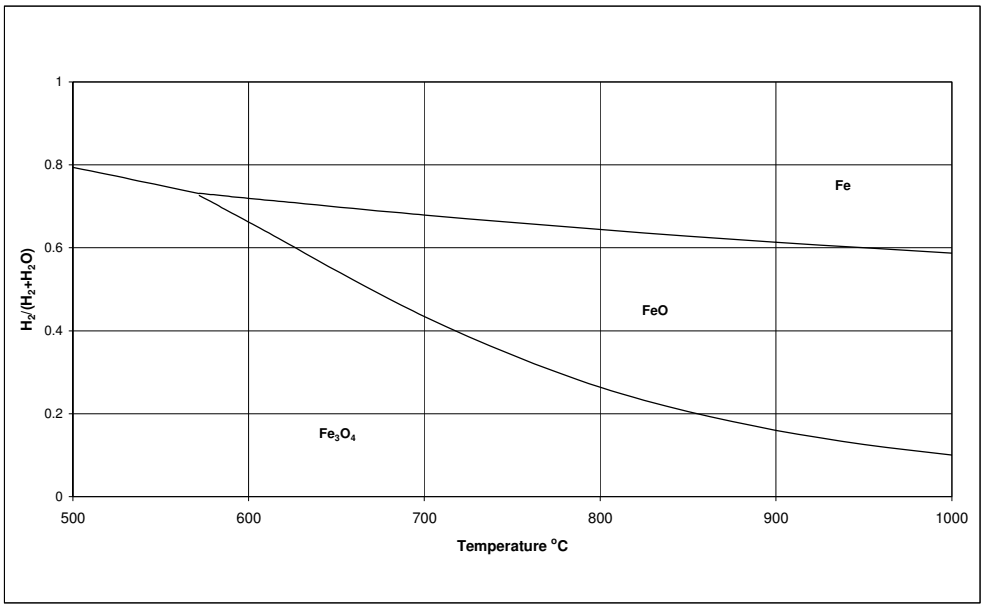

Figure 3.3.5: Equilibrium gas composition for the reduction of Fe_nO_m mixtures of H_2 and H_2O

It is also common to indicate both CO/CO_2 and H_2/H_2O equilibria on the same axis, producing the following figure.

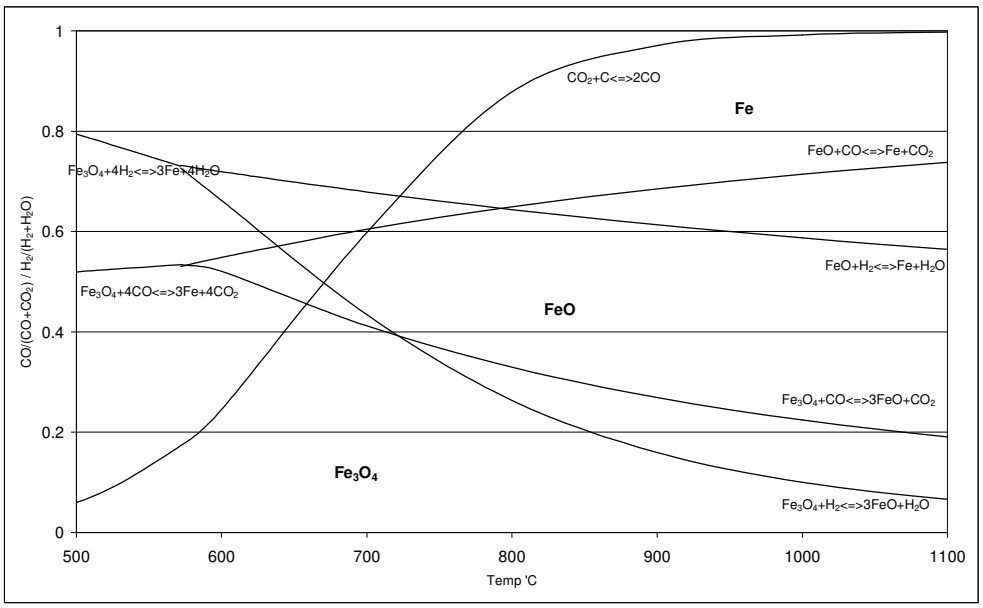

Figure 3.3.6: CO/CO_2 and H_2/H_2O equilibria for the reduction of Fe_nO_m with mixtures of CO and CO_2 and/or H_2 and H_2O.

Assessment

From these diagrams the following deductions may be made:

- Reduction of FeO to Fe requires a higher fraction of CO or H_2 in the reduction gas than does reduction of Fe_3O_4 to FeO or Fe_2O_3 to Fe_3O_4. In the practical reduction temperature regime, (800 - 1100ºC), reduction of FeO to Fe requires a gas of approximately double the fraction of CO or H_2 in the carbonaceous/hydrogenous part of the gas than does the reduction of Fe_3O_4 to FeO.

- The $CO/(CO+CO_2)$ ratio required for reduction of FeO with CO/CO_2 mixtures increases with temperature in the range 600 - 1200ºC. The $H_2/(H_2+H_2O)$ ratio required for reduction of FeO with H_2/H_2O mixtures on the contrary, decreases with temperature in the same range.

- The CO_2 or H_2O volume fraction of the gas after FeO has been reduced to Fe with either CO and H2 at 850ºC cannot be more than 33%. This gas, i.e. with a composition of $CO/(CO+CO_2)$ or $H_2/(H_2+H_2O)$ of approximately 67%, is more than adequate to reduce Fe_3O_4 to FeO and Fe_2O_3 to Fe_3O_4. In fact considering a countercurrent gas reduction process, the complete reduction reaction may be re-written as:

$$6FeO + 18CO_{(g)} \Leftrightarrow 6Fe + 6CO_{2(g)} + 12CO_{(g)} \quad \text{..... [20]}$$

$$2Fe3O4 + 12CO_{(g)} + 6CO_{2(g)} \Leftrightarrow 6FeO + 8CO_{2(g)} + 10CO_{(g)} \quad \text{..... [21]}$$

$$3Fe_2O_3 + 10CO_{(g)} + 8CO_{2(g)} \Leftrightarrow 2Fe3O4 + 9CO_{2(g)} + 9CO_{(g)} \quad \text{..... [22]}$$

This would mean that the reduction gas required to reduce 1t of hematite (66.5% Fe completely with either 100% CO or H_2) at 850ºC would be approximately

1000kg hematite * 66.5%Fe / 55.85kg Fe/kmole Fe / $.333CO_2(CO+CO_2)$ * 22.4Nm^3/kmole = 800Nm^3/t hematite

Or to produce 1000kg Fe under the same conditions would require

1000kg Fe / 55.85kg Fe/kmole Fe / $.333CO_2(CO+CO_2)$ * 22.4Nm2/kmole = 1203Nm^3/t Fe

It stands to reason that if the reduction gas does not consist of 100% CO and/or H_2, but either contain some CO_2 and/or H_2 or inert gases like N_2, the volume of gas required would increase proportionally.

This and the fact that the gas utilisation, i.e. the faction of reduction gas consumed per pass, is rather low (maximum 50% for countercurrent processes), has a major implication on gaseous reduction processes like Midrex, HYL and Purofer as will be seen later.

Performing reduction of hematite at 850ºC in a concurrent reactor would have the implication that the gas composition of the outlet gas, i.e. after having performed total reduction, may not contain more than 33% CO_2 or H_2O. Reaction [11] to [13] may be rewritten as follows.

$$3Fe_2O_3 + 27CO_{(g)} \Leftrightarrow 2Fe_3O_4 + 1CO_{2(g)} + 26CO_{(g)} \quad \text{..... [23]}$$

$$2Fe_3O_4 + 26CO_{(g)} + 1CO_{2(g)} \Leftrightarrow 6FeO + 3CO_{2(g)} + 24CO_{(g)} \quad \text{..... [24]}$$

$$6FeO + 24CO_{(g} + 3CO_{(g)} \Leftrightarrow 6Fe + 9CO_{2(g)} + 18CO_{(g)} \quad \text{..... [25]}$$

The required gas volume for complete reduction under the same conditions as above is now

1000kg Fe / 55.85kg Fe/kmole * 1.5kmol CO2 / kmole Fe / $.333CO_2(CO+CO_2)$ * 22.4Nm^3/kmol

= 1805Nm^3/t Fe which is 50% more than for a countercurrent operation

3.4 Kinetics of the Reduction of Iron Oxides

Whereas the thermodynamics of the reduction of hematite and lower iron oxides may be largely independent of the origin of the hematite, the kinetics of the reduction of hematite is certainly dependent on the origin of the hematite. For this reason it is vital that in any process design employing the reduction of a specific iron ore, the kinetic data for that iron ore is used in the design.

The iron ore envisaged for use in the process under study is a local hematite, since it is been shown that carbothermic reduction of titaniferous magnetite proceeds only to approximately 66% metallization due to the formation of ülvospinel. (Manamela & Pistorius 2005). Only Kumba Resources (from the Sishen mine) or Assmang (from the Beeshoek mine) offer hematite to the local market.

As will be evident from the next chapter the reduction procedures of the process under study is unlike that of pure gaseous reduction processes or pure solid carbon reduction processes. It contains elements of both, but the particle size is more similar to gaseous reduction processes than to processes employing composite pellets. For this reason work conducted on South African hematites using both gaseous and solid carbon reduction will be reviewed.

The rate of reduction of various South African iron ores of a wide range of particles sizes by solid Carbon and CO or H_2 have been studied by various authors, including Beeton (1965), Theron (1985), Van den Berg&Dippenaar (1989), Lourens (2002), Coetsee, Pistorius & deVilliers (2002), Manamela & Pistorius (2005), Pistorius (2005), and others.

3.4.1 Reduction with solid carbon

As far as the reduction of Sishen lump ore with sold carbon is concerned, no relevant previous work was found. The body of work (Lourens (2002), Coetsee, Pistorius & deVilliers (2002), Pistorius (2005) concentrated on the rate of reduction of composite pellets, consisting of blends of fine iron ore and fine coal/char/antracite, in shallow layers under radiative heat transfer.

Manamela & Pistorius (2005) determined the rate of reduction of varying diameters of Titaniferous magnetite from Steelpoort with char, and determined that reduction is indeed strongly dependent on particle diameter.

Wright et al (1981) although not working with Sishen lump ore, used a single pellet with a diameter of approximately 12mm which was heated together with two alumina crucibles containing 20g char each in a furnace. When the items had reached furnace temp, the pellet was placed on top of the char in one crucible and the contents of the second quickly poured over the pellet and the crucible placed back into furnace. After a predetermined reduction time the crucible was taken out, quenched under

inert atmosphere, and the contents analyzed. The tests were all conducted under isothermal conditions with a large excess of carbon ($C/Fe_2O_3 > 5$). The procedure was repeated for various reduction times at various temperatures ranging from 900 to 1200ºC.

Wright et al (1981) found the following:

- Reduction rates in a static bed in the temperature range of 900 ~ 1000ºC were similar to that found for the same raw materials in a rotary kiln, and also similar to that found by other workers for fine ore/fine coal composite pellets
- At temperatures above 1075ºC reduction rates showed a distinct reduction. Pellets reduced at these temperatures were found to contain areas of localized slag formation.
- Dense iron layers were observed in pellets reduced at temperatures above 1157ºC.

He concluded that the reduction of iron oxide with carbon in all but high vacuum conditions occurs through the intermediaries CO & CO_2. This opinion is supported by various other authors (Prakash 1996, Fruehan 1977)

From this premise and the fact that the calculated apparent activation energies were largely similar to those determined by other authors for the oxidation of carbon by CO_2 it was concluded that the reaction rate is primarily controlled by the Bouduard reaction. This conclusion is also supported by other workers (Fruehan 1977).

At temperatures above 1000ºC the reaction rate may be controlled by diffusion of the gaseous intermediaries in and out of the pellet. The formation of localized slag areas and dense iron rings may further reduce the rate of diffusion of the gaseous intermediaries.

However, the work also suffers from some limitations. This includes the fact that a single pellet was used suffers from the limitation that CO formed by the reduction of Fe_2O_3 by C in the top half of the pellet has limited opportunity of engaging in further reaction with iron oxide, since it is expected to flow vertically upwards as that is the only escape route. Similarly does CO formed from the gasification of carbon by CO_2 formed from subsequent reduction of iron oxide by CO have limited opportunity of engaging in more reduction reactions. It is uncertain how the flow of the gaseous products would benefit the reduction

Although Wright et al states that an initial amount of CO is formed by the gasification of carbon with free atmospheric oxygen entrapped in the system during the transferring of the pellet and carbon to the crucible, no further gasification of carbon and the subsequent reduction of iron oxide was investigated.

The apparent similarity between the work of Wright et al (1981) and that of Fruehan (1977) would suggest that the results of research on the reduction of hematite in iron ore/carbon composite pellets might be applicable to the reduction of lumpy ore or pellets reduced with separate carbonaceous materials, however Wright et al does not explore this position adequately.

3.4.2 Reduction with CO and/or H_2

Only Beeton (1965) and Theron (1985) have studied the reduction of lump South African hematite ores by CO and H_2. The work of both researchers is reviewed by Dippenaar, Barczsa & Jones (1988).

Beeton (1965) concentrated on the reduction of lump Thabazimbi hematite. However, the total output from the Thabazimbi mine is presently consumed by Arcelor Mittal South Africa under a 25 year supply agreement with Kumba Iron Ore. This ore is therefore not available for sale to parties outside of the Arcelor Mittal group.

Theron (1985), in the course of studying the sulphur distribution during direct reduction, performed reduction tests on lump Sishen and Thabazimbi hematites with both CO and H_2 using thermogravimetric analysis.

Theron (1985) selected four approximately spherical iron ore particles of diameter -12+10mm by hand from a large sample. These were placed in a porous crucible located inside a temperature controlled furnace. Reduction was affected by a stream of reducing gas flowing over the particles. The mass change during the reduction reaction was recorded as a function of time by a chemical balance on which the crucible was supported.

Reduction was performed with hydrogen, carbon monoxide and with carbon monoxide/dioxide blends. Reduction trials with hydrogen lasted approximately one hour and was performed at a range of temperatures ranging from 650 to 1000ºC while in the case of carbon monoxide trials lasted approximately 100 minutes and was performed at temperatures of 800, 900 and 1000ºC. Full metallization was achieved when reducing with hydrogen at temperatures above 900ºC, but not when reducing with carbon monoxide.

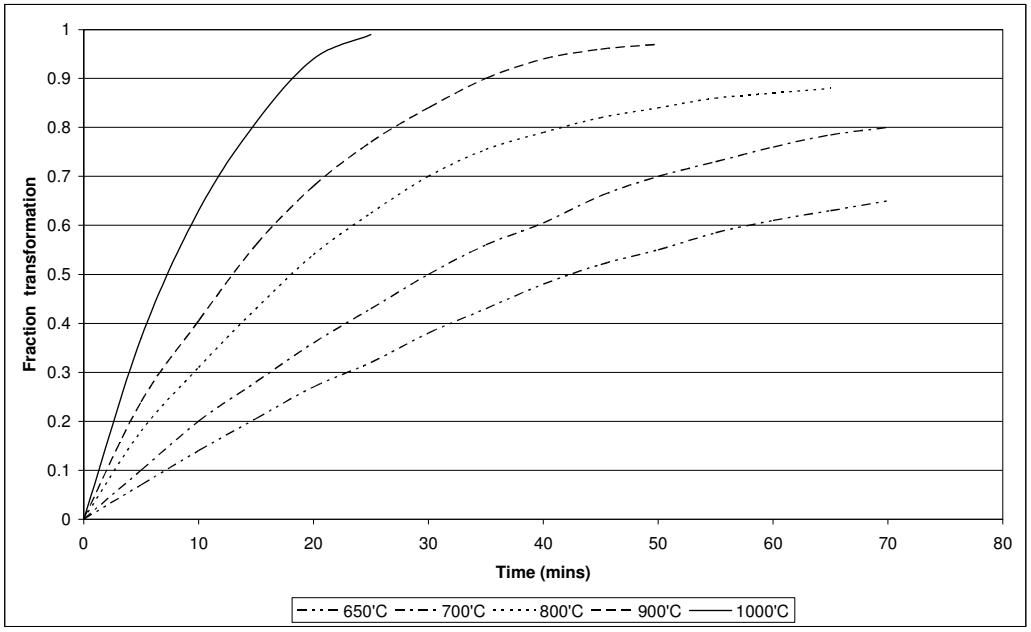

Figure 3.4.1: Reduction of -12+10mm Sishen Hematite with H_2 (Theron 1985)

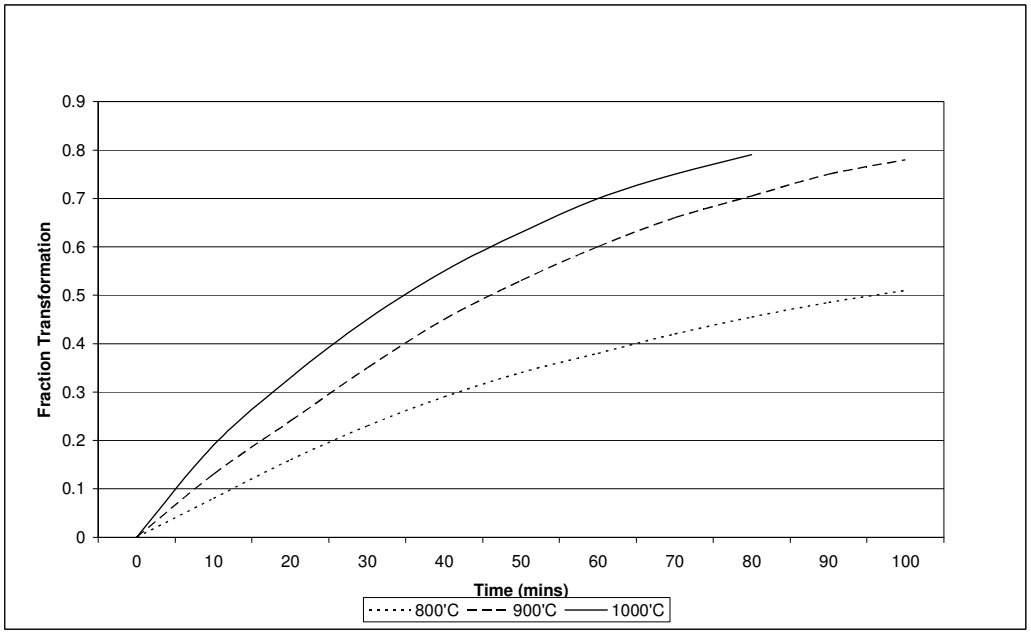

Figure 3.4.2: Reduction of -12+10mm Sishen Hematite with CO (Theron 1985)

In a separate trial Theron performed a reduction test in a stepwise approach with an increasing fraction of CO in a CO/CO_2 gas mixture at 1000ºC. The composition of the gas mixture was as indicated in Table 3.4.1. The gas flow at each step was maintained until it was evident that complete reduction to the species intended had been approached, where-after the gas composition was changed to the next composition.

	CO	**CO_2**
Fe_2O_3 ..... Fe_3O_4	15%	85%
Fe_3O_4 ..... FeO	67%	33%
FeO ..... Fe	100%	0%

Table 3.4.1: Gas composition in stagewise reduction test by Theron (1985)

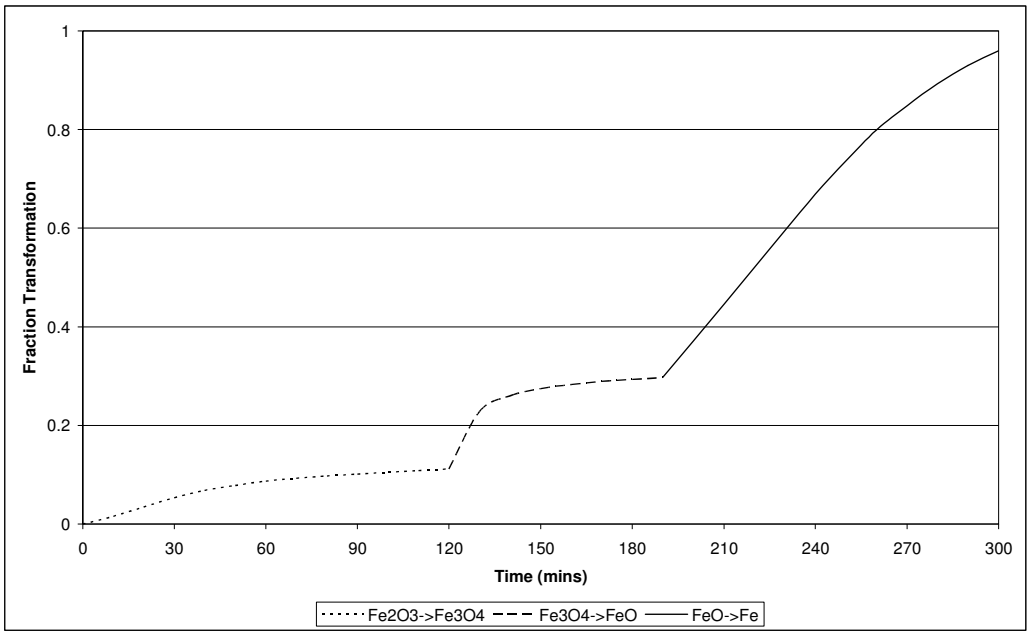

Figure 3.4.3 : Stepwise reduction of -12+10mm Sishen Hematite with CO/CO_2 mixtures at 1000ºC (Theron 1985)

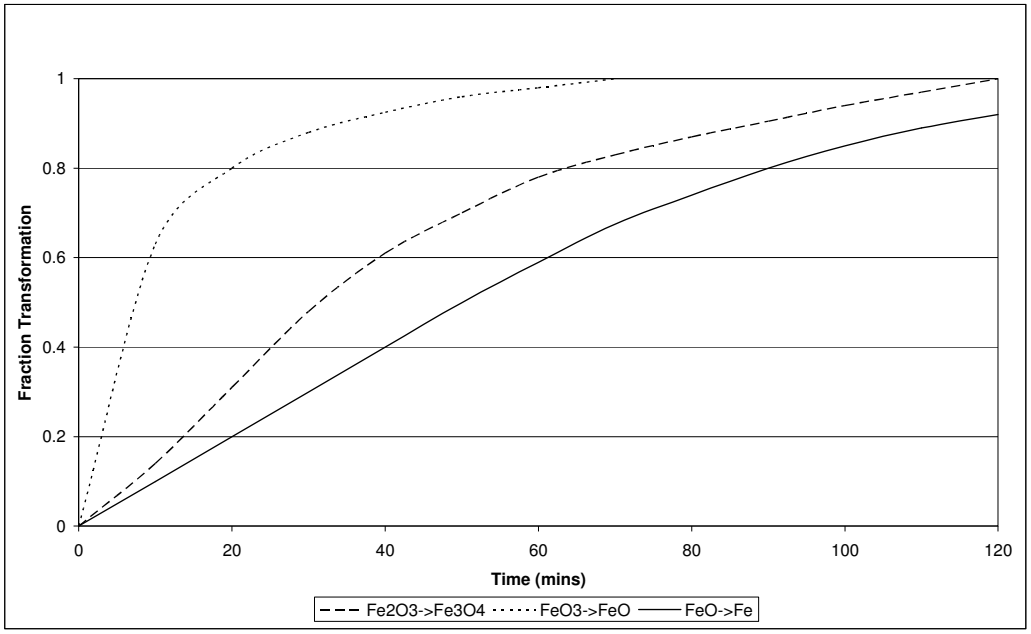

Figure 3.4.4: Stepwise reduction of -12+10mm Sishen Hematite with CO/CO_2 mixtures at 1000ºC (Theron 1985)

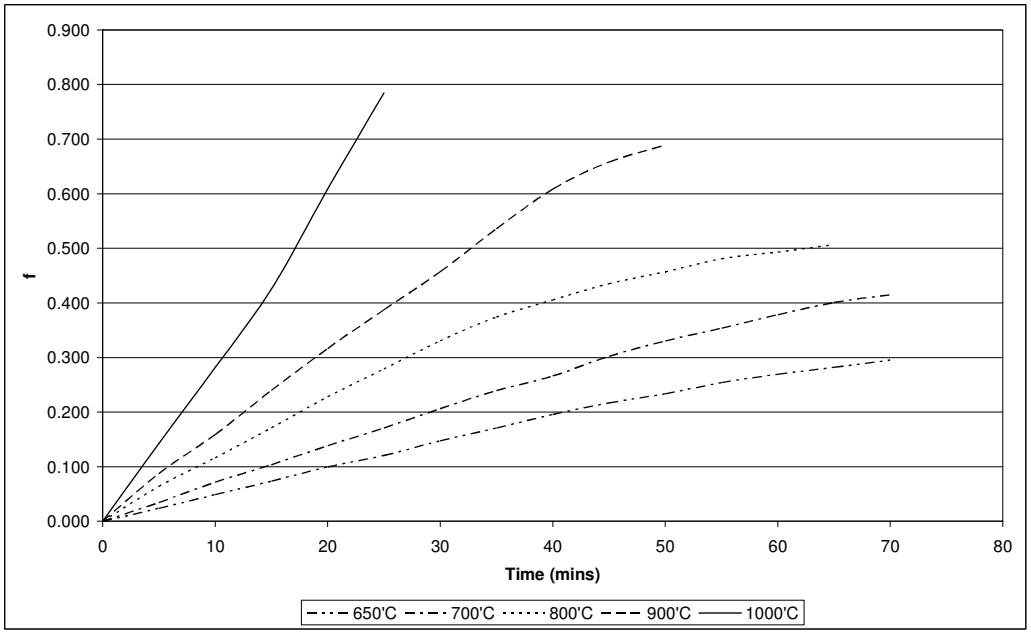

Figure 3.4.5 : f vs time for H_2 reduction of -12+10mm Sishen Hematite (Theron 1985)

Theron deduced the following:

- Complete reduction was approached asymptotically at the higher temperatures (900 & 1000º) regardless of the type of gas used for reduction, albeit at vastly different rates.

- Reduction with hydrogen was approximately 4.5 times faster than reduction with CO.
- When iron oxides are reduced with gas mixtures of analysis equal to that in equilibrium with the next lower oxide, transformation will take place until all the iron has been completely transformed to that species and no further. The reduction reactions of Fe_2O_3 to Fe_3O_4, Fe_3O_4 to FeO and FeO to Fe take place at significantly different rates.
- From the fact that the relationship between the relative penetration of the reaction front and the time could be approximated by a straight line, Theron deducted that the shrinking core model is an appropriate representation to apply when modelling the reduction of hematite. The reduction is chemical reaction rate (topochemically) controlled. This is in accordance with the approach suggested by Levenspiel (1972)

$$f = t/\tau = 1 - r_c/R = 1 - (1 - X)^{1/3}. \quad \text{..... [26]}$$

Assessment

The work of Wright et al (1981) and Theron (1985) provides some insights to the critical questions regarding this work. This includes:

- The reduction of lump iron ore in the presence of solid carbon in all likelihood occurs via the gaseous intermediaries CO, CO_2, H_2 and H_2O, and may have some similarity to the reduction mechanism happening inside composite pellets.
- The reaction rate in a blend of lump iron ore and solid carbon is most likely controlled by the Bouduard reaction in that part of the reactor where gasification of the carbon takes place, and when gasification ceases to play an important role, by the rate of CO and/or H_2 reduction of FeO.
- The time required for complete metallization for 12mm pellets are
    - 2.5hrs when reduced by carbon at 1075ºC
    - 4 hrs when reduced by carbon at 1000ºC
    - 1 hour when reduced by H2 at 900 ºC
    - 25 minutes when reducing by H2 at 1000ºC
- The time required for full reduction of Sishen hematite with CO could not be determined from previous work and needs to be determined.

3.5 Physical processes influencing DRI production

Where-as many physical process may influence a typical DRI production process unit, only two physical processes which may limit the production rate of DRI processes more than others, are discussed here. These are:

- Heat transfer from the combusted product gas to the burden limit the production rate in rotary kilns, but heat transfer from the reduction gas to the burden in shafts may also limit production rate in some instances.
- The pressure drop due to the passage of the reduction gas through the bed limit the production rate in many reduction shafts.

3.5.1 Heat transfer

Heat Transfer in Rotary Kilns

Heat transfer in rotary kilns is extremely complex. In the pre-heating zone of the kiln where the gas temperature is below 800ºC, convection is the main mode of transfer, while in the reduction part of the kiln where the gas temperature may be as high as 1100ºC, radiation is the main mode of transfer. Various attempts have been made to model the heat transfer in a rotary kiln, some succeeding admirably. (Oeters & Ottow 2009, Palmer & Howes 1998). This work is not discussed in detail, however the following conclusions may be drawn from this work.

- Heat transfer in rotary kilns is a complex phenomenon with radiation, convection and conduction all contributing differently at different stages in the kiln process to transfer heat from the gas to the burden and to the kiln wall, and then from the kiln wall to the burden when the heated wall is rotated below the burden.
- Heat is also transferred from the heated top surface of the burden to the rest of the burden when this layer is mixed in with the burden.
- Heat transfer in kilns is diameter specific, with increasing diameters becoming more disadvantageous due to longer radiation distances, and less kiln surface per volume of production area.
- Pre-heating of the burden is rate limiting in large diameter kilns, while reduction is rate limiting in smaller diameter kilns.

Heat transfer in shafts

Heat transfer in shafts is covered in more detail since design of the pre-heat shaft is a key aspect of the pilot plant design. Normally heat transfer is not a limitation to shaft based processes, since as explained previously, a large volume of gas needs to be passed through the shaft to ensure sufficient reduction and reduction with CO is slightly exothermic. However when the reduction gas contains a large fraction of hydrogen, of which the reduction reaction is slightly endothermic, heat transfer may be limiting.

Heat transfer from a gas passing though a bed of broken solids and the solids as well as to the walls of the container have been described by various authors including Löf & Hawley (1948), later reviewed by McCabe & Smith (1976), Caulson & Richardson (1989) and various others. Seshadri & Silva Pereira (1986) reviewed various correlations for the calculation of heat transfer in packed beds.

Two approaches seem to be favoured (Sheshadri & da Silva Perreira 1986). The first is to express the heat transfer coefficient as the conventional with units W/m^2K in terms of parameters influencing the coefficient, like the equation of Ranz-Marshall,

$$h = \frac{k_g}{d_p}\left[2 + 0.6\left(\frac{\mathrm{Re}_p}{\varepsilon}\right)^{1/2}\mathrm{Pr}^{1/3}\right] \qquad \text{..... [27]}$$

whilst the next expresses the heat transfer coefficient as the volumetric heat transfer coefficient with units W/m^3K, e.g. the correlation of Furnas

$$h_v = \frac{A_s U_g^{\,0.7} T_g^{\,0.3}}{d_p^{\,1.35}} M \qquad \text{..... [28]}$$

A_s = 114 for iron ore heating and 137 for cooling

$$M = \ln(13.7472 - 6.8656e^{\varepsilon}) \qquad \text{..... [29]}$$

The average particle diameter, d_p, for blends of particles is calculated from

$$\frac{1}{d_p} = \sum_{i-1}^{n} \frac{x_i}{\Phi_s d_{pi}} \qquad \text{..... [30]}$$

It is important to realise that the normal heat transfer coefficient, h, and the volumetric heat transfer coefficient, h_v, are related in the following way.

$$h_v = hA = h\frac{6(1-\varepsilon)}{d_p} \qquad \text{..... [31]}$$

Values for both the traditional and the volumetric heat transfer coefficient have been calculated for a typical MIDREX shaft of 5m producing 500kt/a. The difference of 290% is in line with the difference found by Sheshadri and da Silva Perreira (1986).

	Ranz-Marshall	**Furnas**
h (W/m^2K)	136.6	369.6
Hv (W/m^3K)	44398	129625

Table 3.5.1: Heat transfer coefficients for a typical Midrex shaft.

When it is borne in mind that the typical bulk density for lump iron ore is $2.55t/m^3$, whilst the density of hematite is approximately $4.5t/m^3$, it follows that the void fraction must be approximately 0.4. Thus the volumetric heat transfer coefficient is approximately 300 times that of the normal heat transfer coefficient for an average ore particle diameter of 12mm. Alternatively, the heat transfer area per unit volume is $300m^2/m^3$. This probably explains why calculated heat transfer coefficients expressed as $W/m^2/K$ does not seem high, but when the shaft height required for heat transfer is determined it seems rather small. This is in line with experience on the first Corex plant in which the burden, which also contained uncalcined limestone, attained a temperature of 800ºC within 1 hour from entering the shaft or merely 2m below the stockline. (Delport 1992).

3.5.2 Pressure drop

It has been shown in Section 3.3 that the volume of reduction gas is a crucial control parameter for the efficient reduction of iron ore particles in a shaft. From a simple forces balance on a shaft it is clear that when $dPA > mg$ the upward forces exceed the downward forces and the bed will tend to "hang". If the gas volume cannot be reduced it is obvious that some other parameter needs to be varied to reduce the pressure drop.

Various equations for the determination of pressure drop though a bed of broken solids have been proposed. Perhaps the most well known is that by Ergun (McCabe & Smith 1976). It may be re-written as follows

$$dP = 150\frac{\mu GL}{\sigma D^2}\frac{(1-\varepsilon)^2}{\varepsilon^3} + 1.75\frac{G^2 L}{\rho D}\frac{(1-\varepsilon)}{\varepsilon^3} \quad \text{.....[32]}$$

With G = Mass velocity (kg/sm^2)

ϱ = Fluid Density (kg/m^3)

μ = Fluid viscosity (Ns/m^2)

D = Effective particle diameter (m)

ϵ = Void fraction

The effective particle diameter is may be determined using equation [30]. However, the most complex parameter to determine is ϵ, the void fraction. The void fraction is defined by

$$1-\varepsilon = \frac{M_p}{\rho_s V} \quad \text{..... [33]}$$

M_p = Mass of particles in container

ϱ_s = Density of a single particle

V = Volume of container

It is not straightforward to predict the bed voidage. While the voidage for beds of single diameter particles may be determined, it is well known that mixtures of different sizes of particles decrease the bed voidage since the smaller particles tend to fill the voids between the larger particles.

Perry & Chilton suggest that bed voidage be determined in a small vessel and that it be corrected for the full scale application since it is known that the ratio of particle diameter to vessel diameter influences the voidage. (Perry & Chilton 1973). More recent work done by a variety of workers on predicting the bed voidage as a function of the volume ratio of binary mixtures of particles have yielded accurate, albeit complex, correlations. (Finkers & Hoffmann 1998).

However, burdens in practical applications never consist of a binary mixture of equal diameters, or even binary mixtures of closely sized particles, but a range of particles of differing diameters. Furthermore, decrepitation of the iron ore particles during reduction increases the fraction of small particles, further decreasing bed voidage and increasing pressure drop. It has also been found that

packed beds act like gravel bed filters to dust that may be present in the reduction gas, and that this increases the pressure drop across the bed strongly. (Delport 1992)

Figures 3.5.1 and 3.5.2 have been prepared for a 5m diameter x 11m high Midrex shaft producing 500kt DRI/a using a reduction gas with a typical gas analysis to illustrate the effect of bed voidage and system pressure on the bed pressure drop. See Appendix 3 for assumptions.

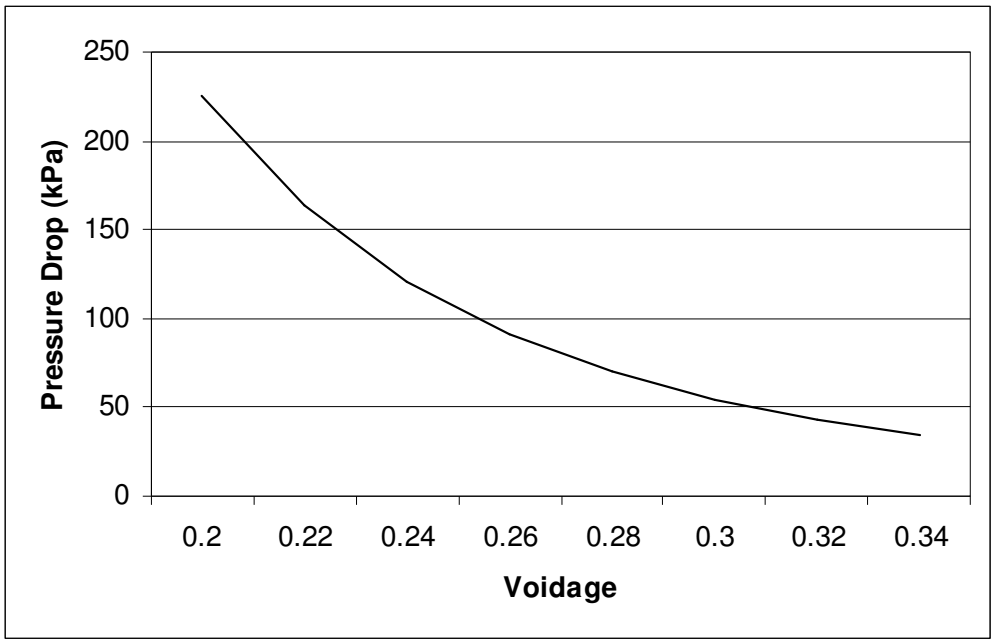

Figure 3.5.1: Effect of voidage on bed pressure drop. (System pressure = 3.5kPa Abs)

In practice, the only parameters that are available to influence pressure drop is ore size distribution, ore shape factor and system pressure.

- **Iron Ore size distribution**

  Most operators attempt to keep the ore size distribution as narrow as possible by specifying the size range as narrow as possible, by limiting over- and under size by screening out the over- and under-size and by selecting iron ores with as low a tendency to decrepitate during reduction as possible (Nair & Kundoo 2003).

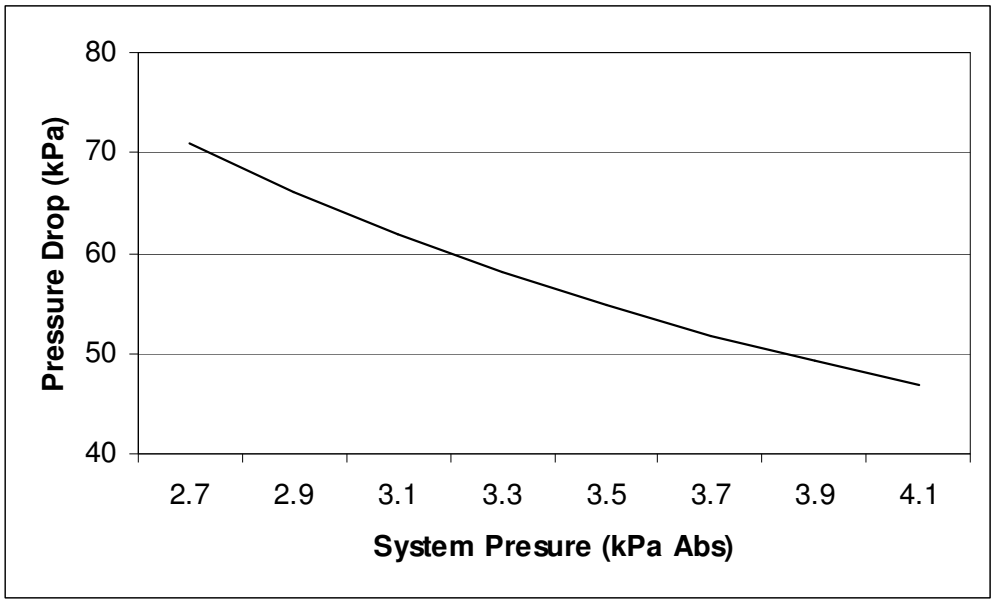

Figure 3.5.2: Effect of system pressure on pressure drop (Voidage = 0.3)

- **Shape factor**

Iron ore pellets are spherical and smooth in shape and therefore have a shape factor of close to 1, while crushed iron ore may have a shape factor as low as 0.65 (Perry & Chilton 1973). Most shaft operators either use only pellets, but since pellets normally commands a premium over lump iron ore, many blend as much lump iron ore into the feed stream as the pressure drop will allow. (Midrex Technologies Inc, 2008)

- **Reduction gas pressure**

The pressure that the reduction shaft is operating on is normally defined during the design stage of the process to get to an operating regime that will allow the operator smooth operation. In practise the operator will operate at the lowest possible pressure that allows stable operation and only increase the pressure when problems with a too high pressure drop is experienced. To reduce the pressure drop, the operator needs to increase the pressure, but the maximum pressure is limited by the design of the shaft.

3.6 Existing DRI Processes

By 1973 1000 processes for the production of DRI had already been patented (Battelle 1973). Many more have been patented since then. Many of these never reached industrial scale application as only perhaps 30 processes have been applied on industrial scale at any time. (Gojić & Kožuh 2006).

3.6.1 Classification of DRI Processes

In view of the fact that such a large quantity of DRI processes exist, various attempts at classifying DRI process have been made. (Batelle 1973, Plaul et al 2009). Classification is possible on the following bases

- Reduction reaction (Solid carbon, CO and/or H_2)
- Ore size (Lump, medium, fine, ultra fine)
- Reductant type (Natural gas, coal)
- Vessel (Shaft, Rotary kiln, Fluidised bed, Rotary hearth)
- Product (DRI, Hot Metal)
- Commercial success/developmental status

The reaction used for reduction is perhaps the most fundamental basis for the classification of DRI Process. Classifying DRI processes on this basis yields the following table

Reaction used	**Process class**	**Comments**
$Fe_2O_3+3C \Leftrightarrow 2Fe+3CO$	Rotary Kiln, Rotary Hearth	Reaction strongly endothermic, external heat has to be supplied, e.g combustion of coal, electricity
$Fe_2O_3+3CO \Leftrightarrow 2Fe+3CO_2$ $Fe_2O_3+3H_2 \Leftrightarrow 2Fe+3H_2O$	Shaft, Fluidised bed	Reduction with CO is slightly exothermic, reduction with H_2 slightly endothermic.

Table 3.6.1: Reduction reactions of iron oxide

Classification of iron production processes based on ore size, reductant type and product is a common classification basis. Table 3.6.2 presents such a classification indicating commercial names of processes. Processes producing liquid hot metal are also indicated. Developmental status or commercial application status is not a criterium. Comprehensive descriptions of all of these processes are available from various publications and reference works and are not repeated here (Plaul et al 2009, Gojić & Kožuh 2006, Battelle 1973).

Product	**Hot metal**	**Hot metal equivalent**	**DRI/HBI**	**DRI/HBI**	**Fe_3C**
Reductant ..... **Ore size ↓**	**Coke**	**Coal**	**Natural gas**	**Coal**	**Natural gas**
Lump, pellet, sinter	Blast Furnace	Corex Redsmelt Oxicup Fastmelt Sidcomelt	Midrex, HYL, Arex, Ghaem, Purofer	SLRN, DRC, Codir, Tisco, Gasifier/DR Kinglor-Metor	
Fine ore		Finex Hismelt Hisarna CCF DIOS Romelt Ausmelt	Finmet, Fior, Circored, Spirex, Novalfer, H-Iron, HIB	4Primus Circofer Comet	
Ultra fine ore, steelplant wastes		Fastmelt	Fastmet, ItMk3, Iron Dynamics, Höganäs	Fastmet	Iron Carbide

Table 3.6.2: Classification of Fe unit producing processes (Plual et al 2009)

As the focus of this study is processes producing solid DRI, processes producing liquid iron or equivalent are forthwith omitted from descriptions. Processes that have reached industrial scale application are much fewer in number than that listed above. In their annual survey of operating DRI processes operating on industrial scale, Midrex Corp (2009) lists only 15 DRI processes operating on industrial scale at the end of 2008. Processes in the course of development and those specifically designed to treat steelplant waste oxides are excluded from the table

Ore\Reductant	**Natural Gas**	**Coal**
Lump ore/Pellets	Midrex (50.67), HYL (21.2), Purofer (.33)	SLRN (1.83), Jindal (1.26) DRC (.93), Codir (.52), SIIL (.38) Tisco (.36), Osil (.25) Dav (.04), Others (19.5), Corex/Midrex (.8)
Fine ore	Finmet (2.2) Circored (.5) Fior (.4),	
Ultra fine ore	Iron Dynamics (.5)	

Table 3.6.3: DRI Processes operating on industrial scale at end Dec 2008 with installed capacity in million t/a in brackets (Midrex Corp 2009)

When the above 15 processes are analysed in more detail, the similarity between the Midrex, HYL and Purofer processes as far as raw materials and reactor vessel is concerned, is immediately apparent. This is also true about the 10 rotary kiln based processes listed and about the Fior and Finmet processes. When the processes are grouped as far as similarity of raw materials and reactor vessels are concerned, table 3.7.3 is obtained.

Process	**% of world production**	**Reactor Vessel**	**Ore feedstock**	**Reductant**
Midrex, HYL, Purofer	72.7	Shaft	Pellet/Lump	Natural gas /Coke, char
SL/RN, Jindal, DRC, Codir, Popouri, SIIL, Tisco, Osil, Dav	25	Rotary Kiln	Pellet/Lump	Coal
Finmet, Circored, Fior	1.6	Fluidised bed	Fine ore	Natural gas
ITMk3, Fastmet	0.7	Rotary Hearth	Ultrafine ore	Coke/char

Table 3.6.4: Industrial scale DRI processes grouped in terms of raw materials and reactor vessel. (Midrex Corp 2009)

Detail of one process in each of the four classes of processes is indicated in Table 3.6.5

Aspect	**Unit**	**Shaft**	**Rotary Kiln**	**Fluid bed**	**Rotary Hearth**
Names		Midrex	SLRN	Finmet	Iron Dynamics
Unit size	Mt/a	0.4 – 1.8	.06 - .18	.55	.5
Ore size	mm	10 - 20	8 - 16	.1 – 1	<1
Reduction temp	ºC	850 - 950	900 – 1000	780 – 800	1000 - 1200
Retention time	hrs	6	8 – 12	2	.25
Operating Pressure	Bar (g)	Ambient – 5	Ambient	14	Ambient
Limiting factor		Pressure drop	Heat transfer in pre-heat or reduction zones	Sticking of DRI fines	

Table 3.6.5: Details of selected DRI processes in each class of the four major classes of DRI processes. (Formanek & Rose 2009) (Hillisch & Zirngast 2001)

3.6.2 Shaft based processes

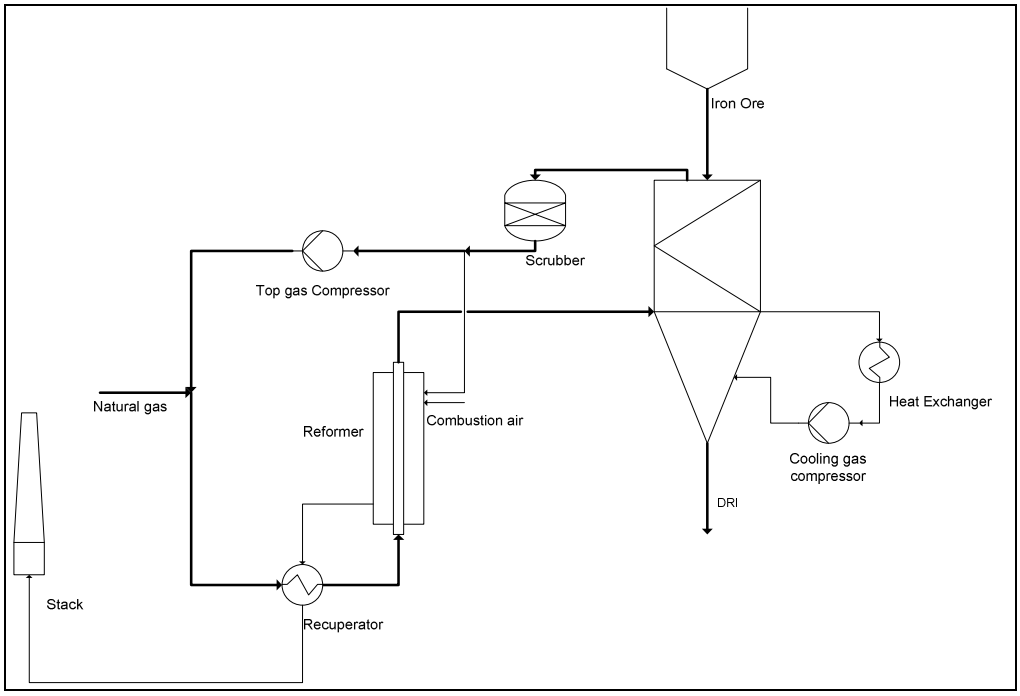

Figure 3.6.1: Simplified schematic flowsheet of shaft based processes

This class of processes include Midrex, HYL and Purofer processes. Newer developments include Arex, Danarex, and Hyl-Energiron, although it is unclear whether these are fundamentally different or merely name changes as an effect of commercial agreements between technology suppliers

The process description is as follows: (Midrex Technologies(1) 2009), Oeters & Ottow 2009, Batelle 1973)

Iron ore is first pre-heated then reduced by hot (850º) reduction gas containing typically 95% CO and H_2 moving counter currently to the burden in the shaft. The iron ore is reduced to DRI with a metallization of at least 93% during its residence time of typically 6hrs and is cooled once it passes the reduction gas entry point to prevent damage to handling equipment and re-oxidation. The top gas which may contain as much as 50% CO_2 and H_2O, is cooled, cleaned and re-circulated to a reformer. In the reformer fresh natural gas is partially combusted or gasified with the CO_2 and H_2O in the recycled top gas over a catalyst, which is typically nickel based. In the application where coal is used to produce the reduction gas, the CO_2 is removed from the top gas and mixed in with fresh reduction gas produced by the gasification of coal with oxygen and steam.

The volume of reduction gas supplied to the shaft is such that after the target amount of FeO has been reduced to Fe, (metallization degree of the DRI, typically 93%), the gas composition would still be marginally above the Fe-FeO equilibrium gas composition at the reduction temperature.

The plant typically consists of three main sections:

- The raw material handling section
- The shaft
- The gas preparation section

The raw material section is normally relatively simple since there is no blending of iron oxide and reductant and/or desulphuriser required. It typically consists of off-loading facilities feeding into long term (week+) storage silos. From these the iron ore passes over screens to short term (shift) storage hoppers before it is lifted by skip or inclined conveyor to the top of the shaft where it enters the shaft.

The reactor vessel or shaft is a vertical retort with a conical bottom. The shaft is kept filled with burden consisting of graded pellets or a blend of graded lump iron ore and iron ore pellets. The iron ore is charged into the reactor at the top and the DRI extracted at the bottom through pressure raising/lowering devices. Since most shafts are operated at elevated pressure, the pressure raising/lowering device (which may be lock hoppers, pressure seals or seal legs depending on the specific design) has the function of allowing burden to pass through whilst preventing reaction gases escaping to atmosphere.

Hot reducing gas is injected into the burden through one or more what is generally referred to a bustle ring or bustle main. The bustle is located at the bottom of the cylindrical section of the shaft. The bustle consists of a distributor ring main and ports through which the gas enters the burden. The ports are generally angled down and open into the burden on an angle to prevent burden from entering the ports.

The gas preparation section differs depending on the raw material used and the specific supplier. When natural gas is used, it typically consists of the reformer, the reduction gas supply system and the top gas cooling, cleaning and recirculation system. After the gas has passed through the shaft it is generally cooled and cleaned in a top gas scrubber after which it is re-circulated back to the reformer by a top gas compressor. Fresh natural gas is mixed in with the re-circulated gas and heated before it enters the reformer which typically consists of tubes filled with a catalyst through which the gas mixture passes. The reforming reaction is either

$CH_4 + CO_2 \Leftrightarrow 2CO + 2H_2$, or

$CH_4 + H_2O \Leftrightarrow CO + 3H_2$ or a combination of both

Gasification of natural gas with oxygen is increasingly being used as a supplement to the reforming process. It is rare for the gas preparation system to consist of only gasification of natural gas. The heat required for the endothermic reforming reaction is obtained from combusting a portion of the top gas with air. Sensible heat in combusted gases is recovered as efficiently as possible by a series of heat exchange steps with combustion air, fresh natural gas and re-circulated top gas. This bleed stream has the additional advantage of removing unwanted inerts like N_2.

When coal is used to generate the reduction gas, the gas preparation system consists of a gasifier in which coal is gasified with oxygen and steam, and the top gas, after being cooled, cleaned and the CO_2 removed, is re-circulated back into the fresh gas stream. (e.g. Wiberg, Midrex with gasification, HYLIII with gasification)

When the reduction gas is the product of another process like the Corex process and contains significant amounts of CO_2, it is mixed in with the re-circulated top gas immediately after the top gas scrubber since it also has to pass through the CO_2 removal system. Pre-heating of the gas might then be somewhat problematic since soot may form when high CO gas is heated indirectly above 550ºC. In this case a two stage pre-heat set-up is used with indirect heating taking the gas to 500ºC and direct heating the rest. (e.g. Saldanha Steel)

3.6.3 Rotary kiln based processes

This class of processes include numerous processes like SLRN, Jindal, DRC, Codir, SIL, Tisco, Osil, Dav and others. It is estimated that there are hundreds of small rotary kilns in India with annual capacities of 10,000 - 30,000 tons per year. The combined total capacity of all rotary kilns operating in India is estimated to be 19.5 million t/a, i.e. 16.16million t/a of unlisted plants. (Midrex(1) 2009)

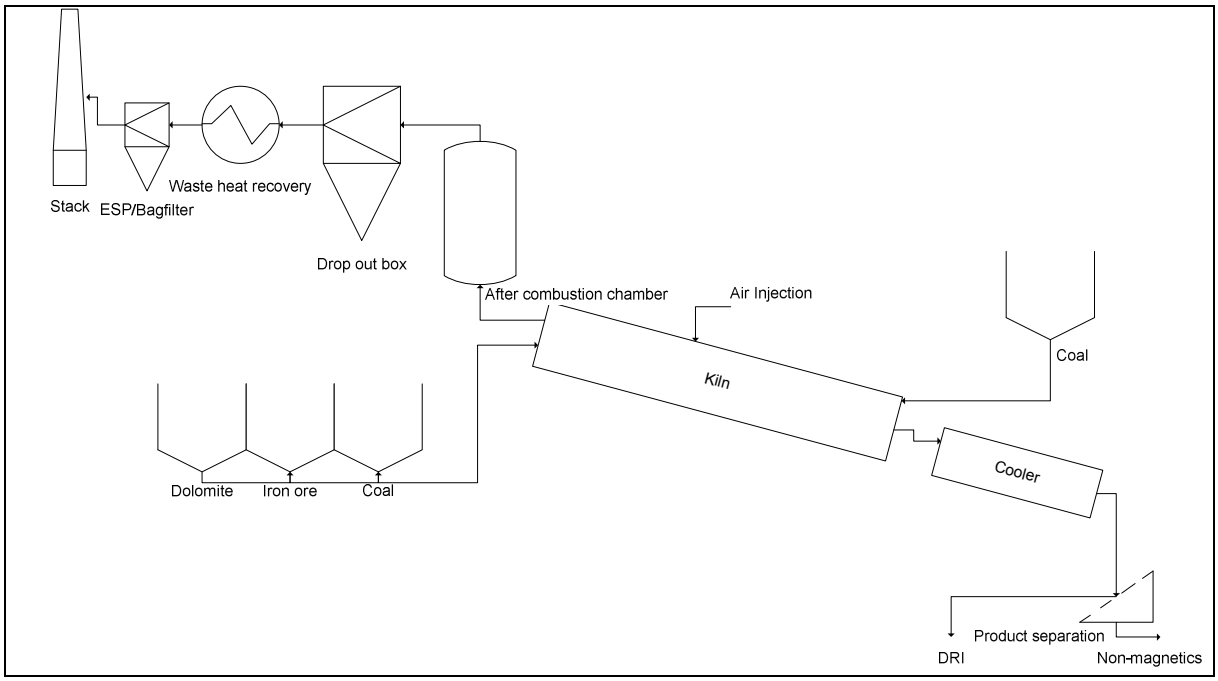

Figure 3.6.2: Schematic flowsheet of rotary kiln processes

The process description is as follows: (Oeters, & Ottow 2009, Mans 1986**,** Batelle 1973)

Iron ore, coal and desulphurising agent are charged into a slightly filled reactor where it is pre-heated by radiation from the combustion of gases from the latter part of the process in the unfilled part of the reactor. The coal dries and devolatilises and when the burden reaches a temperature of approximately 700ºC the char starts reacting with the iron ore. The overall reaction is

$$Fe_2O_3 + 3C \Leftrightarrow 2Fe + 3CO$$

although there seems to be agreement that the solid reaction above only happens at onset, and that the reaction happens through gaseous intermediaries according to the following reactions.

The evolved CO from the reaction above reacts with iron oxide according to the reaction

$$Fe_2O_3 + 3CO \Leftrightarrow 2Fe + 3CO_2$$

Some of the evolved CO_2 may gasify carbon to CO by the Bouduard reaction

$$CO_2 + C \Leftrightarrow 2CO$$

Finally the gas mixture leaves the burden and moves countercurrently with the burden to the exit. The gas is combusted with air injected into the gas stream to supply the heat required for the endothermic reaction and to pre-heat the iron ore and coal.

It is not established whether the evolved volatiles also contribute to the reduction of the iron ore according to the following reaction

$$Fe_2O_3 + CH_4 \Leftrightarrow 2Fe + CO + 2H_2O$$

as the temperature at which most of the devolatilisation is completed (500º) may be too low for reduction to take place, but some H_2 is liberated at higher temperatures though.

The iron ore is reduced to DRI with a metallization of at least 90% during its residence time in the reactor of typically 8 - 12hrs and it, the coal ash and the desulphurizing agent are cooled in an indirect cooler upon exiting of the reactor where-after the DRI is separated magnetically from the dolochar.

Combustibles in the exit gas which may consist of coal volatiles, CO, H_2 and some coal dust, are combusted, and the sensible heat of the off-gas either exchanged to the surrounding air or used for steam generation. The steam generated is typically used for power generation. Finally the off-gas is cleaned before it is emitted to atmosphere.

The plant typically consists of four main sections:

- The raw material handling section
- The rotary kiln
- The product cooling and separation section
- The off-gas treatment section

The raw material section is more complex than that of a shaft based process since blending of the iron oxide, reductant and desulphuriser is required. It typically consists of off-loading facilities feeding into long term (week+) storage silos for each raw material. From these the raw materials may pass over screens (often not) to short term (shift) storage hoppers before it is transported by conveyor to the top of the feed hoppers from where it enters the rotary kiln.

The reactor vessel or kiln is a refractory lined, inclined horizontal retort rotating slowly thereby transporting the burden along the bottom. Inclination depends of the characteristics of the burden and varies between 1.5 – 2.5º. Rotational speed also depends on burden characteristics and varies between 1 and 3 rpm. The kiln is only filled to a filling degree of approximately 15% and the burden continuously climbs up the side of the kiln to the angle of repose of the material then slips down to an angle lower than the angle of repose as the kiln rotates. This rolling and slipping motion improves contact between iron ore and char.

The kiln is equipped with gas seals on either end preventing gas escape. Burden is fed from the feed end (highest end) and air is injected at the discharge end. Some coal may be injected together with the air from the discharge end. Shell air fans mounted on the shell supply further combustion air into the kiln gas cavity.

The product cooling and separation section consists of an unlined inclined retort with water sprayed on the outside, cooling the product to below 100ºC to prevent conveyor damage. After cooling, the DRI is separated from the coal ash and dolomite, typically called dolochar, by magnetic separation. Excess char may be returned to the reactor.

The off-gas treatment section typically consists of a post combustion chamber, a waste heat recovery boiler and either an electrostatic precipitator or a bag filter. The generated steam is used for either electricity generation or process heat. Some plants do not recover heat from the off-gas and cool the gas in trombone coolers.

3.6.4 Fluid bed based processes

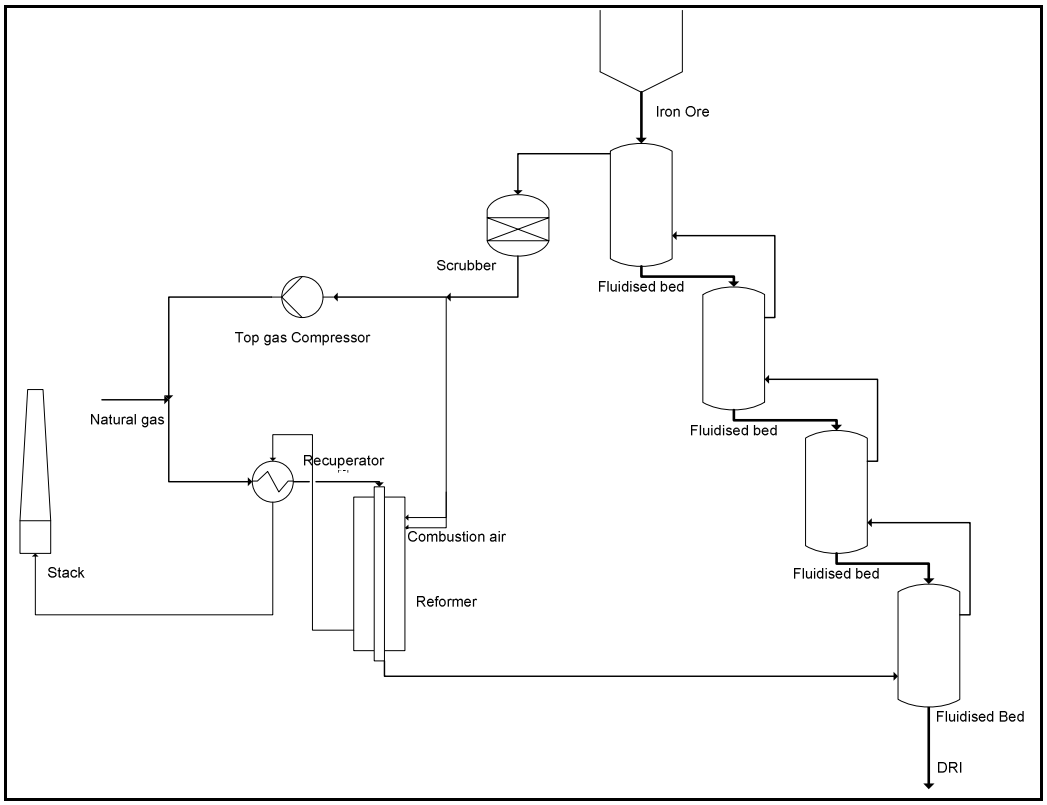

Figure 3.6.3: Simplified schematic flowsheet of Fluid Bed based DRI Process.

This class of processes include Fior, Finmet, Circored and Circofer

Fluid bed processes like Fior and Finmet are remarkably similar to shaft based processes and share the description given above bar the reactor used and the differences that causes. The flowsheet of Circofer is somewhat different to Fior and Finmet. (Oeters, & Ottow 2009, Brent 1999, Batelle 1973)

Since a fluid bed approaches a CSTR, it would mean that when supplying just enough reduction gas to a single fluid bed to reduce 93% of the FeO to Fe as in a countercurrent shaft process, it will result in a lower metallization than required since the gas may encounter some higher oxides of iron (Fe_2O_3 and Fe_3O_4) also and the gas composition may be such that it oxidises Fe back to FeO. Two solutions are possible, namely supplying enough gas so that even after 93% of the Fe_2O_3 is reduced to Fe the gas composition is still above the Fe-FeO equilibrium or having multiple reactors and thereby simulating a countercurrent operation. The latter seems to be preferred (Fior, Finmet).

Another typical complication with fluid bed applications is the fact that when the ore particle diameters vary in a wide range, creating gas flow conditions that will fluidise the largest particle would mean that the smaller particles are elutriated from the bed and need to be separated from the gas and either re-circulated back to the bed or taken to the product section directly.

Since the size grading of the produced DRI is typically very fine, the product is normally hot briquetted to form so called Hot Briquetted iron (HBI)

Sticking of fine iron particles also seems to be a common problem.

3.6.5 Rotary hearth based processes

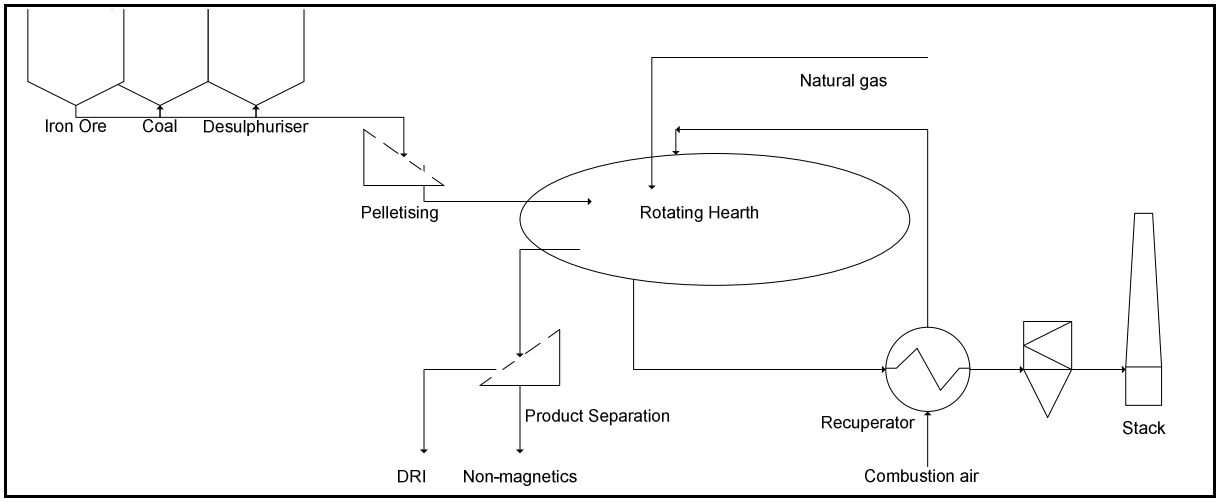

Figure 3.6.4: Simplified schematic flowsheet of RHF processes.

Rotary hearth type processes include Fastmet, Iron Dynamics, ITMk3, and the reducing part of the Fastmelt process.

Process description: (Midrex Technologies(2) 2009, Oeters & Ottow 2009, Batelle 1973)

Ultra fine iron ore or fine waste oxide is blended with fine coal, charcoal or coke and either pelletised using a binder or briquetted in a composite ball. Pellets are dried before charging, briquettes not. The pellets or briquettes are laid out in a shallow layer on the hearth of the rotary hearth of the furnace and the temperature is rapidly raised to typically 1050ºC by radiation from flames burning immediately above the burden. Reduction at this temperature occurs rapidly and retention times of only 15 minutes are required to attain complete reduction. Any emitted combustibles like coal volatiles and CO from the reduction reaction are also combusted. The product is discharged from the hearth after one revolution of the hearth. Reactions involved include

$Fe_2O_3 + 3C \Leftrightarrow 2Fe + 3CO$

CO evolved inside the pellet may react with FeO whilst diffusing out of the pellets, according to the reaction below, but due to the fact that heating, and therefore the reduction front penetrates the pellet from the outside to the inside, it is uncertain whether evolved CO may react further with iron oxide.

$Fe_2O_3 + 3CO \Leftrightarrow 2Fe + 3CO_2$

By the same token, the contribution of the regenerated, evolved CO with C may be limited.

$CO_2 + C \Leftrightarrow 2CO$

The plant typically consist of four main sections:

- The raw material handling section
- The rotary hearth furnace
- The product cooling and separation section
- The off-gas treatment section

The raw material section is more complex than that of a shaft based process since blending and agglomeration of the iron oxide and reductant is required. It typically consists of off-loading facilities feeding into long term (week+) storage silos for each raw material. From these the raw materials are proportioned and transported by conveyor to a blending drum where binder is added is required. From the blending drum it either pelletised, then pass over a screen with the undersize re-circulated back to the pelletizing step, or briquetted and stored in a short term storage hopper (shift). The pellet is dried if water was used in the agglomeration step. From this hopper it is fed into the rotary hearth furnace.

The reactor vessel is a refractory lined hearth rotating in a high temperature tunnel furnace. Burners located above the hearth are fired with natural gas, fuel oil or pulverised coal. The burners raise the temperature of the pellets on the rotating hearth very rapidly.

The product cooling and separation section consist of a screw feeder running outside of the hot zone above the rotating hearth which removes the reduced pellets from the hearth. Cooling is performed by variety of means, mostly indirect cooling in a water cooled screw conveyor. After cooling, the DRI is briquetted or used as is.

The off-gas treatment section typically consists of a settling chamber, a waste heat recovery boiler and either an electrostatic precipitator or a bag filter. Recovered waste heat may be used to preheat combustion air and or to generate electricity.

3.6.6 Limitations of Existing Processes

All of the process groups suffer from one or more limitations.

- Shaft and fluidised bed based processes are to a large extent dependent on the availability of natural gas, and whereas this has for a long time been regarded as an advantage, the recent steep increase in oil prices has turned this into a liability leading to the temporary shut-down of a number of shaft based direct reduction plants. (Midrex Corp 2009). Both Midrex and HYL are actively promoting the use of coal gasification coupled to their standard shaft processes as an alternative to natural gas. At present only Arcelor/Mittal's Saldanha Steel operates such a process assembly while HYL has several coal gasification projects underway in China. (MBM 2007). Other efforts are directed towards finding a more direct coal based direct reduction process.

- Rotary kiln based processes suffer from low thermal efficiency and since the coal in gasified inside the reactor, the ash remains with the product leading to high gangue content in the product and low specific productivity. (Manning & Fruehan 2001).

- Rotary hearth based processes, although being a relatively new development in the DRI arena, suffer from high specific capital investment costs. This is most likely due to the combination of relatively complex mechanical equipment required and the high temperatures attained in the process. Future developments will in all probability reduce this cost somewhat

These and other factors have led to an increased urgency in the search for an alternative to natural gas based or rotary kiln based DRI processes.

3.6.7 DRI Processes operating in South Africa

South Africa produced approximately 1.2 million t/a of DRI in 2008, down from 1.7 million t/a in 2007 (WSA 2009). This was produced at 5 different locations using 12 different units. Details about the DRI production facilities are indicated in Table 3.7.1.

Allthough the 13 rotary kilns producing pre-reduced titaniferous magnetite at Highveld Steel could also be regarded as producing direct reduced iron, (albeit at a lower degree of metallization) they are excluded from this table, since the product is regarded as a unique intermediate product not fitting the description of DRI.

Process	**SLRN**	**DRC**	**Codir**	**Dav**	**Midrex**
Location	Vdbijlpark	Germiston	Dunswart	Cullinan	Saldanha
Reactor	Kiln	Kiln	Kiln	Kiln	Shaft
No. of units	6	3	1	1	1
Capacity of units (kt/a)	6 x 180	2 x 90 1 x 150	1 x 150	1 x 40	1 x 800
Diam x Length (m)	4.8 x 80	3.6 x 80(e) 5 x 80	4.6 x 73		6.6 x 9
Coal rate (kg/t DRI)	800	750			
Investment cost ($/annual ton)	190(2007) Brownfield (1)	280(1997) New (2)		Converted cement kiln	

Table 3.6.6: DRI Production facilities in South Africa in 2009 (Midrex Corp 2009, (1) Creamer 2007, (2) Prnewswire 1997)

3.7 New DRI Processes

Details of new processes under development normally only appear in the public domain when the developer feels that the state of development has reached a stage where wider communication is warranted. For this reason information on new processes in the early stages of development is limited.

After much activity in the new liquid iron- and steelmaking process arena a decade ago, especially in the so-called direct steelmaking processes, interest in direct steelmaking processes seems to have reduced somewhat, and developments at present seem to concentrate on new liquid iron processes, including HiSmelt, Ausmelt, Technored, and Oxicup processes. (Gojić & Kožuh 2006)

Development activity in new DRI processes, which produces iron in the solid state, seem to be limited to two classes of processes, namely coal based gas generation for traditional shaft based processes and fine ore/coal composite reduction processes mostly based on rotary hearth technology.

Technical detail of a DRI processes developed in South Africa, called Finesmelt, is limited, but is based on an externally heated rotary kiln processing a fine ore/char composite blend. (IMBS 2009)

Detail of new developments are indicated in Table 3.7.1

Vessel	Ore type	Reductant	Developer	Developmental status
Shaft	Pellet/Lump	CO/H_2 from coal gasification	Corex, Midrex, HYL	Corex industrial scale. Midrex 1 plant, HYL some plants under construction
Rotary Hearth Furnace	Fine ore	Coal	ITMk3, Fastmelt, Hi-Quip, Primus	Demonstration plants
Rotary kiln	Fine ore	Coal	Finesmelt	Demonstration plant

Table 3.7.1: New DRI processes under development. (Gojić & Kožuh 2006)

3.8 Existing Gasification processes

Since natural gas is one of the minerals South Africa is not richly endowed with, prospective local users of shaft based DRI processes are compelled to use coal as reducing agent and have to generate a suitable reduction gas by gasifying coal using a suitable gasification technology.

Gasification is an old and well established technology. Gasification was discovered in 1798 and by 1850 the technology had developed to such an extent that many European cities were lighted with "town gas". (Reed & Das1998). Various gasification processes have been developed over the years with gasification agents ranging from cold air to mixtures of hot air, steam, oxygen and even alternatively air and H_2O.

As is to be expected, gasification processes exist that process coals of all particle size groups, namely, lump (cobbles, nuts, peas), fine (duff) and ultrafine (pulverized) coal. Examples of gasification processes operating on the different coal size gradings are indicated in Table 3.8.1 (Schilling et al 1985)

Where-as many similarities exist between gasifiers within a particular class, important differences exist. In most instances the reactions that take place in the different gasifiers within a class are similar, and the differences exist in oxidant, (e.g. air or oxygen and steam), operating pressure (atmospheric or

pressurized) and in raw charging and ash discharge mechanisms. A typical gasifier from each class has been selected to demonstrate important differences. (See Table 3.8.2).

Reactor..... Coal Size↓	**Fixed bed**	**Fluidised bed**	**Entrained bed**
Lump	SASOL-Lurgi, Welmann-Galusha, Kerpely, Power Gas, UGI, Kellogg, PCV, Intergral Engineering, Il Gas Integrale, GE, Demag		
Fine		HT Winkler, Cogas, CO_2-acceptor, Synthane, Hygas	
Ultrafine			Koppers-Totzek, Texaco, Bi-gas, Hygas, Russel-Otto,

Table 3.8.1: Classification of Gasification process by coal size and reactor type. (Schilling et al 1985)

Type	**Fixed bed, Air blown**	**Fixed bed, Oxygen & steam blown**	**Fluidised bed**	**Entrained bed**
Names	Welmann-Galusha	SASOL-Lurgi	HT Winkler	Koppers-Totzek
Coal size	6 – 50mm	6 – 40mm	< 8mm	< 0.1mm
Gasifying medium	Water saturated air	O_2 + steam	O_2 + steam	O_2 + steam
Pressure	Atmospheric	20 – 30bar	Atmospheric	Atmospheric
Temperature	600 - 650ºC	700 - 900ºC	800 - 1000ºC	1500 - 1900ºC
CO_2	3.4%	27 – 32%	13 – 25%	7 – 12%
Strengths	Simple operation	Successful on large industrial scale	Very little pyrolysis products in gas	Very little pyrolysis products or dust in product
Weaknesses	Countercurrent operation causes pyrolysis products to end up in the gas.	Countercurrent operation causes pyrolysis products to end up in the gas.	Fluid bed reactor causes high dust content in gas	Complex

Table 3.8.2: Selected details of gasification processes (Schilling et al 1981)

A common disadvantage that fixed bed gasifiers have is that of tar formation. As the coal entering the gasifiers is pre-heated by the hot gasifier gas exiting the gasifier, it de-volatilises. (Reaction [19]) The tars in the volatiles, apart from being environmentally problematic, if not treated properly, cause a variety of problems in gas lines.(Sutton et al 2009)

A gasification technology that is often overlooked is that of downdraft gasification. Although the size of downdraft gasifiers were usually small (<100kW thermal), the technology was used on an extensive scale during WWII for the generation of a combustible gas to replace vaporised gasoline fuel in internal combustion engines. It is estimated that as many as 1 million gasifiers existed during this time to operate cars, trucks, boats, trains and electric generators. (Reed & Das 1998, Di Blasi 2000)

Two versions of the downdraft gasifier exist, i.e. the so-called throated and the stratified downdraft gasifier (alternatively called the un-throated, open top or topless downdraft gasifier). The throated downdraft gasifier, of which the Imbert gasifier is the best known example was the most common design in WWII. The throated downdraft gasifier is again gaining ground for gasification of biomass for a variety of applications, including heating and drying, irrigation and power generation applications mostly on a small scale. Industrial application of the design is mostly limited to areas with ample supply of wood such as Brazil and Indonesia (Reed & Das 1998). The throated downdraft gasifier is limited in size to approximately 500kW.

The un-throated or stratified downdraft gasifier is less common, but nevertheless overcomes some of the limitations of the throated downdraft gasifier. It is at present applied most commonly for the gasification of rice husk, but it has not been widely commercialized. Extensive research and modeling work has been done on this type of gasifier however. (Reed, et al 1983, Di Blasi 2000)

The downdraft gasifier operates on lump feed (biomass or coal) similar to the Welman-Galusha or SASOL-Lurgi gasifier, but the main advantage that the downdraft gasifier has above the updraft gasifier is the fact that the pyrolysis sone is located above the oxidation zone with the significance that the coal volatiles are also gasified, circumventing the problem with handling the tars, whilst at the same time gaining the advantage of generating reduction gas from the volatiles.

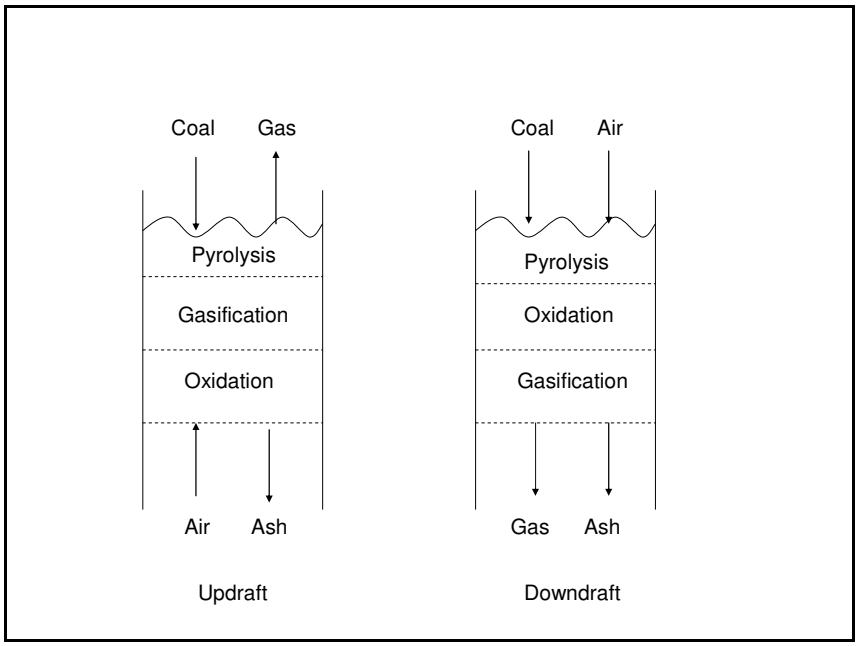

Figure 3.8.1: Schematic flow diagram of updraft (countercurrent) and downdraft (concurrent) fixed bed gasifiers (Reed and Das 1988)

Two important design considerations for downdraft gasifiers include the equivalence ratio and the superficial velocity. (Knoef 2008, Reed & Desrosiers 1979, Reed et al 1999)

- The equivalence ratio (ER) is defined as the quotient of the actual air:fuel ratio and the air:fuel ratio for complete combustion. Figure 3.8.2 indicates some pertinent facts about the ER

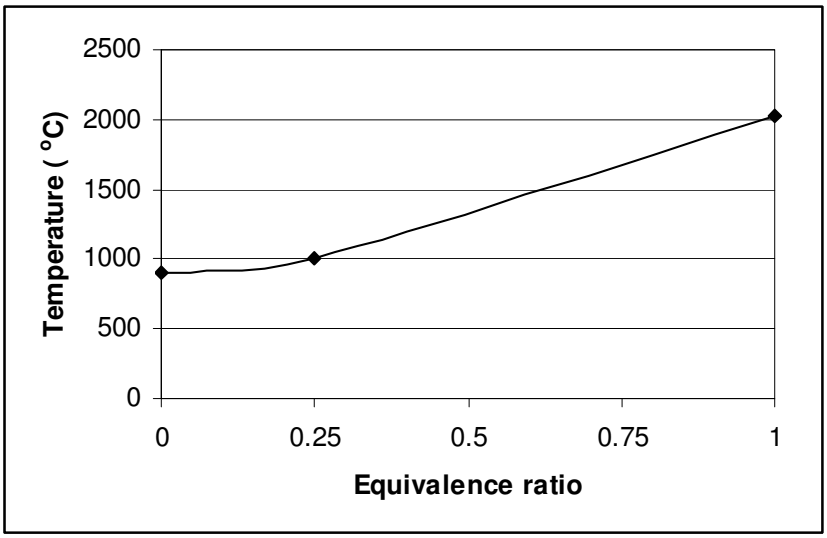

Figure 3.8.2 Equivalence ratio vs. Temperature for biomass gasification (Reed & Desrosiers 1979)

ER = 0 represents pure pyrolysis, i.e. devolatilisation in the absence of air

ER = 0.25 represents the point where all char has been gasified, and is often referred to as the optimal gasification air:fuel ratio.

ER = 1 represents complete combustion, i.e. all carbon has been combusted to CO_2 and all hydrogen to H_2O

The area $0 \leq ER \leq 0.25$ is referred to as the flaming pyrolysis area, i.e. some char has been gasified

- The superficial velocity (SV), sometimes also referred to as the hearth load of the gasifier, is the quotient of the volume of gas produced (Nm^3/s) and the hearth area (m^2). When referred to as the hearth load the units are ($Nm^3/s/m^2$), and when referred to as the superficial velocity the units are (m/s). Stratified downdraft gasifiers typically operate best at SV = 0.2m/s

Chapter 4

CONCEPTUAL DESIGN, THEORETICAL VERIFICATION, PILOT PLANT DESIGN AND OPERATION OF THE NEW PROCESS

This chapter covers four aspects

- Conceptual design of the process
- Theoretical Verification of the process
- Laboratory testing of kinetics of Sishen iron ore reduction
- Design, construction & testing of the pilot plant

4.1 Requirements for the DRI Processes.

Many DRI processes and plant offerings with low technical risk exist from which the prospective DRI producer may select. The process that the prospective DRI producer will select needs to conform to general and specific requirements regarded as crucial for success in the specific environment that the process is intended for. The requirements have been discussed in Chapter 2. Requirements that could disqualify some processes process are:

- Volume: <100 000t/a
- Capital cost < $100/annual ton
- DRI delivered cost < 80% of HMS#1 scrap price
- No oxygen use
- No excessive environmental compliance cost

Manning & Fruehan (2001) state that due to increasing cost and environmental pressure on steelmaking operations worldwide, prospective plant builders are compelled to set additional requirements for new Iromaking processes. These are:

- Very high efficiency with respect to energy and materials usage.
- Greater flexibility in feed materials – use coal directly, use fine /lump ore and/or waste oxides without agglomeration.

- Reduced capital costs – process should be capable of being operated on a smaller unit scale without compromising efficiency.
- Operational flexibility – ideal process would be capable of operating at a range of production rates without compromising efficiency or economics.
- Capable of producing steel or low carbon iron directly.

To test the compliance of existing DRI processes to the requirements set, one specific process in each of the four classes of processes presently applied on industrial scale was analysed in detail. The analysis is indicated in tabular format (Table 4.1.1):

Requirement	**Units**	**Shaft**	**Rotary Kiln**	**Fluidised bed**	**Rotary Hearth**
Process	Name	HYL Mini-module	SLRN	Finmet	Fastmet
Production capacity	kt./a	200 - 2500	30 - 108	550	150 - 500
Capital cost	$/t/a	150 for 450kt/a (1) excluding gasification (2)	175 for 360kt/a brown field expansion (3)	220 for 500kt/a (4) excluding gasification	470 for 500kt/a (5)
Coal & hematite use	Yes/No	Hematite yes, coal with gasification	Yes	Hematite yes, coal with gasification	Yes
No oxygen required	Yes/No	Oxygen required for gasification	No	Oxygen required for gasification	No
Environ mental	Issues	None	Dolochar disposal	None	None
Disqualifying Cost issues	Yes/No	No	No	No	No
Qualify?	Yes/No	No	No	No	No

Table 4.1.1: Compliance of four DRI process classes to specific requirements set. Shaded cells indicate non-compliance. Sources: (1) Duarte et al 2002 (2) Visagie 1982 (3) Creamer 2007, (4) Smith 2001 (5) Midrex Technologies(1) 2009

The fact that natural gas is not readily available in South Africa made it an essential requirement that the process had to use coal. For this reason the traditional shaft- and fluidised bed based processes were

judged as not complying with the requirements, as the only way to use these processes would be to use a gasifier to gasify coal with oxygen and steam to generate the required reduction gas. It is reported by Visagie (1982) that this option nearly doubled the capital cost of a shaft based DRI plant investigated for erection at Vanderbijlpark. It would require the use of oxygen, also a disqualification. Both existing coal based process classes had a higher capital cost than the set capital cost limit and therefore were also judged as non-compliant to the requirements set.

Since none of the existing classes of processes conformed to the specific requirement, it was endeavoured to design a new process that would fit the requirements.

4.2 Conceptual design of the process

The design draws on the experience gained with the commissioning and operation of the first Corex process during 1986 to 1992 (Delport & Hollaschke 1990, Delport 1992). The design also takes cognisance of the strengths and weaknesses of existing DRI processes and attempts to obtain the best of all worlds.

Low capital cost was, after simplicity, regarded as the crucial attribute for the process, therefore fluidised bed and rotary hearth reactors were disregarded as the reactor selection as they were regarded as too expensive and complex. This left a shaft and a rotary kiln reactor as possible reactor choices. Analysing Rotary Kiln and Shaft based DRI processes for strengths and weaknesses yield the following table.

Reactor	**Strengths**	**Weaknesses**
Rotary Kiln	Utilises coal directly/ not affected by pressure drop limitations	Poor heat & mass exchanger / rotating vessel more complex than stationary shaft
Shaft	Excellent heat & mass exchanger	Cannot utilise coal directly/susceptible to pressure drop limitations

Table 4.2.1: Strengths and weaknesses of shafts and rotary kiln reactors

To design a new process, a wide range of factors influencing the design of the process had to selected. This included the particle size of the raw materials, since this in turn influenced the selection of the reactor vessel. Also selection of the oxidant influenced the process flow as will be seen in the next section. The following table indicates details of the design choices made for the design as well as the main reasons for making the selection.

Parameter	Selection	Comment
Iron oxide	Lump hematite	Capital cost tends to rise with the use of fine ore as either a pre- or post agglomeration step is generally required when fine ore is used.
Reductant	Lump Coal	Lump coal, i.e. peas, nuts or large nuts as a rule have lower ash content than the fine fraction, also called duff. Lump fractions are often the only fractions that are washed. Duff coal is rarely washed.
Oxidant	Air	Air is selected as oxidant since selecting oxygen would require the installation of an air separation plant, either by the operator or a supplier. Selecting air as oxidant, especially if ambient operating pressure is also selected, however disqualifies counter current shaft operation due to pressure drop
Vessel	Shaft	A stationary shaft is regarded as the lowest capital and maintenance cost vessel option
Operating pressure	Ambient	Although elevated pressure might increase the specific production rate, it invariably increases complexity and capital cost
Reduction gas generation	Internal	Gasification is performed internally in the reduction shaft similar to a rotary kiln process to keep capital costs low.

Table 4.2.2: Design preferences for the new DRI Process

Perhaps the most fundamental aspect of the process design is the selection of a shaft furnace as processing reactor, but to perform gasification inside the reactor. Various processing arrangements could be utilized to perform coal gasification. However, performing gasification with air internally in a shaft left only two choices, namely counter current and concurrent operation.

Counter current operation was abandoned due to three reasons

- In counter current flow, the coal charged with the iron ore is pre-heated by the hot gases. When the coal reaches a temperature of approximately 400ºC the coal starts to devolatilise. The volatiles, which contains amongst others, tars and pitches, are stable at these temperatures, and leave the reduction shaft with the top gas. Upon cooling they have a tendency to form accretions in pipes, and they also present an environmental problem that has to be managed.
- Air injected at the bottom of the reduction shaft where all or most of the carbon has been consumed and the ore has been reduced to a degree of 93% metallization, may re-oxidise the

formed DRI. This may be the reason why ancient indigenous smelting operations managed to produce a high FeO fluid slag at temperatures below 1250ºC in a simple counter current furnace blown with cold air (Friede et al 1982)

- Counter current reduction in a shaft with reduction gas generated by air gasification of coal would certainly lead to pressure drop complications in the shaft because of the high nitrogen content and therefore high reduction gas requirement.

To achieve the aim of low capital cost requirements, gasification with air in a vertical stratified downdraft gasifier in which the reduction is also accomplished, is employed. The gas generated by coal gasification therefore flows concurrently with the iron ore and coal.

However, whilst gasification with air already approximately doubles the volume of reduction gas required to affect the required reduction due to the dilution of the gas with nitrogen, concurrent flow, whilst circumventing pressure drop problems, increases the amount of reduction gas required even further. Concurrent flow requires that the $CO/(CO+CO_2)$ ratio of the exit gas to be not lower than the Wüstite/Iron equilibrium ratio at the gas temperature. This represents a waste if not utilised, or alternatively, an opportunity to reduce the coal rate if it can be utilised. Therefore a second shaft is envisaged in which this gas may be combusted with air to pre-heat the iron ore.

The process arrangement therefore consists of two shafts, a pre-heat shaft placed above a gasification/reduction shaft. Iron oxide is charged into the pre-heat shaft, pre-heated and lightly reduced using reduction gas from the reduction shaft flowing counter-currently with the burden. The iron oxide flows under gravity into the reduction shaft where a suitable reductant like coal is introduced together with some gasification air. Gasification occurs, forming CO and H_2 which performs the reduction, while the gas flows co-currently with the burden and both the DRI and reduction gas leave the reduction shaft at the lower end.

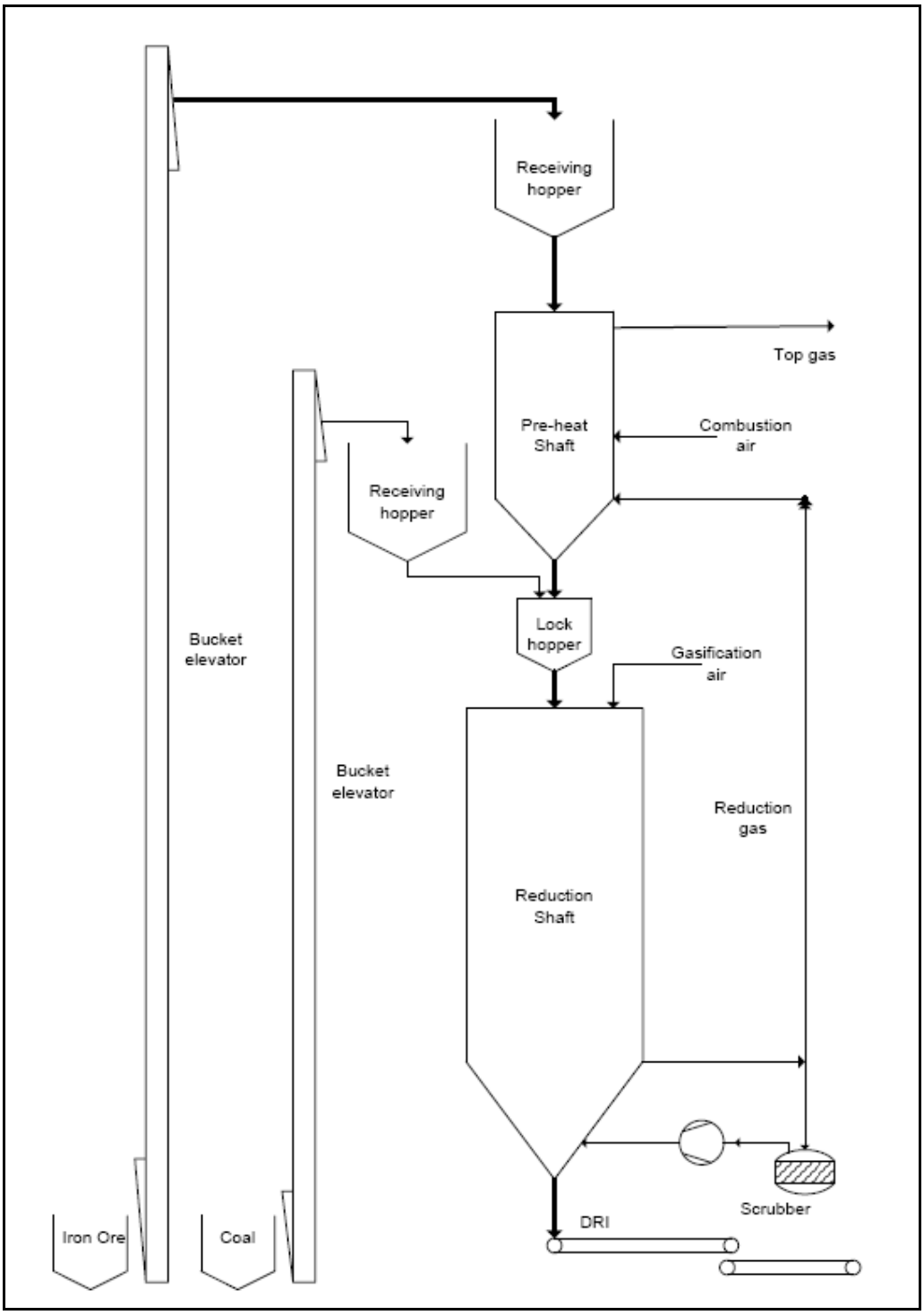

Figure 4.2.1: Schematic flow diagram of the conceptual process

4.3 Theoretical Verification of the Concept

Requirements for carbothermic reduction of hematite (Fe_2O_3)

To reduce iron oxide with either carbon or carbon monoxide two fundamental energy quantities need to be provided to the reaction system, i.e.

- The Enthalpy of formation of the iron oxide from its components, being iron and oxygen
- The sensible heat acquired by all the products of the reaction, i.e. the iron and the $CO/H_2/CO_2/H_2O$ as well as any unused char and any ash that might have been in the consumed reductant and any Nitrogen that may enter the reduction vessel.

There are two sources of this energy, namely

- The Enthalpy of formation of the product/s of reduction
- The Sensible heat that might be in the reagents

There are basically only two reaction systems for the carbothermic reduction of hematite, i.e. reduction with solid carbon or reduction with CO and/or H_2. For the purpose of this explanation only reduction with CO will be considered. (H^f_{298} figures from Peacy & Davenport 1979)

- Reduction with solid carbon

$Fe_2O_{3(s)} + 3C_{(s)} \Leftrightarrow 2Fe_{(s)} + 3CO_{(g)}$ $\quad H^f_{298} = 493\ 000$ kJ/kmole Fe2O3

- Reduction with CO

$Fe_2O_{3(s)} + 3CO_{(g)} \Leftrightarrow 2Fe_{(s)} + 3CO_{2(g)}$ $\quad H^f_{298} = -23\ 000$ kJ/kmole Fe2O3

The generation of the CO required for reduction may be performed outside of the reduction reactor like in the COREX/MIDREX set-up, or it may be generated inside the reduction reactor. When generated inside the reduction reactor, and concurrent flow is used, the $CO/(CO+CO_2)$ ratio of the outlet gas may not be lower than 0.67 at 850ºC. The reaction then is:

- Reduction with CO with internal gasification

$Fe_2O_{3(s)} + 9C_{(s)} + 4½O_{2(g)} \Leftrightarrow 2Fe_{(s)} + 3CO_{2(g)} + 6CO_{(g)}$ $\quad H^f_{298} = -1\ 022\ 000$ kJ/kmole Fe_2O_3

It must be noted that the H^f_{298} values are indicated at 298K and reduction processes typically take place at 850ºC. The sensible heat in the products of the reaction, i.e. 2 kmoles Fe and 3 kmoles CO, or 6 kmoles of CO and 3 kmoles of CO_2, have to be obtained from somewhere. Also, when the CO is obtained from

gasification of carbon with air, the sensible heat required to heat the N_2 associated with the oxygen to the reduction temperature, has to be accounted for also.

The enthalpy balance is shown in graphical form in Figure 4.3.1.

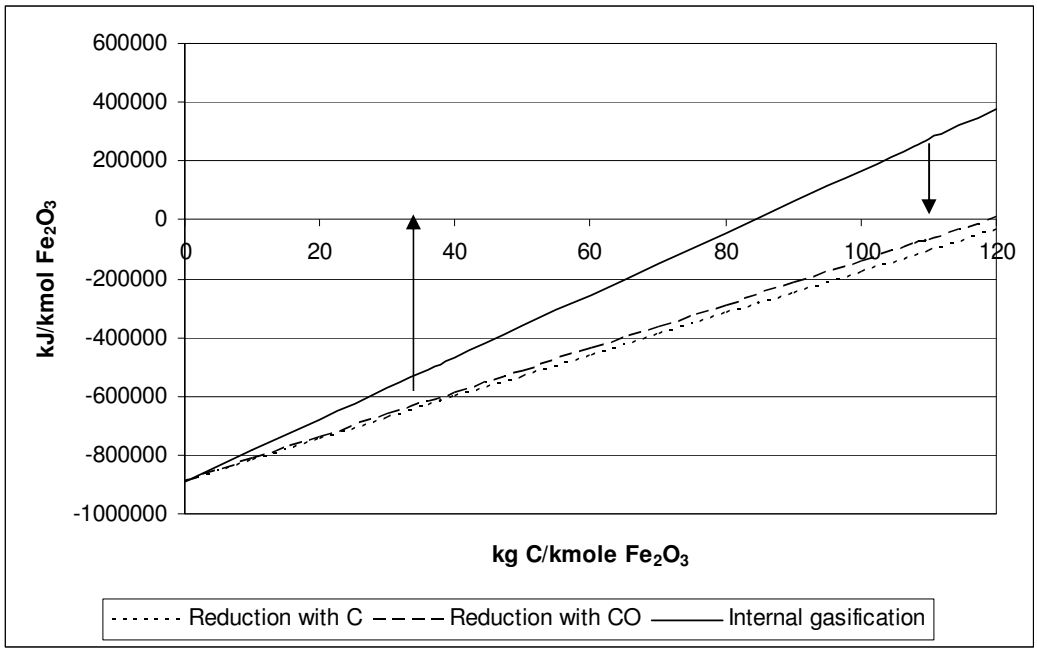

Figure 4.3.1: Enthalpy balance for different reaction schemes for the carbothermic reduction of hematite. The sensible heat in the N_2 associated with the required O_2 is also accounted for.

From the graph the following aspects are clear

- Reducing Fe_2O_3 with solid carbon requires only 3 kmoles or 36kg of Carbon per kmole Fe_2O_3, but requires a substantial energy input (1574 kWh/t Fe) from an external source, e.g. electric heating like in the Hiveld, Finesmelt or similar processes, or combustion of the formed CO and additional carbon like in rotary kilns

- Reducing Fe_2O_3 with CO at 850ºC generated outside of the reduction vessel in a concurrent arrangement, requires 981kg Carbon and 144kg O_2 per kmole of Fe_2O_3, but the reduction is exothermic and no additional energy input is required.

- However, when gasifying the carbon in the same reactor as where reduction takes place, the excess heat available from CO generation may be applied to fuel solid carbon reduction. Also the CO that is formed in the solid carbon reduction of Fe_2O_3 may further reduce Fe_2O_3, until the $CO/(CO+CO_2)$ ration reaches 0.67. It can be shown that only 0.8 moles of C needs to be gasified to CO to balance this reaction scheme. It can be shown that when reducing Fe_2O_3 with a

combination of solid carbon and CO, a substantially lower coal rate is required. Producing only 5.9 kmoles of CO by gasifying carbon with air, forming 0.8 kmoles of CO by solid carbon reduction and 2.2 of CO_2 by CO reduction of Fe_2O_3 yields a reaction system in enthalpy balance with a coal rate of 723 kg carbon per tonne Fe.

- By also using the export gas to pre-heat the iron ore and or the gasification air or oxygen, the coal rate may be reduced even further. Pre-heating only the ore reduces the coal rate to 559kg C per tonne of Fe.

Physical processes that have an influence on the process concept

Two physical processes limiting existing processes have been identified in Chapter 3. These are heat transfer and pressure drop.

- **Heat transfer**

It has been shown that heat transfer is the limiting factor in rotary kilns, but that heat transfer in packed beds is extremely efficient. Since the rate of heat transfer is dependent on shaft dimensions and material properties as well as specific flow rates and material properties, the rate of heat transfer needs to be confirmed in the final design.

- **Pressure drop**

The pressure drop across the shaft has been shown as limiting the volume of gas passing through the shaft. It has also been indicated that producing a reduction gas with air nearly doubles the volume of reduction gas required. However, due to the fact that the direction of flow is downward, the balance of forces is now extremely advantageous to material flow, i.e. all forces act in the same direction. The exact pressure drop across the shaft needs to be determined in order to specify the fan pumping the gas through the system.

4.4 Thermodynamic Simulation

4.4.1 FactSage Simulation

The computational thermo-chemistry Simulation software package FactSage, was used to simulate the conceptual process. When using a program like FactSage, the following has to be kept in mind:

- The software only simulates equilibrium conditions and does not consider physical or kinetic considerations
- Unlimited time to reach equilibrium is assumed
- The standard equilibrium calculation approach is that all reagents enter the process at the same temperature and all reaction products are at the same temperature after the reaction.

The simulation was performed in two stages, namely:

- Simulation of most basic reaction scheme
- Simulation of the effect of coal volatiles and ash on the reaction

Simulating the most basic reaction scheme

In the first simulation varying amounts of carbon is reacted with varying amounts of air in the presence of 1g of hematite. The amount of carbon and air is varied until 100% metallization of the iron is achieved. Reagents enter the process at 25ºC and zero heat loss is assumed. See Figure 4.4.1 and 4.4.2. Alpha indicates the amount of oxygen in grams.

The minimum amount of carbon required to metallise 1g hematite fully is determined to be 0.371g carbon per gram hematite or 530 kg C/t Fe. The temperature of the reaction products at this point is 652ºC and the $CO/(CO+CO_2)$ ratio of the gas computed to 0.58. This value is equal to the $CO/(CO+CO_2)$ ratio in equilibrium with FeO at this temperature as computed an indicated in Figure 3.1.3.

This most basic of simulations indicates that a high degree of reduction is thermodynamically possible when carbon is gasified with air in the presence of hematite in a concurrent reaction arrangement.

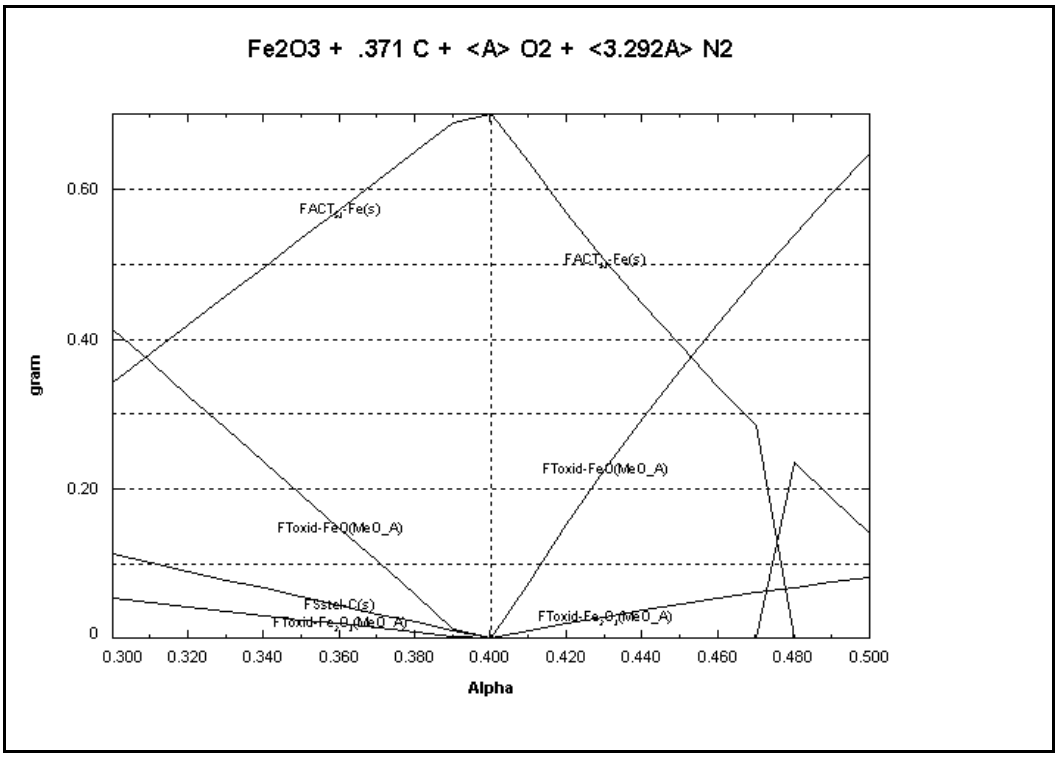

Figure 4.4.1: FactSage calculation of the effect of a varying amount of air on metallization

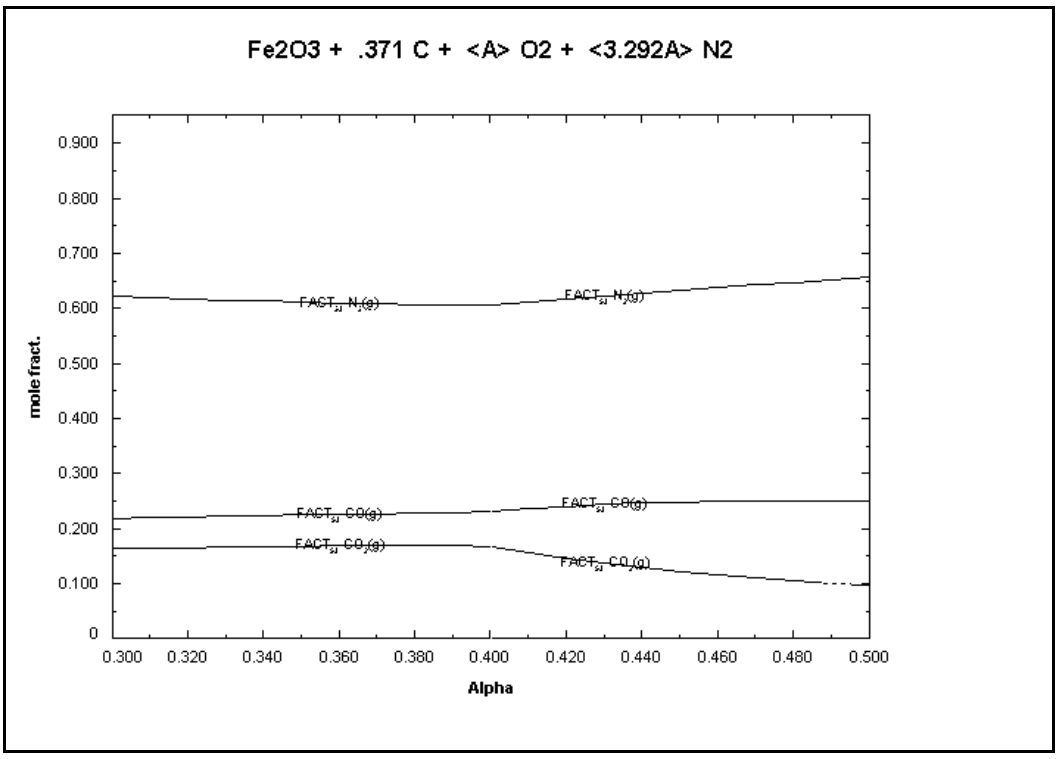

Figure 4.4.2: FactSage calculation of the effect of a varying amount of air on gas composition

Simulation of the effects of coal volatiles and ash

When coal is gasified in a downdraft gasifier the coal devolatilises when it is heated by radiation from the oxidation zone. See chapter 3 for a schematic diagram of a downdraft gasifier. These products of pyrolysis have to pass through the oxidation and gasification zones. This is an advantage since it prevents the condensation of tars from the outlet gas, and it gasifies the volatiles to produce more reduction gas. However, it is unclear what the effect of this might be on the reaction scheme.

To calculate the composition of the volatile matter that would arise when a typical South African coal used for direct reduction in rotary kilns is devolatilised, the analysis of Leeupan DR, (Anon(4) 2007) was entered in the model prepared by Mathesius et al (1987) to predict the composition of the volatile from coal during slow pyrolysis. See Appendix 2 for the calculation of the volatiles matter composition.

Coal was then entered into FactSage as a combination of the volatile matter and ash components to determine the effect of volatiles matter in the gasification of coal. Coke was entered as graphite and tars, being mostly combinations of aromatic rings, as Benzene (C_6H_6). Using this approach, 100g of coal was reacted with 180g hematite and varying amounts of air (indicated by Alpha on the figure). From the simulation it is clear that the process scheme envisaged is indeed thermodynamically feasible. The increase in coal rate to 794kg/t iron is expected because of the ash content of the coal.

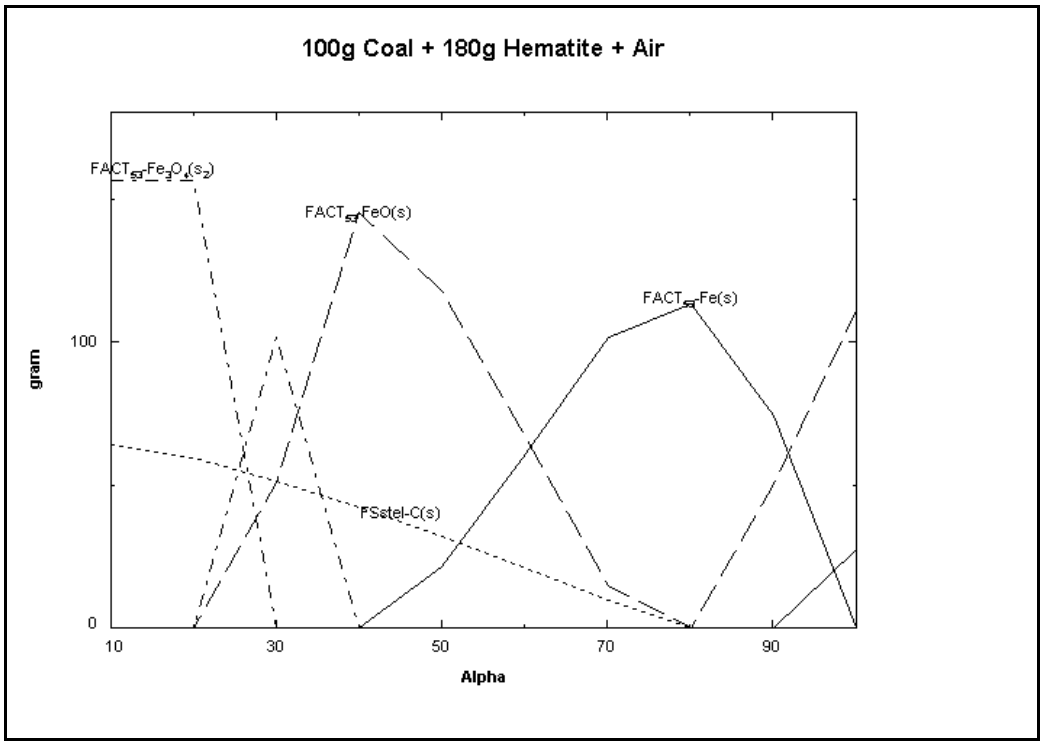

Figure 4.4.3: FactSage simulation: Effect of varying volumes of air on degree of reduction

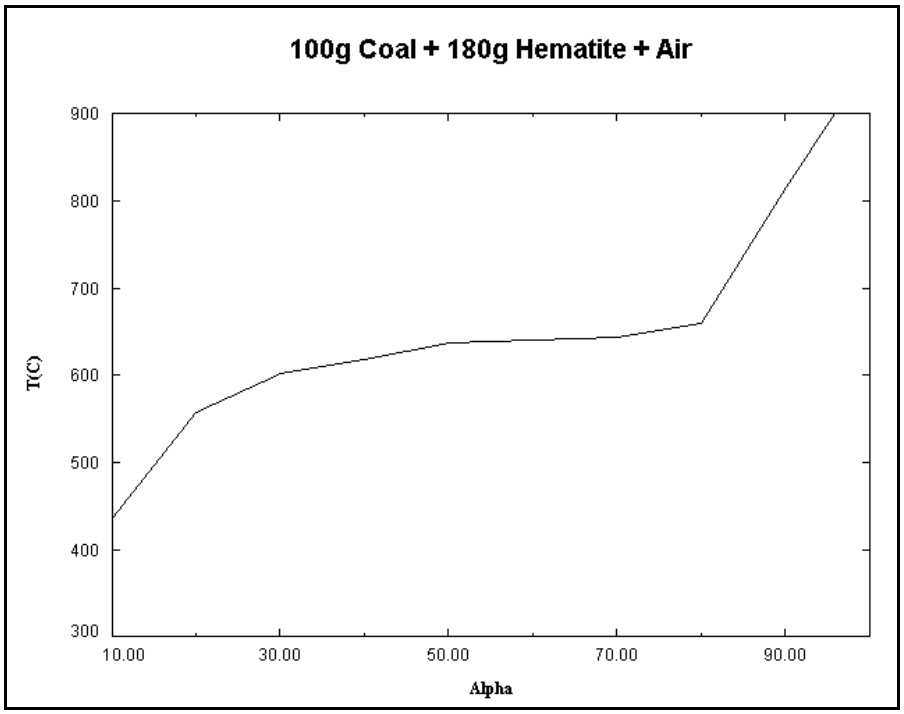

Figure 4.4.4: FactSage simulation: Effect of varying volumes of air on reaction temperature

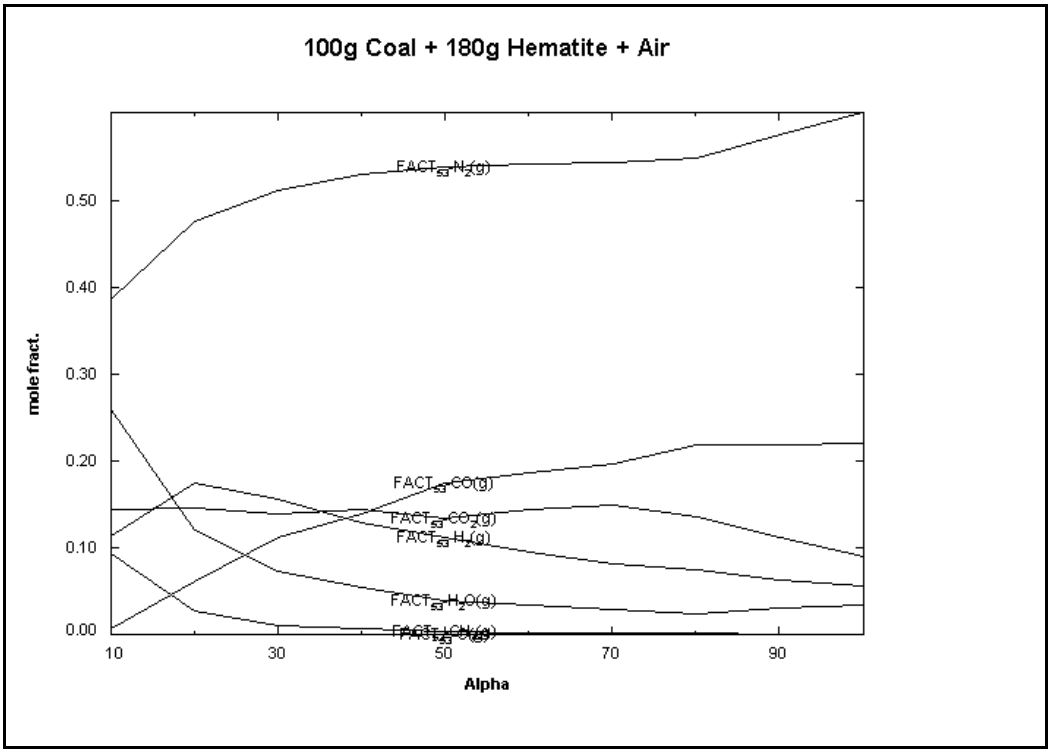

Figure 4.4.5: FactSage simulation: Effect of varying volumes of air on gas composition

4.4.2 Mass and Enthalpy Balance

To calculate raw material requirements and to test the effect of aspects such as pre-heat of raw materials, and the heat loss on the process, a mass and enthalpy balance was prepared for the process. (See Appendix 3). The mas and enthalpy balance assisted greatly with the design the pilot plant.

The calculation approach followed is the following:

- Independent variables include
    - Analyses of raw materials
    - The degree of metallization required
    - The production rate
    - Temperature of gasification air and feed ore
    - Reduction degree of the feed oxide
- Since it is known that the $(CO+H_2)/(CO+CO_2+H_2+H_2O)$ ratio may not be lower than the equilibrium value of this quotient with Wustite at the reduction shaft exit, this figure is used to calculate the volume of gasification air required to bring the gas analysis to this composition taking into account the mass of oxygen removed from the iron ore.
- Using the sensible heats of the incoming raw materials, the heats of reaction and the heat loss from the reduction shaft, an enthalphy balance is constructed for the reduction shaft. If the enthalpy demand is in balance with the enthalpy supply, the mass balance is finished. If not, the coal rate is varied to increase the enthalpy supply.
- Linked spreadsheets calculate heat transfer coefficient, heat loss, pressure drop and other important parameters

		Pre-heat Shaft					Reduction Shaft				
	Unit	Ore	Comb Gas	Comb Air	Top Gas	Oxide	Coal	Steam	Gas. Air	DRI	Red Gas
Moist	%	1.50					3.90				
B.D.	t/m3	2.55				2.55	0.65				
Fe	%	65.82				65.81	0.00			90.1 1	
SiO_2	% (in ash)	3.50				3.50	47.10			4.79	
Al_2O_3	% (in ash)	1.40				1.40	38.90			1.92	
CaO	% (in ash)	0.06				0.06	2.45			0.08	
MgO	% (in ash)	0.04				0.04	1.07			0.05	
Other	% (in ash)	0.90				0.90	10.27			1.23	
S	%	0.01				0.01	0.78			0.01	
Ash	%						12.40				
C	%						70.51				
H	%						3.40				
O	%	28.28		23.30		28.28	7.40		23.30	1.81	
N	%			76.70			1.61		76.70		
CO	Vol %		26.5		0.0						26.5
CO_2	Vol %		13.1		23.8						13.1
H_2	Vol %		8.6		0.0						8.6
H_2O	Vol %		4.3		7.8			100.0 0			4.3
N_2	Vol %		47.5		68.4						47.5
Mr	kg/m3		27.4		31.0			18	28.84		27.4
Kmoles	Kmoles(O_2)		**8.29**	1.46	13.8	8.07	21.59	0.00	5.30	8.07	42.32
	Kmoles std			6.9		0.050	0.13		25.25	0.05	0.26
Mass	Rate (t/h)	0.68	0.23	0.20	0.43	0.68	**0.29**	**0.00**	0.73	**0.50**	1.160
Vol	Vol (Nm3/h)		186	155	309			0.0	566		948
Temp	Temp (℃)	25	35	25	200	1200	25		25	850	850

Table 4.4.1 Mass balance for DRI Process

4.5 Laboratory Tests

In order to determine what the minimum retention time is that the iron ore particles have to spend in the reduction zone of the process to produce DRI of an acceptable quality, it was necessary that the reduction rate of the intended iron ore with CO was known. Pertinent information was found in literature, e.g. the thermogravimetric analysis work done by Theron (1985) on Sishen hematite. However, the work had to be verified and the range extended.

Thermogravimetric analysis (TGA) may be described as a testing technique in which the mass of a sample is observed continuously during the course of a reaction. Factors which may influence the rate or extent of the reaction may be kept constant or varied either continuously or in a pre-determined program during the course of the analysis. The extent of the reaction may be determined by analysis before and after the test, or, if the analysis of the sample and the nature of the reaction are known, the mass difference may be used as the indicator, as done by Theron.

4.5.1 Apparatus

To perform TGA work on the reduction of Sishen iron ore an experimental set-up had to be created since none was available ready made. A TGA experimental set-up capable of accepting samples of up to 10g in mass typically consists of a tube furnace, a chemical balance, a support rod supporting the crucible on the pan of the chemical balance whilst holding it in place in the temperature controlled region of the tube furnace, and a gas mixing and metering set-up. It is crucial that neither the crucible nor the supporting rod arrangement touch the furnace in any way, or that the gas flowing past the sample does not influence the mass measurement in any way.

The tube furnace used in this set-up was a Carbolite STF1500 tube furnace of which the temperature controlled region was 700mm from the bottom of the furnace tube. To insert the sample into this region of the furnace, the support rod had to be at least 700mm long and the chemical balance had to able to be moved up by at least the same distance.

Most TGA arrangements keep the tube furnace stationary while moving the chemical balance up and down. Chemical balances are sensitive devices that require careful leveling when placed in a new position. In order to avoid anticipated problems with leveling of the chemical balance when moving the balance up or down, it was decided to rather move the tube furnace up or down. The furnace was mounted in a steel frame which in turn was mounted on to a hydraulic pallet lifter. By setting up the arrangement in a perfectly vertical position and by using the hydraulic lifting arrangement of the pallet lifter the furnace could be lowered over the sample without affecting the arrangement of chemical balance.

To be able to pass a controlled volume of gas over the sample whilst still ensuring that no interference exist between any part of the sample support arrangement and the furnace, it is required that the chemical balance be included in the gas system. Including the chemical balance into the gas tight circuit requires that effective seals be devised to avoid leaking of the gas, especially if reduction of iron ore with CO is being studied.

Two water seals were devised, one which seals the contact area between the Perspex box covering the chemical balance and the base, and one which seals the top of the Perspex box with the furnace tube.

To facilitate the use of a water seal between the furnace tube and the top of the perspex box, and to allow for the introduction of the reaction gas, an aluminium gas inlet manifold was attached to the bottom of the furnace tube. The seal between the manifold and the furnace tube, consists of two flanges, one with a diameter slightly larger and one with a diameter slightly smaller than the furnace tube. The flanges are chamfered to accept an o-ring between them which was compressed slightly to seal on the furnace tube.

A complete description of the experimental arrangement is provided in Appendix 4.. Figure 4.5.1 is a schematic drawing of the TGA arrangement indicating salient features

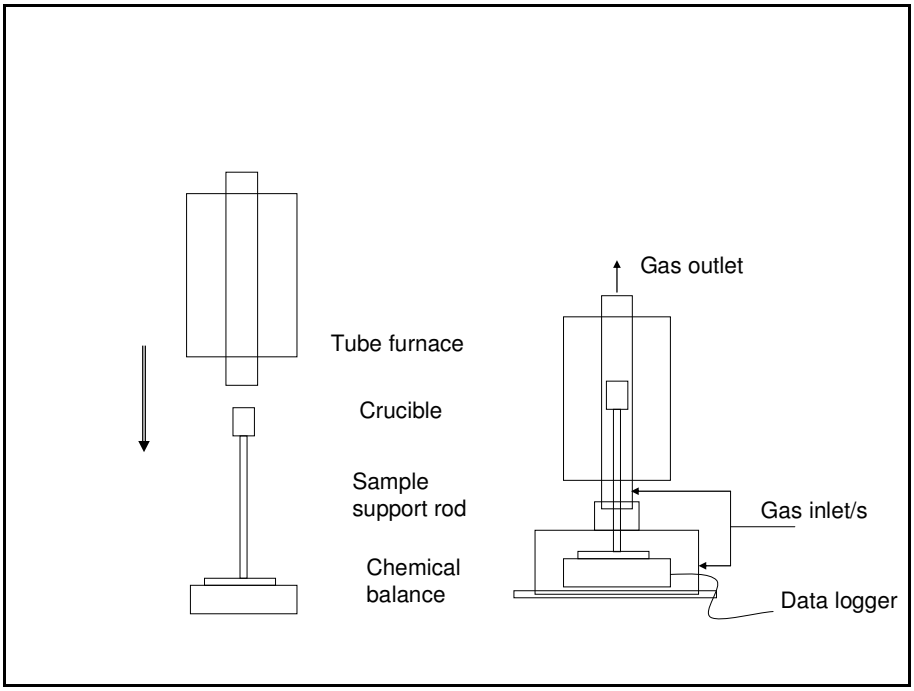

Figure 4.5.1: Schematic drawing of TGA apparatus indicating lowering of the furnace over the sample, and creation of the gas tight system

4.5.2 Experimental methods

Calibration of Apparatus

Determination of furnace temperature profile

To determine exactly where in the furnace the sample should be located, a calibrated thermocouple was inserted at various depths in the furnace whilst the furnace temperature was being maintained at a constant temperature. The following graph is an indication of the furnace temperature profile.

Calibration of rotameter

The rotameter was calibrated by determining the time it took a soap bubble to travel between the 0 and 100ml marks in a glass tube

Calibration of RS232 Data Logger

The Eltima RS232 data logger was used to log the scale reading. However, the chemical balance used, a Sartorius 214S could not be programmed to print the scale reading at predetermined intervals, but printed continuously at a programmed baud rate. The baud rate was set to the lowest selectable and the number of data points logged was therefore a function of the connectivity between the chemical balance and the personal computer. Figure 4.5.2 indicates the number of data points logged per unit time. From the graph it is clear that after an initial burst of 16.43 data points, the rate of logging is constant at 2.497 data points per second.

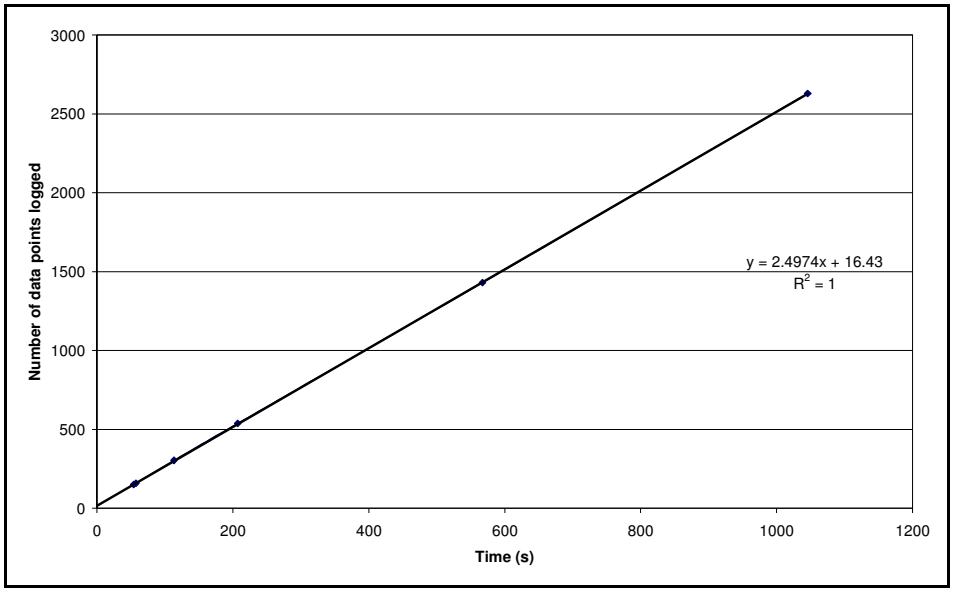

Figure 4.5.2: Number of data points logged versus time

Test procedure

An iron ore specimen was selected by hand from a sample of dried -12.5+10mm Sishen ore. The aim was to obtain a particle of approximate spherical shape with a mass of approximately 5g. The sample was weighed accurately and placed into the crucible held up by the support rod and chemical balance. The furnace was lowered over the sample and purging with argon started. During initial purging gas was introduced into the scale enclosure and into the manifold. After a purging period of approximately 5 minutes the gas inlet into the scale enclosure was closed and argon was introduced into the manifold only. After another purging period the Argon was closed and the CO introduced. A CO flow of 5.5l/min was used. The CO at the outlet of the furnace tube ignited spontaneously within 2 to 3 minutes and burned in a stable blue flame flame for the duration of the test.

The scale reading was logged continuously on a personal computer using a RS232 to USB data interface and data logging software. After the intended time for the test had elapsed, or the mass loss became very small, the CO was closed and argon introduced. As soon as the CO flame had died down, the top of the furnace tube was closed with rockwool to counter the chimney effect and the furnace raised to a position previously determined to position the crucible directly opposite to the gas inlet in the manifold. The sample was kept in this position for some 10 minutes, determined to be the time required to cool the sample down to approximately 100ºC, after which the furnace was raised completely, the sample removed and cooled down further under argon until it could be weighed finally.

Calculation method

Scale drift was experienced and had to be accounted for. This was done by weighing the ore particle before and after the reduction test, and subtracting the mass loss greater than the determined mass loss evenly over the time of the experiment. The reduction degree was calculated by expressing the corrected mass loss as a fraction of the maximum possible mass loss, which in turn was calculated from the bulk analysis of the iron ore.

Species	**Mass %**	**Species before reduction**	**Oxygen associated with this specie (g)**	**Specie after reduction**	**Oxygen lost (g)**
Fe	66.15	Fe_2O_3	28.43	Fe	28.43
SiO_2	2.97	SiO_2	Included	SiO_2	0
Al_2O_3	0.95	Al_2O_3	Included	Al_2O_3	0
K_2O	0.13	K_2O	Included	K	
P	0.053	Apatite		P	
S	0.016	FeS		S	
Sum	70.27		98.7		28.43
Other	29.73	CaO, MgO	1.3	CaO, MgO	0

Table 4.5.1 Calculation of maximum possible mass loss

At least 2 TGA experiments were conducted on each temperature. Where results differed too much, another experiment was performed on the same temperature.

4.5.3 Results of Reaction rate experiments

The fractional reduction, R, defined as the mass of oxygen removed expressed as a fraction of the total oxygen associated with hematite in the ore, as an indication of the progress of the reduction reaction, was calculated and plotted against the time over the course of the reaction. Selected examples of these progression trends are shown in Figure 4.5.3.

The following observations were made. These observations are very similar to that made by Theron (1985).

- Two types of iron ore particles were distinguishable. One type with a layered structure and another with a dense type structure. The reduction behavior of these two types differed appreciably. Particles with the same observable type of structure also showed some difference in their reduction behavior.

- Although spherical particles were sought, it was not always possible to find exactly spherical particles and particles as close to spherical were then selected. It is known from work done by Kang et al (1998) that particle shape does affect reduction rate. It is not clear what the magnitude of influence of shape was on the reduction rate determined in this work.

- The rate of reduction of hematite with CO is characterized by a larger than expected standard deviation. Theron does not report the exact standard deviation for CO reduction, but he reports the standard deviation for H_2 reduction. The standard deviation was 1.2 minutes on a mean time for 50% reduction at 900ºC of 11.4 minutes. On a second batch of iron ore the average time required for 50% reduction had reduced by 22% to 8.9minutes and the standard deviation had increased to 1.7 minutes.

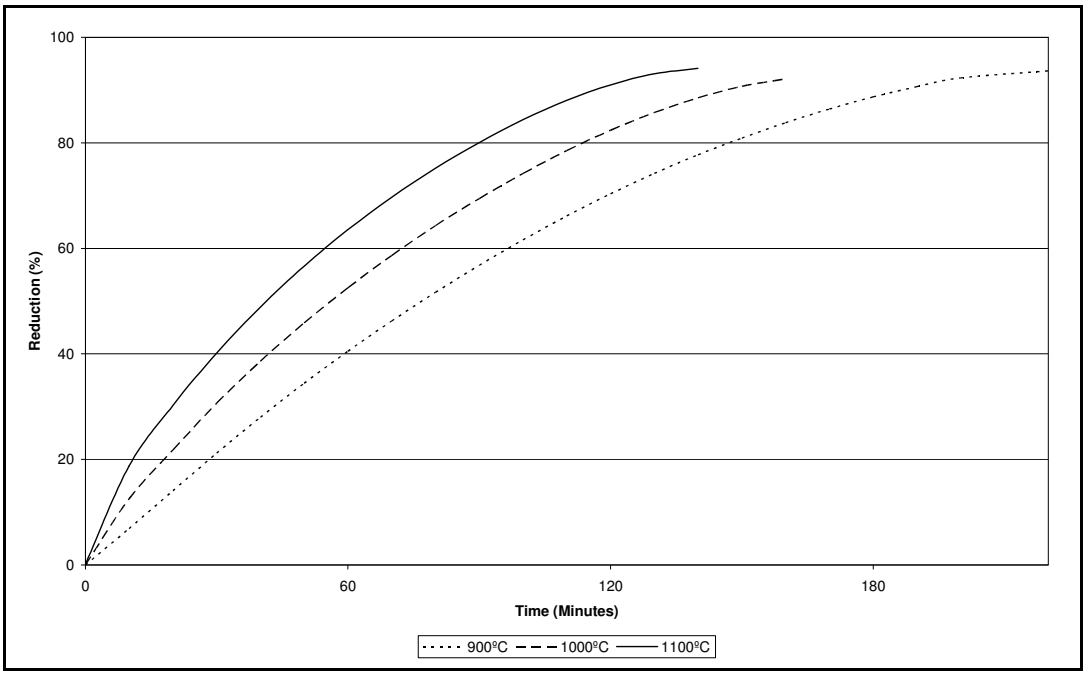

Figure 4.5.3: TGA analysis of CO reduction of Sishen Iron ore

The results of the thermogravimetric experiments indicate that at least 3 hours retention time is required to reduce a -12 + 10mm hematite particle to 93% metallization using 100% CO at 900ºC. From this result it was decided to use a retention of 4 hours in the pilot plant design due to the following reasons

- The shaft temperature may not be above 900ºC in all areas
- The reduction gas will not consist of 100% CO and/or H_2, but will in all probability contain some CO_2 and/or H_2O.

4.6 Pilot Plant Design, Construction and Testing

4.6.1 Background

To test the principle of the process it was decided to design & construct an extremely small and simple pilot plant with the sole aim of proving the principle, i.e. that a high metallization could be achieved using the process as proposed.

The advantage of using a small sized plant included the fact that construction cost and time would be kept to a minimum whilst raw materials requirements would also be kept low. It was understood that there were also various disadvantages to constructing such a small pilot plant, but the view at the time was that the advantages inherent in such a pilot plant outweigh the disadvantages. Disadvantages foreseen included an extremely high specific heat loss and possible problems associated with using full sized raw materials in a small diameter plant, which could include bridging.

It was recognised that such a small plant would not be suitable for determining production rate and consumption figures, however, the rationale adopted was that if the principle could be proven, a larger pilot plant would be constructed in which production rates and consumption figures could be determined. The cost of constructing a pilot which would become redundant once testing is completed could however prevent such a venture.

EAF based steel mills generate between 25 and 50kg of EAF dust per ton of steel produced. This dust could contain as much as 29% zinc and 3% lead in oxide form depending on scrap characteristics. The balance is mostly hematite, silica and lime. (Tateishi et al 2008), Recycling of the EAF dust not only obviates the need to dispose of the EAF dust in a landfill at cost, but presents and opportunity at generating income if it can be recycled and the zinc, lead and iron recovered.

It was recognised that due to the concurrent process flow, the process could be used to recycle pelletised EAF dust. The intention therefore was to design the larger pilot plant to serve as a EAF dust recycling plant once testing regarding DRI production was completed. Pelletized EAF dust was therefore also tested in both TGA tests and pilot plant runs. The results of those tests is however deemed to fall outside the scope of this report.

4.6.2 Pilot Plant flow scheme and production volume

The flow scheme of the process was simplified to include only the gasification/reduction reactor. This had the limitation that the effect of pre-heat of the oxide on metallization would not be able to be tested, but the limitation was regarded as acceptable because of the simplification it meant with regard to

construction. The piping and instrumentation diagram of the pilot plant as constructed is indicated in Figure 4.6.1

To decide on the dimensions of the shaft, diameters of Midrex and HYL reduction shafts were located in literature. (Midrex Technologies(1) 2009, Energiron 2009). A remarkable degree of agreement was found. Since Midrex indicated both low and high production rates for a specific diameter shaft, it was decided to model the diameter on the average production rate as indicated by the Midrex range of production volumes. See Figure 4.6.2. Using the correlation obtained the diameter of the shaft was determined to be 150mm which then meant the height had to be 500 mm.

The pilot plant consisted of a single shaft and a simplified gas and water treatment system. The design production rate was 50 kg DRI/d or 2.1 kg DRI/h. With a calculated coal rate of 500kg coal/t DRI and a retention time of 4 hrs, the volume of the active part of the shaft calculated to be 8 liters.

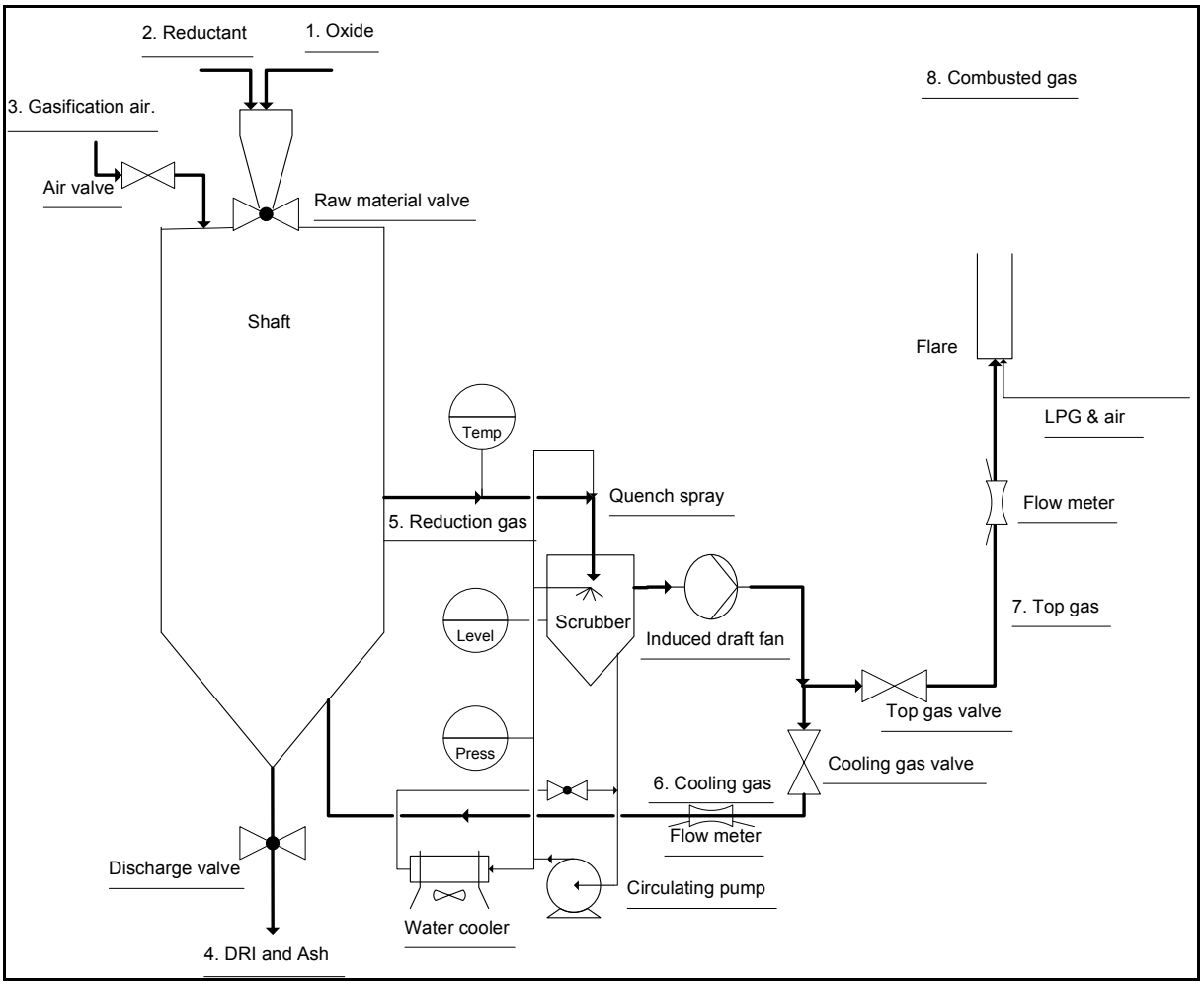

Figure 4.6.1: Pilot Plant Piping & Instrumentation diagram

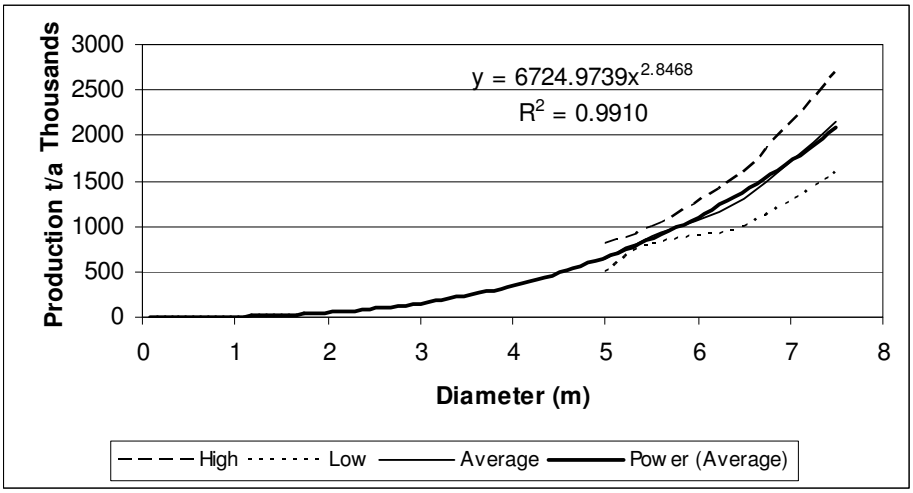

Figure 4.6.2: Midrex shaft Production vs. Diameter

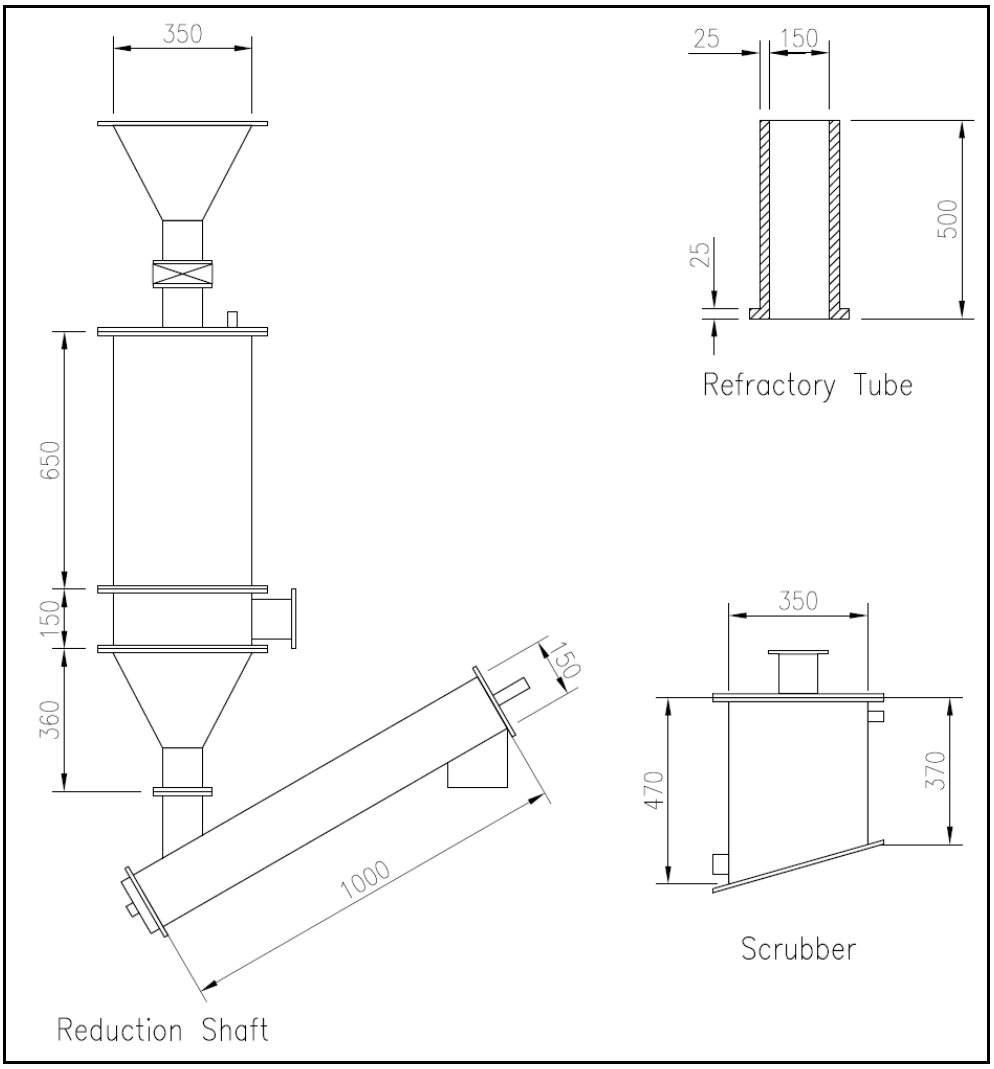

Figure 4.6.3. Dimensions of Pilot Plant Vessels

4.6.3 Raw Materials

It was decided to use raw materials available in the market and as far as reasonably possible use the raw in the format they are available in the market. This entailed using iron ore and coal in the size fraction -25 + 10mm.

- Iron ore

A sample of iron ore together with a bulk analysis of the sample was obtained from Kumba Resources Saldanha. The sample mass was approximately 60 kg. The ore was dried, crushed and screened in the fraction -19 + 8mm.

Component	**Mass %**
Fe	66.15
SiO_2	2.97
Al_2O_3	.95
K_2O	.13
P	.053
S	.016
+20mm	7.9
-8mm	2.5

Table 4.6.1: Chemical analysis of Sishen Iron Ore (Bed no BO449LC)

- Carbonaceous material

Four types of carbonaceous materials were tested, namely charcoal, bituminous coal, anthracite and crushed electrode. All were obtained from the general trade. The proximate analyses of the carbonaceous materials are indicated in the table.

Component	**Charcoal**	**Coal**	**Anthracite**	**Crushed electrode**
Name	Braaimeester	Inyanda peas	Dixon peas	Ucar
Moisture	<1	2.5	1.0	0
Ash	1 – 15	14.7	14.1	1%
Volatiles	25 – 30	23.8	8.7	0
C-fix	55 – 72	59.0	76.2	99
Source of analysis	Reed & Das 1998	Supplier	DME 2009	Supplier

Table 4.6.2: Proximate analysis of carbonaceous raw materials

4.6.4 Pilot plant design

The pilot plant as depicted in the figure was designed, fabricated and constructed using materials available in the general trade in a three month period. Salient features of the pilot plant include

Aspect	Specific	Comment
Production rate	2.1kg DRI/h	50kg/d was deemed to be a practical size in terms of raw material requirements
Coal rate	500kg/t/DRI	Depends on the coal analysis
Ore retention time	4hrs	4hrs is seen as the minimum retention time to ensure 93% metallization
Gas flow rate	12Nm3/h	
Pressure	Atmospheric	
Max reaction temp	1200ºC	
DRI discharge temp	100ºC	
Gas outlet temp	850ºC	

Table 4.6.3 Pilot plant salient design features

Vessel	Dimensions	Manufacturer
Shaft	350mm diameter x 650mm high 6mm Mild steel flanged	J&A Engineering
Bustle section	350mm diameter x 150mm high 6mm Mild steel flanged	J&A Engineering
Cooling cone	350diameter x 100mm outlet x 350mm high 6mm Mild steel flanged	J&A Engineering
DRI screw	Shell: 150 diameter x 1000mm long Screw: Inlet 100mm round Outlet 140mm square Shell 3mm mild steel, Screw 3mm 304SS	J&A Engineering
Scrubber	350mm diameter x 360/420mm high, 6mm Mild steel flanged Inlet 100mm, Outlet 50mm Packing material: 100mm SS pot scourers	J&A Engineering
Flare	100mm diameter x 1.2m high open ended Gas inlet 200mm from bottom Pilot flame 200mm from bottom	Trade

Table 4.6.4: Pilot plant vessel details

Refractory item	Description	Supplier
Shaft working lining	140mmID x 25mm thick x 500mm high loose liner Verocrete 1400 castable K = 1.1W/mK @ 1000ºC	Cape Refractories
Insulation layer	2 x 25mm layers Thermablanket	

Table 4.6.5: Pilot Plant Refractory materials details

Equipment	**Detail**	**Manufacturer**
Induced draft fan	Single stage centrifugal fan 750mm H_2O max p Motor 1800W	Kirby Model: Heritage II
Process water pump	Single stage centrifugal Motor: 0.37kW 2850rpm Flow 0.6 - 2,4m^3/h Head 32 - 9m water	Flomax Model: KF/1
Water to air heat exchanger	Finned tube heat exchanger 300mm wide x 450mm high 26 tubes 15mm x 2mm	
Air fan	Axial fan Blades 5 Diam 250mm	

Table 4.6.6: Pilot plant process equipment details

Valves & Instrumentation	**Detail**	**Manufacturer**
Material charging valve	100 butterfly Disk CF8, Seat NRD	Natco Tozen
Gasification air valve	DN25 Ball	Boston
Top gas flow control valve	32mm manual ball PP	EFFAST
Cooling gas flow control valve	32mm manual ball PP	EFFAST
Top gas Flow meter	Sharp edged orifice Φ12.5mm	
Cooling gas flowmeter	Sharp edged orifice Φ10mm	
Thermocouple	Chromel-Alumel 3mm SS sheath	Unitemp
Piping	32mm pp	

Table 4.6.7: Pilot plant valves and instrumentation details

- **Design of DRI screw**

Common guidelines for screw conveyor design generally suggest that the screw diameter be at least 4 x the maximum particle diameter and that the gap between the flight and the shell be at least 2 x the maximum particle diameter.(OCW 2009) Further design guidelines suggest that the pitch of the screw be the same as the diameter of the screw. Since the top size of the iron ore is approximately 20mm, the resultant screw conveyor has a discharge rate far in excess of the pilot plant production rate.

The implication of this was that for continuous operation a reduction gearbox of excessively large reduction ratio would be required which in turn put the price of such a device outside of what was

deemed affordable for the project. It was decided therefore that the screw conveyor would be operated by rotating it by hand through a predetermined rotation angle at predetermined times.

4.6.5 Pilot Plant operational Methods

4.6.5.1 Cold tests

A number of calibration tests were conducted before the plant was commissioned

Calibration

- Screw conveyor discharge rate calibration

The screw feeder was operated with material of a similar screen size analysis as the expected DRI screen size analysis to determine the volumetric discharge rate. Three tests of 10 revolutions were performed and the volume of the discharged materials measured. A volumetric discharge rate of 0.6 l/revolution was determined.

This meant that for a production rate of 2.1kg DRI/hr which has a bulk density of 2kg DRI/l, the screw feeder had to be rotated through 630º per hour, or 90º every 7 minutes.

- Flow meter calibration

The orifice flow meter was designed according to the design procedure set out in Perry & Chilton (1973). (See Appendix 3). Differential pressure was determined by a u-tube filled with water. The flow meter accuracy was checked by using a Silva propeller type anemometer to determine the maximum velocity inside the stack. From the correlation given by Perry & Chilton (1973), the average velocity was calculated and from this the flow inside the stack determined. This flow was correlated with the flow measured inside the top gas line. Good correlation was found.

- Quench and packing wetting sprays supply pressure calibration

The supply pressure of both the reduction gas quench spray as well as the packing wetting sprays were set by operating the pump with an opened scrubber, and visually selecting a pressure that yielded satisfactory spray patterns for both the sprays by varying the supply pressure by adjusting the cooling circuit flow control valve. The pump supply pressure was noted and in subsequent tests the system pressure was adjusted to this value previously determined to provide satisfactory spray patterns on both spray systems.

Commissioning of the plant

After construction and calibration of specific pieces of equipment, the plant was cold commissioned by operating all the subsystems of the plant individually, including the water system, gas treatment system and materials discharge system. Adjustments were made and most favourable operational regimes detected and noted. Once the subsystems were functioning acceptably, hot trials commenced.

The first number of hot trials were used to commission and detect and correct any design problems on the plant.

4.7 Pilot plant operation

The testing procedure used in all pilot plant tests is as follows

Plant preparations included the following

- System pressure test

  The system was pressure tested by removing the interconnecting pipe between the scrubber outlet and the induced draft fan inlet and plugging the scrubber outlet with a rubber plug. All inlet valves, (raw material valve, air valve) and all outlet valves (top gas flow control valve, DRI discharge valve) were closed, the cooling gas valve was opened fully after which the induced draft fan was operated to pressurise the system. The system was checked for leaks with soapy water. If leaks were found, they were repaired.

- Water system filling, testing

  The scrubber was equipped with a level indicator consisting of a length of transparent pipe fitted between two elbows inserted through the scrubber wall, one low down and one above the highest possible water level. The required level was marked on the transparent pipe to coincide with a level 25mm below the opening of the scrubber inlet pipe.

  The scrubber was filled with water by connecting an external water source to the circulating pump discharge line and filling the scrubber up to a level somewhat above the required level to compensate for a decrease in the level due to the filling of the pipe system.

Start-up

Start-up followed a typical procedure including

- System check
- Safety check

- Start of water system

The start-up and operation procedure was developed by trial and error. The procedure was as follows

- Fill the reactor vessel with raw material
    a. Fill the bottom cone with suitable filler material
    b. Fill the shaft with low volatile material, i.e. charcoal or electrode coke
- Add high reactivity combustible material on top
- Ignite an ignition source externally and place on top of the bed
- Start the ID fan
- Adjust the top gas flow to the required flow
- When the level has dropped to a suitable level add the intended fuel
- Inspect the fire zone
- When the bustle temperature has reached the threshold level (200ºC) start adding the prepared reaction blend
- Rotate the DRI screw the required revolutions at the required times
- Maintain the level by adding reaction blend
- Note the required parameters

Hot Testing

Main testing commenced after hot commissioning of the plant was completed. The operation of the plant was found to be extremely straightforward. After filling the bottom hopper with a suitable material, the lower portion of the shaft was filled with a low volatile material. An externally ignited ignition source (fire lighter) was the placed on top of the burden and the induced draft fan started. Once the flame front had developed, it was only necessary to rotate the DRI screw at the predetermined times and keep the shaft filled.

Table 4.7.1 presents a list of all pilot plant experiments executed during the course of the work. A number of trials ended pre-maturely due to a particular problem, which included apparatus or procedural problems, process related problems or exogenous factors. Of the 23 trials executed, 15 were regarded as successful in terms of running for the planned duration of the test.

Tests were generally ended after the required time, calculated for the first DRI to pass through the reduction zone, had elapsed.

Trial	Date	Carbon	Oxide	Coal rate	Dur	Bustle Temp	Blow rate	Reason for stoppage
				kg/t ore	Mins	°C	Nm³/h	
1	12 Jun	Charcoal	None	3000	5			CO leakage
2	19 Jun	Charcoal	None	3000	5			CO leakage
3	22 Jul	Charcoal	Pellets	3000	150	350		Water too hot, flare problems
4	28 Jul	Charcoal	Pellets	3000	40	100		Export gas pipes overheated
5	29 Jul	Charcoal	Pellets/ore	3000	180	350		Cooling gas inlets hot
6	4 Aug	Charcoal	Pellets/ore	3000	5			Gas leakage cooling cone ports
7	6 Aug	Anthracite	Pellets/ore	3000	180	300		Flange on screw conveyor hot
8	18 Aug	Anthracite	Sishen	1500	300	380		Fused layer
9	1 Sept	Coal	Sishen	1200	170	440	17.5	Bridge formed
10	3 Sept	Coal	Sishen	700	290	410	17.5	Bridge formed & cone hot
11	12 Sept	Coal	Sishen	700	335	340	7.8	Normal stop
12	17 Sept	Coal	Sishen	700	235	240	7.6	Bridge formed
13	9 Oct	Coal	Pellets	1250	365	280	7.6	Normal stop
14	15 Oct	Charcoal	None	3000	60	106		Normal stop
15	21 Oct	Coal	Pellets	1350	120	372	17.5	Fan clogged up
16	23 Oct	Charcoal	Pellets	750	250	326	10.5	Orifice clogged
17	25 Nov	Charcoal	Pellets		5			ID Fan leaks
18	26 Nov	Charcoal	Pellets	833	250	356		Normal stop
19	5 Feb	Electrodes	Sishen	750	265	340	10.32	Ore bridges, bed falls 3hrs RT
20	27 Mar	Electrodes	Sishen	1400	240	185	12	Normal stop
21	6 May	Electrodes	Sishen	1400	240	160	12	Normal stop
22	1 Oct	Coal	Sishen	1500	180	275	12	Fan blocks with volatiles
23	15 Oct	Electrodes	Sishen	2000	240	424	14.4	Normal stop

Table 4.7.1: Chronological list of all pilot plant experiments

The success or otherwise of the trail was instantly apparent upon visual inspection of the internal structure of the cut samples. The results were evaluated after each test and possible reasons for not achieving the reduction degree considered, after which a new test was planned. In many instances repairs or alterations had to be affected to the plant before a subsequent test could be performed.

Special Testing

When specific measurements were required, e.g. burden temperature measurements or gas temperature and analysis, they were planned beforehand, and the equipment required to execute it e.g. thermocpouples, gas sample holders etc, obtained and prepared. The tests were executed at appropriate times during the trial according to the procedures planned.

Shut-down

After testing various shut-down procedures it was found that by far the most simple and effective procedure was to bank the furnace, i.e. shut all openings to and from the reactor, and leave the plant

overnight. After 18 hours the plant and contents had cooled down to such an extent that the product could be removed without fear of re-oxidation, and analysed.

Burden removal

Burden removal consisted quite simply of rotating the DRI screw so as to remove all contents of the shaft. In one case was it necessary to remove accretions to the sides of the gasifier with forcible means due to fayalite formation.

Problems encountered

A number of problems were encountered during the test work. The problems may be grouped into those relating to equipment inadequacy, and those relating to process deficiencies. Two equipment related problems that warrant description include air ingress in the low pressure section of the plant and the difficulties with containment of the produced CO.

- Air ingress

  Air ingress resulted in damage to the top gas piping during one test as combustion occurred in the piping resulting to overheating. It was established that the DRI screw outlet was the main source of air ingress and an additional DRI screw outlet flap was manufactured and installed to prevent air ingress from this opening.

- Containment of CO

  Containment of CO in the general vicinity of the pilot plant to below 25ppm, the safe TWA exposure limit, presented a challenge. Sources of CO included

  - Leaks in the elevated pressure part of the process, i.e. induced draft fan, piping, valves and orifice flow meter. Careful pressure testing of the plant assisted in finding smaller leaks in the piping, so that they could be sealed. Sealing of the fan shaft and valve spindles proved difficult, and could only be solved by selecting equipment with adequate design.
  - Incomplete combustion of the top gas in the flare proved to be most challenging. Experimentation with different flare arrangements including the size and location of the pilot flame resulted in an effective combustion system of the produced top gas, which resolved the problems.

Problems of a process nature that warrant mentioning include

- Volatiles

It was found that when the shaft is filled initially with carbonaceous material containing a significant volatile matter content such as bituminous coal, serious tar blockages occurs in the induced draft fan. The mechanism is thought to be the following: During start-up, the combustion of carbon source starts in the top layer of the bed. The hot gas from the combustion process is drawn through the cold burden by the action of the fan, and starts to heat the burden. When the temperature of the high volatile material reaches 350ºC it will start to de-volatilise. As the volatiles do not pass through a high temperature region it will remain stable and will exit the shaft with the reduction gas. Upon leaving the shaft it will first go through the quench spray where it is cooled down to approximately 35ºC. At this temperature the solubility of the volatiles in the gas is low and it condenses and remains in the gas as a fine mist. It has been found that they pass through the scrubber and only coalesce in the fan, probably due to the centrifugal force where they cause serious blockages.

- Bridging

Bridging of the iron ore in the oxidation zone of the shaft occurred quite frequently. Collapsing of the formed bridge by poking was found to resolve the problem. It was deduced that the bridging occurred due to the small diameter of the shaft in comparison to the top size of the ore particles. The problem is probably exacerbated by the rapid thermal expansion of the ore due to the fast temperature increase.

- Formation of accretions

During trials with anthracite accretions were found to form on the walls of the shaft directly below the high temperature section of the shaft. The accretions had to be removed by force. These were not found during operation with any other source of carbon. This problem could be described as of a serious nature to further operation.

The following observations were made

1. Gasification, regardless of the reductant used, worked particularly well. After ignition the flame front was stable near to the top surface of the material.
2. The plant operation was stable. After initial adjustment of the top gas flow, it was rarely required to make adjustments to control the top gas flow at the required rate.
3. The pressure drop though the bed is low

4.8 Sample preparation and analysis

4.8.1 DRI sampling and analysis

After each test samples were taken of the reduced product. Analysis consisted of visual inspection and SEM analysis. The particles selected from the DRI sample for analysis were cut by diamond saw, coarse and finely ground and inspected visually. The appearance of the particles was compared to that of samples from other DRI processes and TGA tests with a known high metallization degree. Selected sample were prepared for, and analysed by SEM analysis. The results confirmed the visual assessment. It is reported that the appearance of a reduced particle of iron is an acceptable method of roughly assessing the degree of reduction.

4.8.2 Gas analysis

Gas analysis was performed by sample collection in glass sample holders and analyzing by gas chromatograph. A gas and temperature sampling probe was manufactured by installing a 700mm x 3mm thermocouple through a T-piece inside a 680mm x 6mm stainless pipe. The thermocouple passed through the straight leg of the T-piece while the gas sample was drawn through the elbow end of the T-piece. Care was taken to seal the thermocouple where it exited the T-piece. The sampling probe was also pressure tested by connecting it to a compressed air source and testing with soapy water. The gas sample was cooled by passing it through a 4mm ID x 3m length of coiled copper tubing placed inside a water bath immediately upon exiting the sampling probe.

The samples were drawn into the sample holders by evacuating a 50ml syringe connected to the outlet of the gas holder and ejecting the collected sample to atmosphere. The syringe was operated a predetermined number of times. The number of evacuations required were calculated by measuring the diameter and length of the total tube and that of the gas holder and allowing for a safety factor of at least 2.

CHAPTER 5.

RESULTS AND DISCUSSION

In this chapter the results of the pilot plant experimental work is presented and discussed. The chapter has three subsections, namely

- Method employed to evaluate the degree of metallization of partly metallized iron ore particles
- Presentation and analysis of experimental results.
- Discussion of experimental results

5.1 Method Employed to Evaluate the Degree of Metallization of DRI Particles

Acknowledged analytical techniques for the determination of the degree of metallization of DRI include

- X-Ray diffraction
- ICP
- Magnetic techniques (Satmagan)

However, all the above techniques require pulverising the entire particle which has the implication that material from the different phases of reduction are combined and the result therefore represents an average degree of metallization for the complete particle. The average degree of metallization may suit the requirements of industrial consumers of DRI, but when it is known that the degree of metallization is low and the required information from the analysis is in fact a qualitative indication of the progress of metallization, the techniques above may not be the most appropriate to use. An alternative technique was sought that is:

- Less time consuming
- Less expensive

From the discussion on the thermodynamics of the reduction of iron oxides with CO and/or H_2 presented in Chapter 3, and the thermogravimetric work performed and reported on in the previous chapter, it is evident that the reduction process may be accurately modelled using a shrinking core model.

The following characteristics of the reduction reaction of hematite may therefore be affirmed

- Transformation happens from the outside in,

- Transformation progresses along a known sequence of increasing thermodynamic difficulty, consisting of
    - $Fe_2O_3 \rightarrow Fe_3O_4$
        - $Fe_3O_4 \rightarrow FeO$
            - $FeO \rightarrow Fe^o$
- Oxygen, which constitutes as much as 30% of the mass of the structure, (See Figure 2.2.1) is removed during reduction without reconstituting the structure of the original iron ore, leaving a porous iron matrix after metallization.

From the foregoing it may be asserted that the internal structure of a DRI particle, of which the metallization was halted before completion, will consist of concentric rings of different species of iron starting with iron metal on the outside followed by oxides of iron of increasing oxidation state. The presence of a specific ring, and the thickness of that ring will vary depending on the degree of metallization achieved.

Various researchers (Kang et al 1998, Bonalde et al 2005, Manamela & Pistorius 2005, Thurnhofer et al 2005, Theron 1978) indicate that the different stages of transformation that take place during metallization of an iron ore particle to DRI is identifiable when the prepared (cut & polished) particle is viewed under low magnification.

It was therefore decided that for the purposes of this work visual inspection of prepared particles may be a more appropriate method to determine the extent of metallization qualitatively, provided it is properly calibrated. Calibration included two aspects, viz. visual calibration and SEM techniques.

Calibration

Calibration of visual inspection procedure

Samples of unreduced iron ore, highly metallised DRI, and ore particles with three stages of metallization in between, namely low, medium and high, were cut and mounted in a 25mm resin matrix and ground and polished to serve as references. Photographs of these standards are shown in Figures 5.1.1 to 5.1.5.

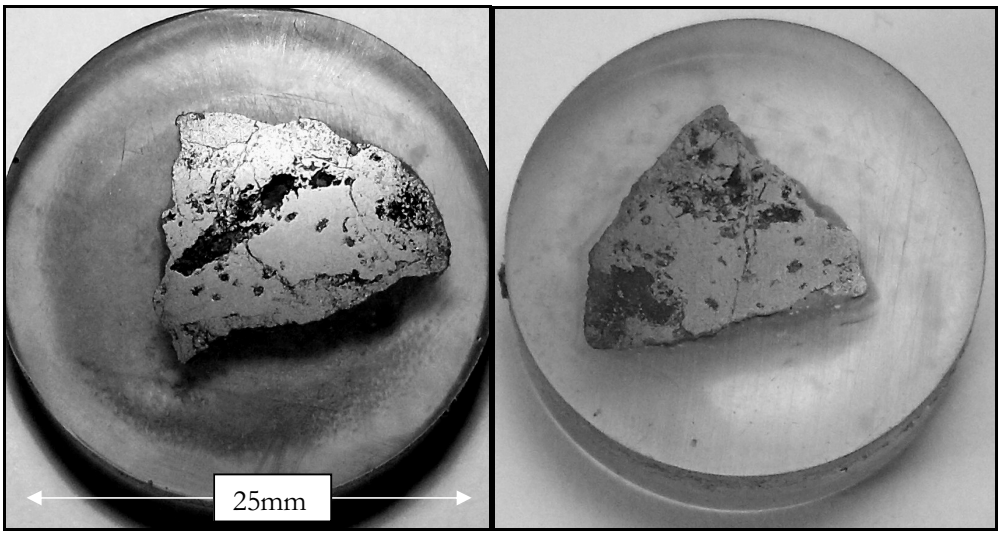

Figure 5.1.1: Optical image of the internal structure of unreduced hematite

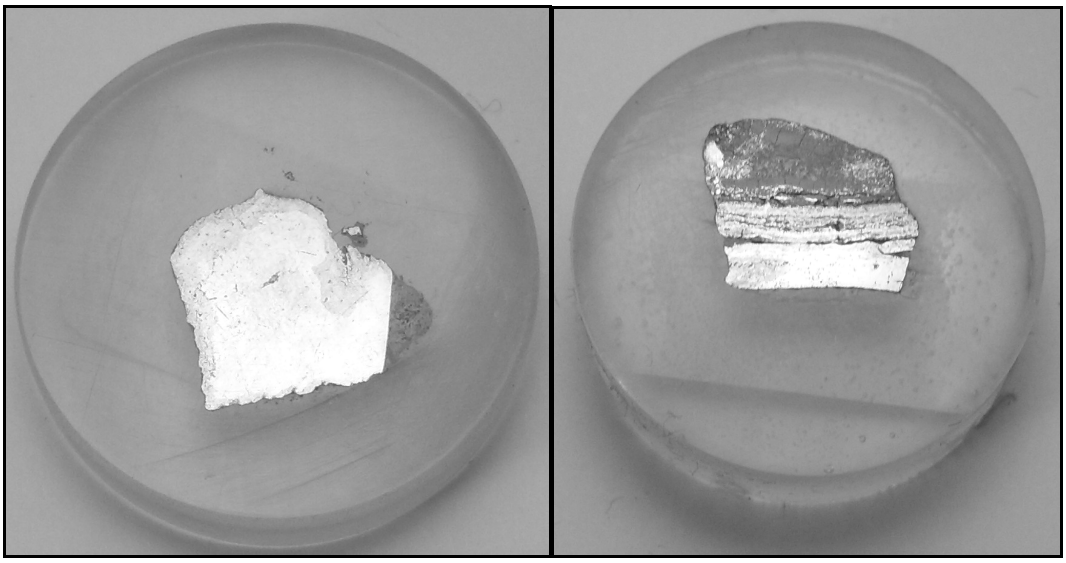

Figure 5.1.2: Optical image of the internal structure of highly metallised DRI

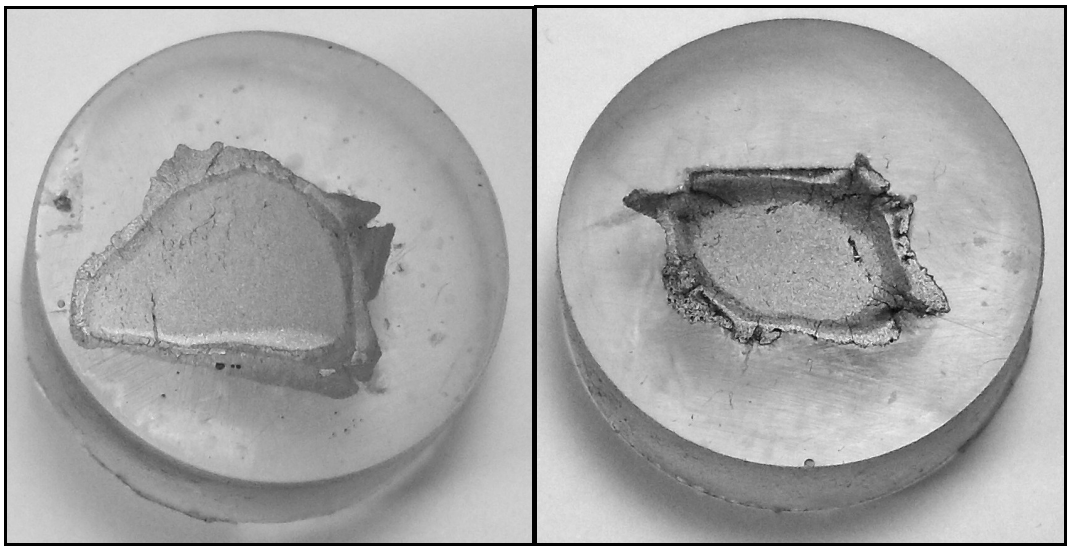

Figure 5.1.3: Optical image of the internal structure of two typical DRI particles with a low metallization degree

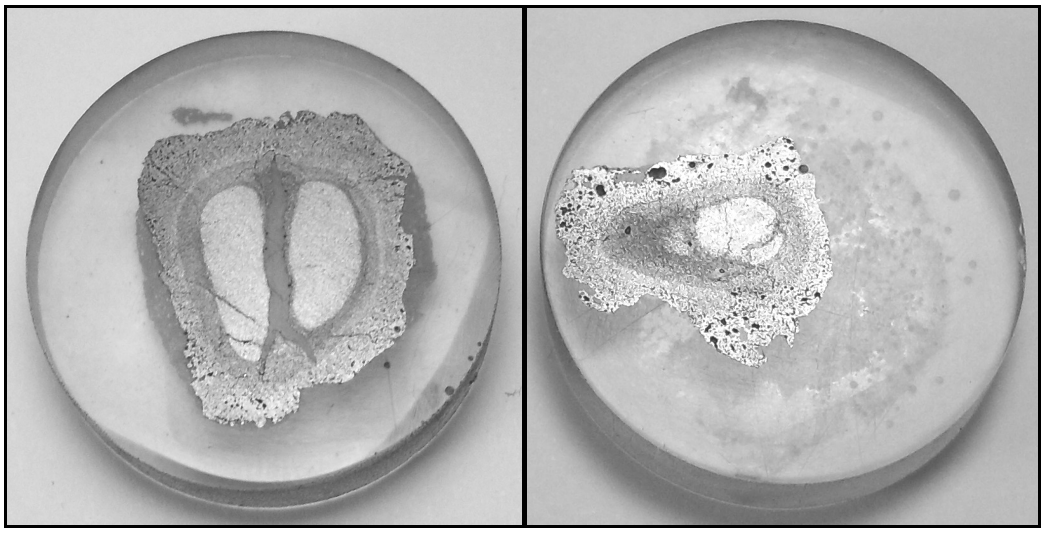

Figure 5.1.4: Optical image of the internal structure of two typical DRI particles with medium metallization degree

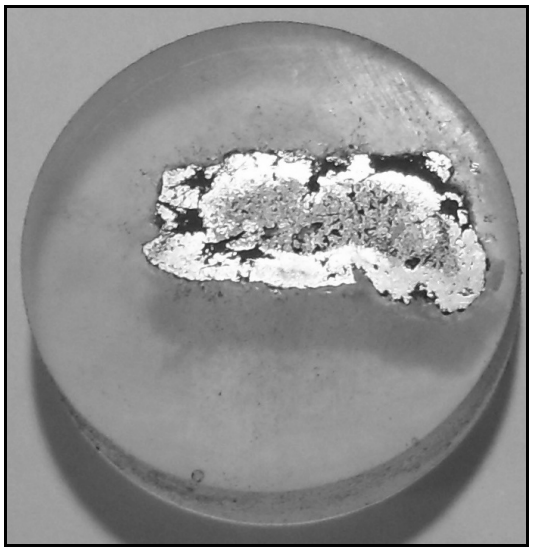

Figure 5.1.5: Optical image of the internal structure of a DRI particle with a high metallization degree

For analysis purposes the metallization of the different classes of DRI particles were classified as indicated in Table 5.1.1 based on the areas of the iron phase present. The image of each sample was partitioned in concentric rings of 5 mm and into 8 sectors of 45º each. The sectors were then classified by the predominant phase present, namely hematite, mixed magnetite/wustite and iron. Finally the number and area of the sectors of each specie were added and the total area of the iron phase expressed as a % of the total area.

Appearance of cut surface	**Surface of iron phase as % of total surface**	**Descriptive metallization degree**	**Designated metallization index**
Unreduced ore	0	None	0
Narrow ring of transformed materials around a large core of unreduced ore	0 – 40	Poor	1
Broad transformed ring with some metallization around a core of unreduced ore	40 – 60	Fair	2
Broad metallic ring around a core of transformed material	60 – 80	Good	3
Metallic ring with no/small black core of lightly reduced ore	> 80	Fully metallised	4

Table 5.1.1. Description of metallization degree of partly reduced iron ore particles

SEM analysis of the internal structure of DRI particles.

SEM analysis of selected DRI particles was undertaken to determine quantitative metallization degree figures. Elemental analysis were performed at different positions across the diameter of the particle. Fe O, Si, and Al contents were determined, and working from the premise that Si and Al with their higher

affinity for oxygen will be present in the oxide form, the Fe specie components were determined. (See Appendix 5.1)

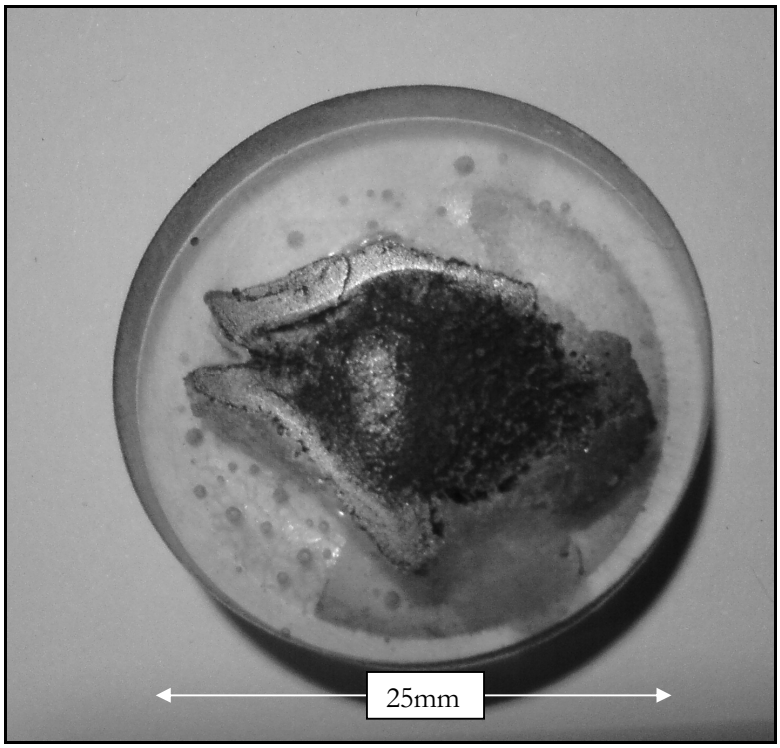

Figure 5.1.6: Optical photo of mounted sample

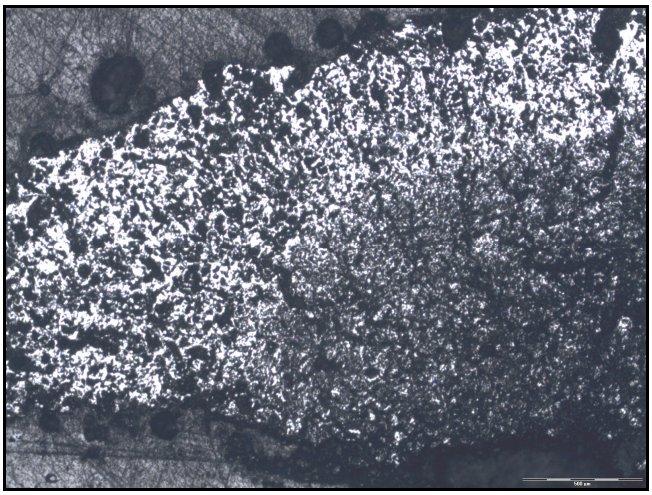

Figure 5.1.7: Optical photo of section of sample (Magnification 5X)

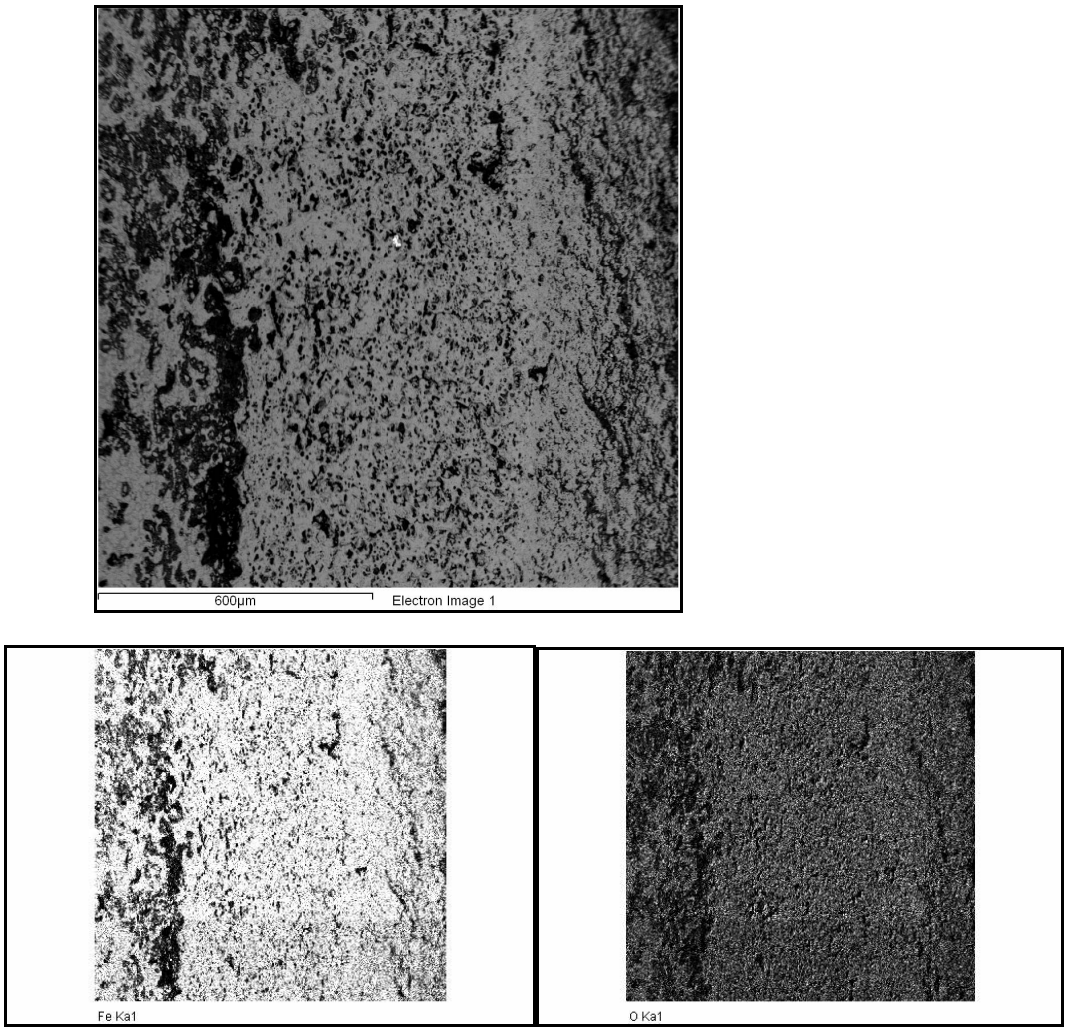

Figure 5.1.8: SEM photographs of a DRI particle

	Analysis Weight %				
Spec	**Al**	**Si**	**Fe**	**O**	**Total**
1	1.27	0.22	80.00	18.52	100.0
2	1.14	0.35	79.80	18.72	100.0
3	0.78	0.10	76.50	22.62	100.0
4	0.61	0.14	73.88	25.36	100.0
5	0.57	0.46	74.05	24.92	100.0
6	0.48	1.09	72.93	25.51	100.0
7	0.36	0.09	73.23	26.32	100.0
8	0.57	0.37	79.86	19.20	100.0
9	2.29	5.16	71.66	20.89	100.0

Table 5.1.2: SEM spectrum analysis of DRI sample

5.2 Presentation and Analysis of Experimental Results

5.2.1 Results of Pilot Plant Experiments

Pilot plant experimental runs were performed using the procedures and techniques discussed in the Chapter 4. Numerous DRI samples were taken from the outlet of the DRI screw after each test. Particles with a diameter of approximately 20mm were selected for cutting and inspection. As was expected it was found that the best metallization occurred in the particles that had spent the longest time in the reduction zone. In general the degree of metallization varied from no metallization in the particles near the burden level to the highest degree of metallization achieved in the test in particles lowest in the shaft, corresponding to the different retention times spent inside the shaft. The overall metallization for the trial noted was the best metallization found in any particle inspected.

The success of the trial, as characterized by the degree of metallization, was instantly apparent upon visual inspection of the internal structure of the cut samples. The results were evaluated after each test and possible reasons for not achieving the required metallization degree considered, after which a new test was planned. In many instances repairs or alterations had to be affected to the plant before a subsequent test could be performed.

The results of the 10 trials in which Sishen iron ore was reduced with different reductants, are indicated in Table 5.2.1.

Trial	Carbon	Oxide	Prod	CR	BT	GFR	Reason for stoppage	Met. degree	
			kg/h	kg/t	ºC	Nm^3/h		Descr	Nr
8	Anthracite	Sishen	1.5	1500	380	16.8	Fused layer	Good	3
9	Coal	Sishen	1.5	1200	440	17.5	Bridge formed 500 below level	Good	3
10	Coal	Sishen	2.7	700	410	17.5	Bridge formed cone hot	Poor	1
11	Coal	Sishen	2.7	700	340	7.8	End of test Raw materials finished	Poor	1
12	Coal	Sishen	3.3	700	240	7.6	Bridge formed	Poor	1
19	Electrodes	Sishen	3	750	340	10.3	Ore bridges, bed falls 3hrs ret time	Fair	2
20	Electrodes	Sishen	1.5	1400	185	12	Air ingress at fan	Fair	2
21	Electrodes	Sishen	1.5	1400	160	12	Air ingress at fan	Fair	2
23	Electrodes	Sishen	1.8	1000	424	14.4	Overoxidise	Fair	2

CR = Coal rate kg/t ore, BT = Bustle temperature ºC, GFR = Gas flow Rate Nm^3/h

Table 5.2.1: Results of pilot plant trials

5.2.2 Analysis of Pilot Plant Experimental Results

The principal aim of the experimental runs was to prove that industrial quality DRI could be produced in the pilot plant. From Table 5.3.1 it is clear that mixed results were achieved. While it was possible to achieve a high degree of metallization in two trials, thereby proving that the process is in fact feasible, only fair metallization was achieved in four runs and poor metallization was achieved in three more trials.

Various factors influence the degree of metallization. These include but are not limited to the coal rate, retention time of the ore in the reduction zone, production rate, and chemical analysis of the raw materials, including the moisture in the air. Whilst it was deemed outside of the scope of this work to attempt to quantify the effect of all of the above, the impact of some of the most prominent factors on the degree of metallization was analysed by correlation analysis.

Notable correlation between metallization index coal rate (positive) and production rate (negative) was expected. Single parameter correlation yielded a significant correlation with both coal rate (r^2=0.818) and production rate (r^2=0.694), in line with expectations. See Figures 5.2.1 and 5.2.2

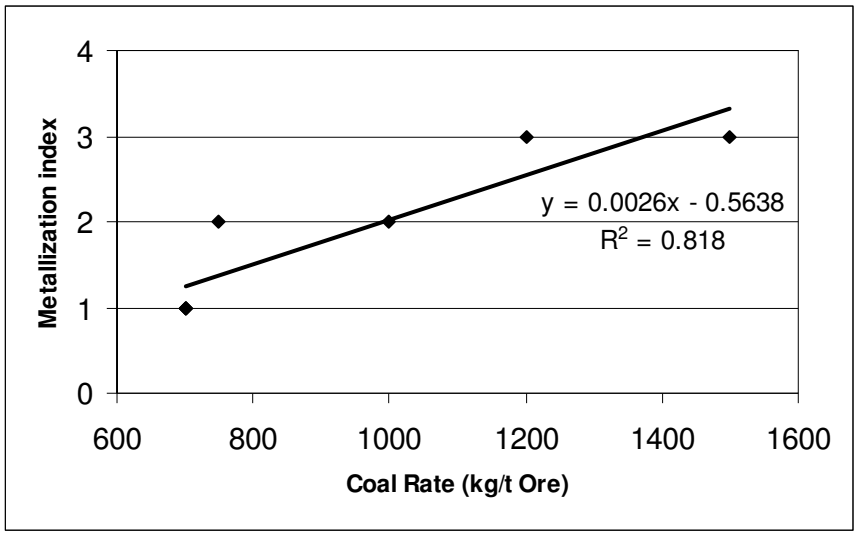

Figure 5.2.1: Metallization index vs. coal rate

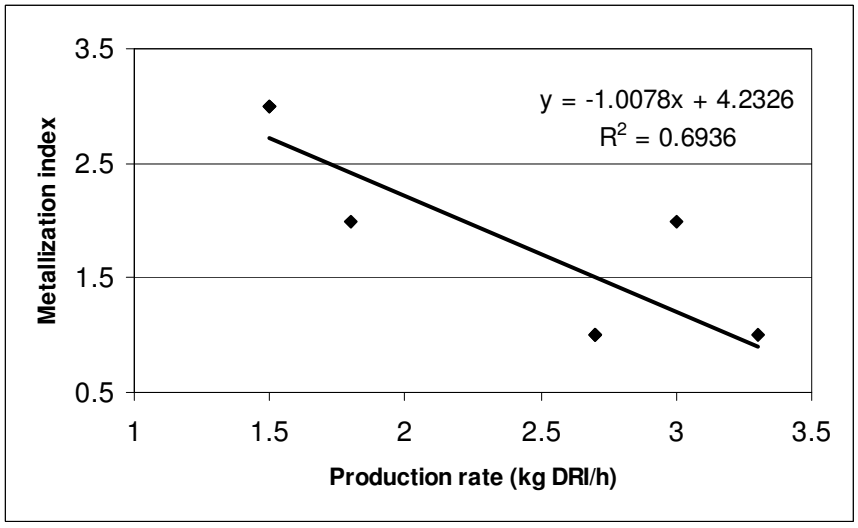

Figure 5.2.2: Metallization index vs. production rate

As mentioned in Chapter 3, the hearth load, or gas flow rate per unit area of hearth is regarded, after the equivalence ratio, to be the most important design parameter for downdraft gasifiers. The gas flow rate, which corresponds with the hearth load since the hearth area remained constant during all the runs, was correlated with Metallization index. The correlation did not prove to be significant (r^2=0.362). This is probably due to the fact that the effect of hearth load is overshadowed by the impact of coal rate and/or production rate.

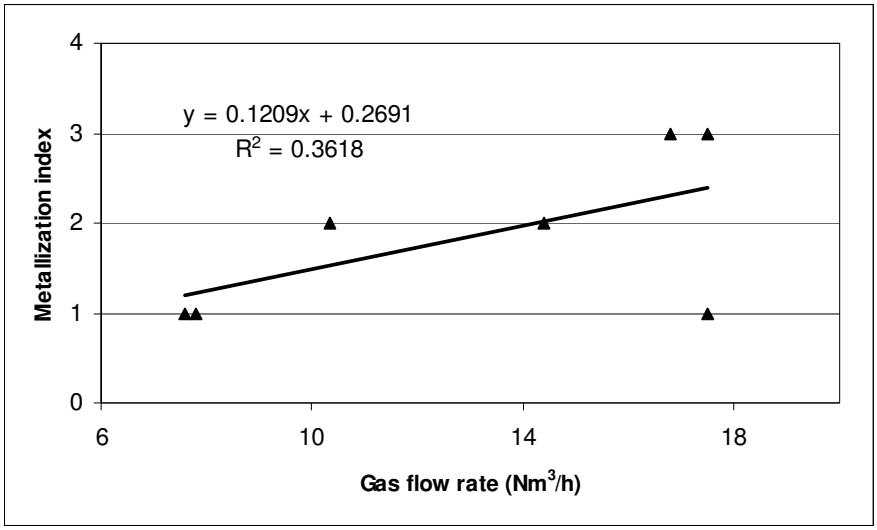

Figure 5.2.3: Metallization index vs. Gas flow rate

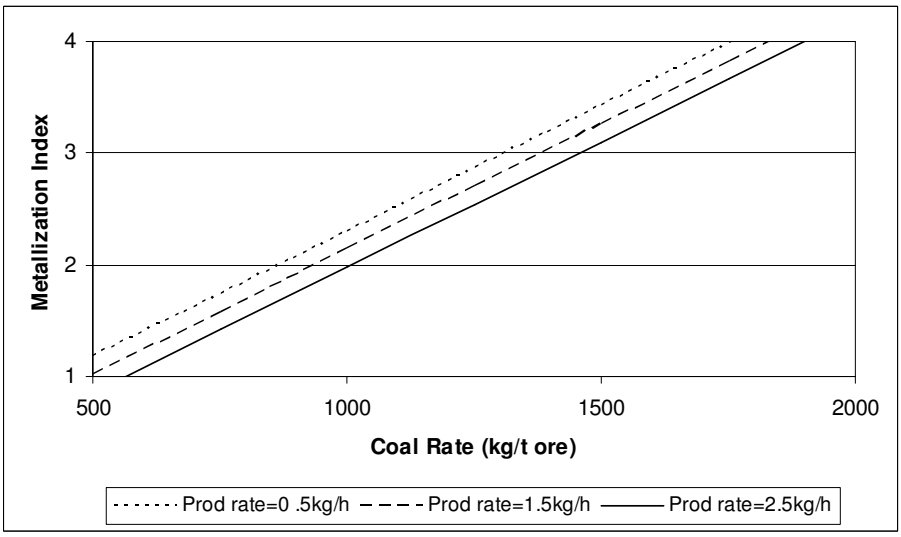

Figure 5.2.4: Correlation of Metallization index with Coal rate and Production rate

Multivariable regression performed on the test results yielded the following correlation: (See figure 5.2.4)

Metallization index = 0.00225*Coal rate – 0.161*Production rate + 0.13.

Multiple R = 0.906 and r^2 = 0.821 .

5.3 Discussion of possible reasons for lower metallization in some trials

From Figure 5.2.4 it would seem that simply by using coal at a coal rate of 1750kg/t ore and operating the pilot plant at a production rate of approximately 1kg DRI/h would have ensured a metallization index of 4, which if correctly calibrated corresponds to 93% metallization. This was not known during the trials since the correlation had been performed yet.

Perhaps as important as understanding what conditions would have made good metallization possible, is to understand the reasons why a higher degree of metallization could not be achieved in some trials.

From the discussion in Chapter 3 it is clear that the gas composition and the gas temperature determine the driving force for the reduction reaction. This is illustrated in Figures 3.3.6 and 3.4.3. From the thermogravimetric test work done by Theron, (1985) and the work done in this study, it also evident that even if the reducing gas contained 100% CO or H_2, a definite period of time is required to reduce 93% of the Fe in an iron ore particle of specific diameter at a particular temperature to Fe metal.

From the above it may be concluded that two factors will determine the degree of metallization in the tests performed. These are:

- The composition and temperature of the reducing gas achieved
- The time the iron ore particles spent in the reducing conditions

Composition and Temperature of the Reducing gas

The temperature of the reduction gas leaving the gasifier, referred to as the bustle temperature, was lower during the trials than that measured inside a stratified downdraft gasifier of comparable diameter of 150mm gasifying biomass with air. The temperature of the gas at the outlet of the gasifier was approximately 1000ºC. (Reed & Das 1998). See figure 5.3.1.

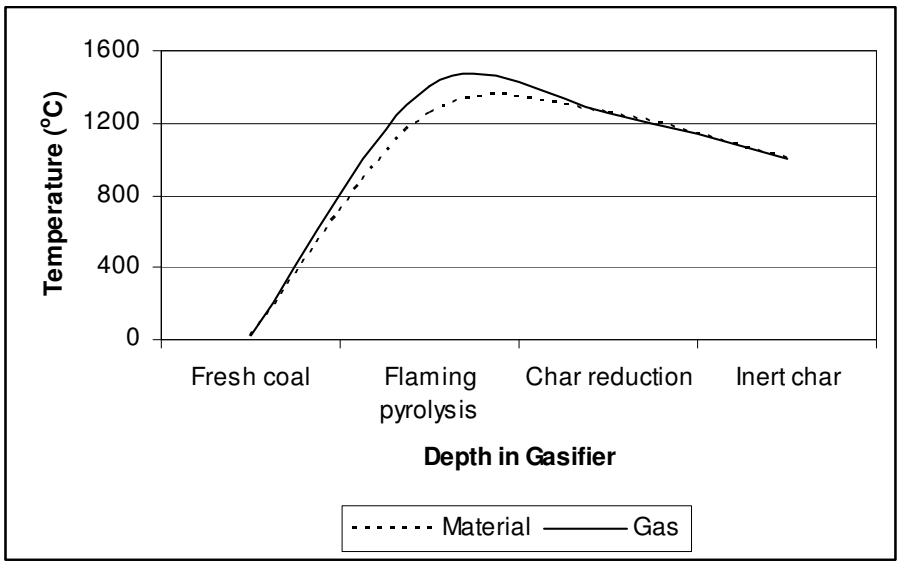

Figure 5.3.1: Material and gas temperatures inside a stratified downdraft gasifier operating on biomass (Reed & Das 1998)

To determine the whether the level of temperatures inside the reduction shaft correlated with that inside the gasifier, an 8mm Alumina sheath was installed in the bed. This made measurement of the bed temperature at any depth possible by inserting a thermocouple in the sheath to any depth in the sheath. Unfortunately the alumina sheath fractured numerous times in the hottest part of the bed, probably due to the fact that the tensile force of the burden acting on the sheath exceeds the tensile strength of the sheath at the temperature. In spite of this the bed temperature was measured various times using a variety of probes inserted from above. Figure 5.3.2 is an indication of the temperatures at various depths in the bed. Since the level of the bed is controlled by manual feeding of batches of burden material, it is to be expected that the bed level may fluctuate somewhat. The bed temperature at a specific point in the bed may therefore fluctuate also.

The maximum temperature attained was found to be generally in good agreement with that reported by Reed & Das (1998). However, a distinctive deviation from the temperature reported was the extent of the drop in temperature below the oxidation zone.

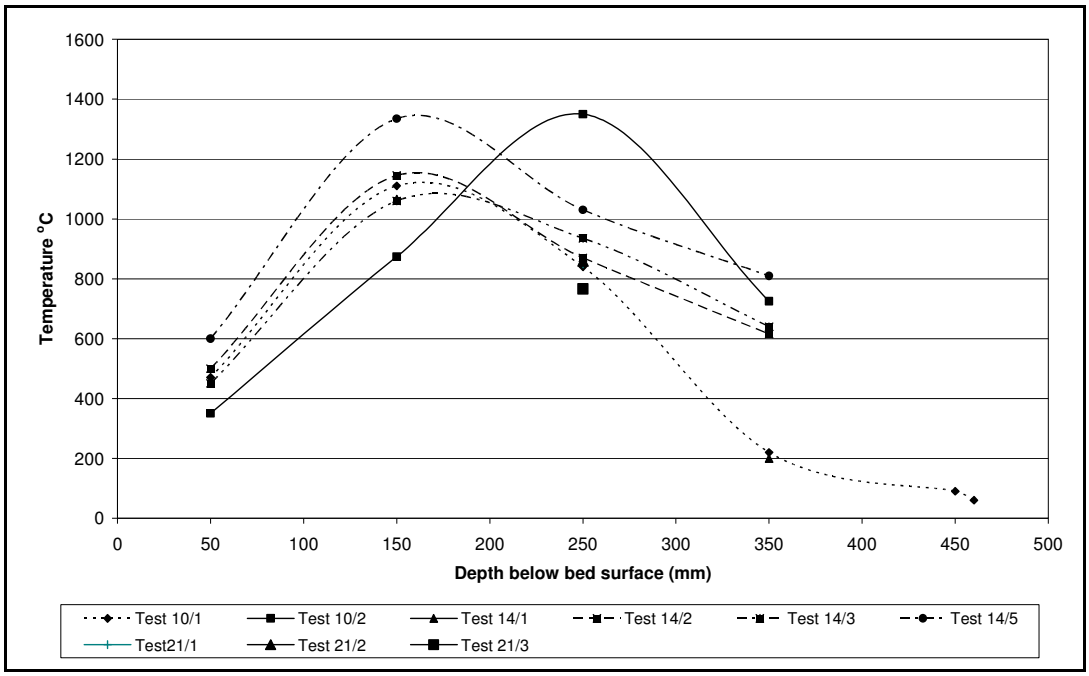

Figure 5.3.2: Gas temperature measurements inside the reduction shaft. (Legend indicates test number and the number of measurements)

Higher than expected heat demand

The sharp drop in the measured temperature was evidently due to either a larger than expected heat consumption in the shaft caused by either an endothermic reaction or a higher heat loss than in the case of Reed & Das (1998). It was uncertain whether a high heat consumption would cause the symptoms experienced, i.e. low degree of metallization and a low bustle temperature. The effects of a high heat consumption in the reduction shaft was therefore investigated.

A FactSage simulation was performed to test the effect of a high heat consumption on metallization and gas temperature. Using a simplified reaction, namely 1g of pure hematite reacted with 0.7g of pure graphite and air, the volume of air was varied to determine the optimum air feed rate for the reaction. Using this feed rate, the heat consumption in the reactor was varied to determine the effect on the gas analysis, gas temperature and metallization. The results are indicated in figures 5.3.3 to 5.3.7.

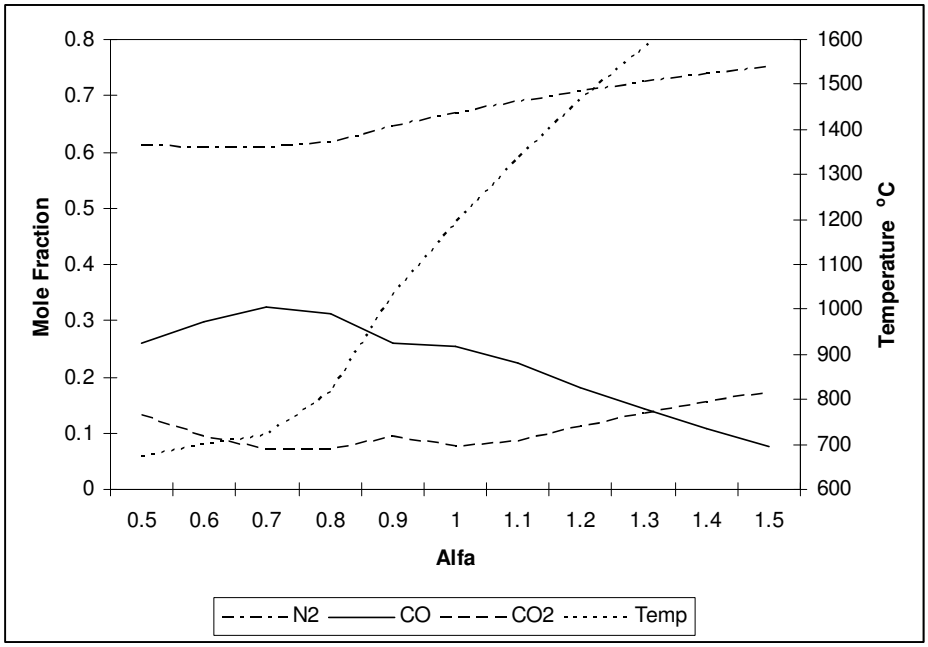

Figure 5.3.3: FactSage simulation of effect of air feed rate on gas analysis and gas temperature

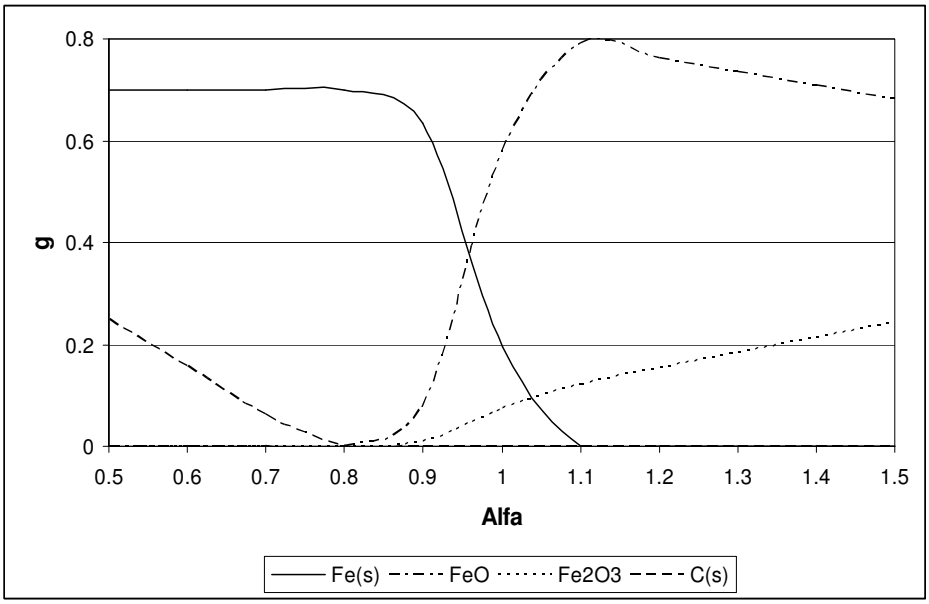

Figure 5.3.4: FactSage simulation of effect of air feed rate (equivalence ratio) on metallization

From Figure 5.3.4 it is evident that the best metallization is obtained at an Alfa value of 0.8 or 0.8g O_2 for every .7g of carbon. Using this value the heat loss is now varied from 0 to -10 000J.

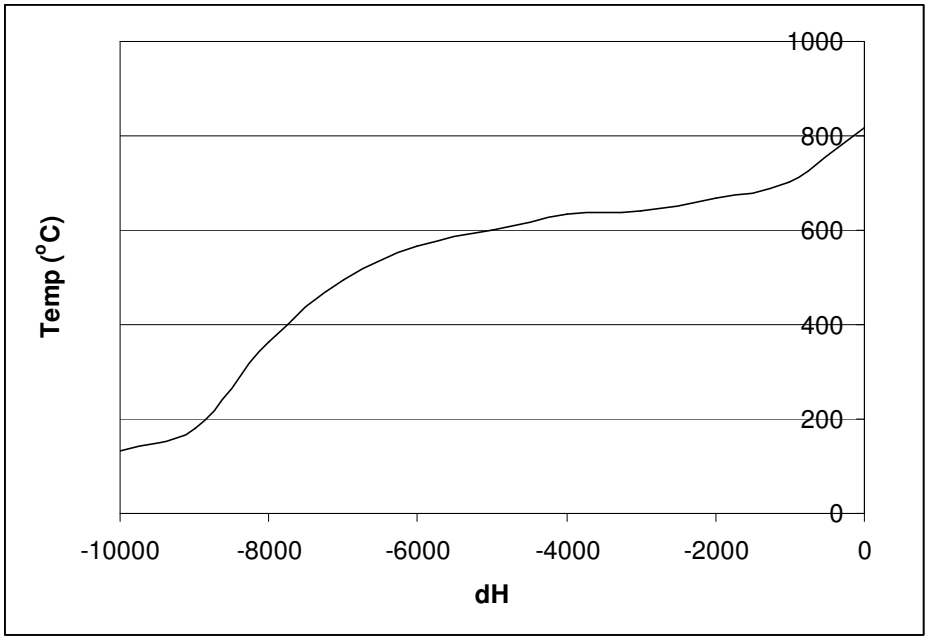

Figure 5.3.5: FactSage simulation of effect of heat loss on gas temperature

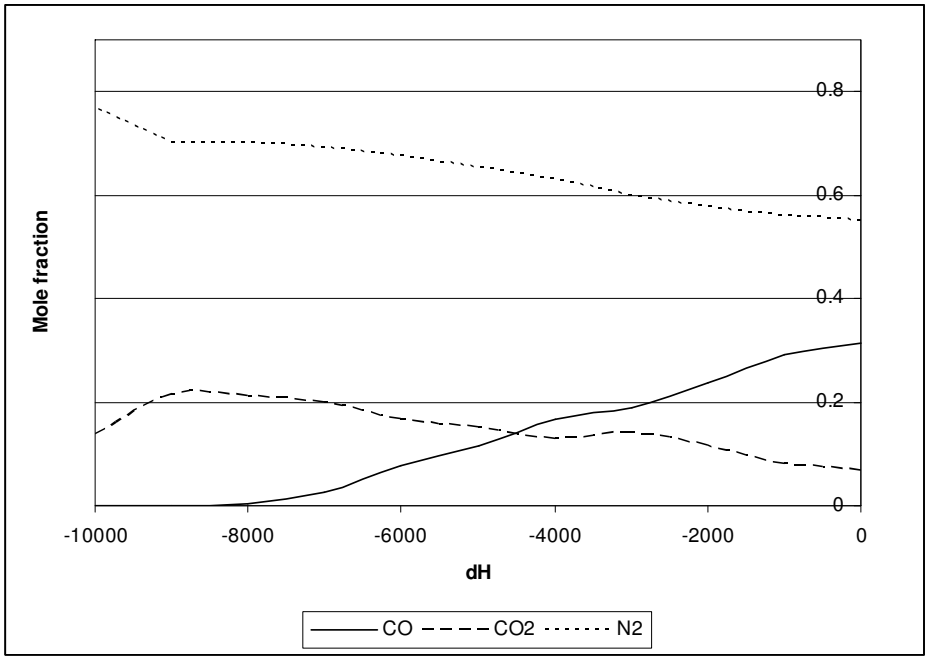

Figure 5.3.6: FactSage simulation of effect of heat loss on gas analysis

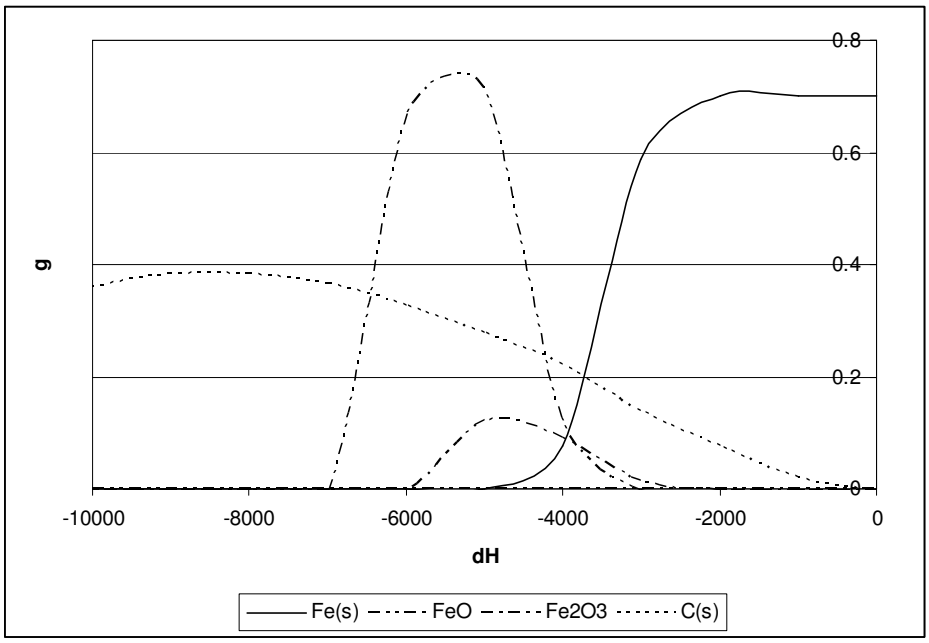

Figure 5.3.7: FactSage simulation of effect of heat loss on metallization

The simulation indicated that starting from a zero heat loss with a metallization degree of 100%, increasing the heat loss initially does not affect metallization, but once the heat loss increases above 3000J the degree of metallisation reduces rapidly to a null metallization at a heat loss of 5000J. From the figure a heat loss of approximately 4000J for a DRI production rate of .7g DRI/hr or 5714kJ/kgh. is equated with a metallization degree of approximately 20%.

Causes for the high energy consumption was investigated, and since the heat required to heat the hematite to the reaction temperature and the heat of reaction of the reduction of hematite had already been accounted for in the simulation, only heat requirements other than these had to be considered. The following three possibilities were identified:

- Heat of Devolatilisation of the coal
- High heat loss
- Unsteady state conditions

Heat of Devolatilisation of the coal

Devolatilisation of the coal, which occurs during pyrolysis of the coal, was identified as an enthalpy requirement in the top part of the reduction shaft, (See schematic diagram of downdraft gasification Figure 5.3.8). Since the magnitude of the heat of devolatilisation was unknown it was regarded as a possible reason why the bustle gas temperature was lower than expected.

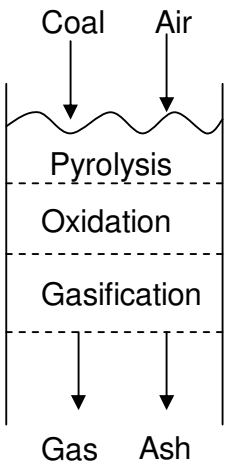

Figure 5.3.8: Schematic drawing of downdraft gasification

Coal may be portrayed as a blend of complex carbohydrates and devolatilisation of the coal involves destruction of these carbohydrates into a volatile component and solid carbon. Tomeczek & Palugnio (1996) quantified the enthalpy of devolatilisation of 5 different Polish coals over the temperature range 0 - 1500ºC. They concluded that the enthalphy of devolatilisation is slightly endothermic below 800ºC for all coals (-120kJ/kg coal) and either endothermic or exothermic above 800ºC (±200kJ/kg coal) depending on the type of coal.

In order to estimate the magnitude of the heat of devolatilsation of a typical South African coal the following analogy was used. When the Heat of Combustion of any hydrocarbon is compared with the sum of the Heats of Combustion of the elements, the difference equates to the Heat of Formation of the hydrocarbon. Using this method of calculation the Heat of devolatilsation may be approximated for any hydrocarbon. The principle is proved by performing the calculation for a simple (CH4) as well as a complex hydrocarbon (C6H6).

The volatiles released during the devolatilsation of coal, are elements and coumpounds (H_2, CH_4, CO etc), so the sum of the Heats of Formation of these compounds need be deducted from the sum of the Heats of Combustion of the elements, which presumes that all C and H_2 is combusted to CO_2 and H_2O. The composition of the volatiles is calculated using the model proposed by Matthesius et al (1987) which estimates the composition of the volatiles during slow pyrolysis. (Appendix 2)

$$Coal(C_nH_m) \xrightarrow[Heat]{} Char(xC_{(s)}) + Volatiles(C_{n-x}H_m)$$
$$C_{n-x}H_m \rightarrow CH_4, C_2H_6, CO, CO_2, H_2, H_2O, NH_3, H_2S, Tar(C_zH_y)$$

Figure 5.3.9: Simplified reaction for pyrolysis of coal (Components of volatiles as by Matthesius et al 1987)

The calculated heat of devolatilisation for Leeupan DR fraction is approximately -40kJ/kg, which falls within the range determined by Tomeczek & Palugnio (1996).

	Heat of combustion kJ/kmol	Sum of Heats of Combustion of elements (kJ/kmol)	Difference (kJ/kmol)	Heat of Formation (kJ/kmol)
C	-393500			
H2	-241800			
S	-395192			
CH4	802300	-877100	-74800	-74898
C6H6	-3169500	-3086400	83100	82982
	Calorific Value Mj/kg	Sum of Heats of Combustion of elements (MJ/kg)	Difference (MJ/kg)	Heat of Formation (MJ/kg)
Leeupan dr	-27650	-27328	322	
Volatiles				-362
Heat of devolatilisation				-40

Table 5.3.1: Heat of devolatilisation of Leeupan DR Coal (Mathew & Rogers 1974, Perry & Chilton 1973). (Appendix 2)

The magnitude of the heat of devolatilsation is however so small as to not be a probable cause for the low bustle temperature. This was confirmed by performing various pilot plant trial runs using electrode chips with a near zero volatiles content. The bustle temperature during these tests were not any higher than during tests with charcoal or coal.

High Heat loss

To determine the magnitude of the heat loss from the reduction shaft in relation to that from operating shafts, a comparison was made with operating reduction shafts. Using the correlation of shaft diameter vs. annual production prepared for the design of the pilot plant (figure 4.6.2) and the fact that the retention time of the iron ore in operational shafts is approximately 6 hours (Batelle Institut 1973) the volume of any size shaft may be determined. With the diameter, production volume and the internal volume of the shaft known, the height of the shaft and therefore the specific heat loss area may be calculated. Figure 5.2.9 indicates the specific heat loss area for shaft of different diameters.

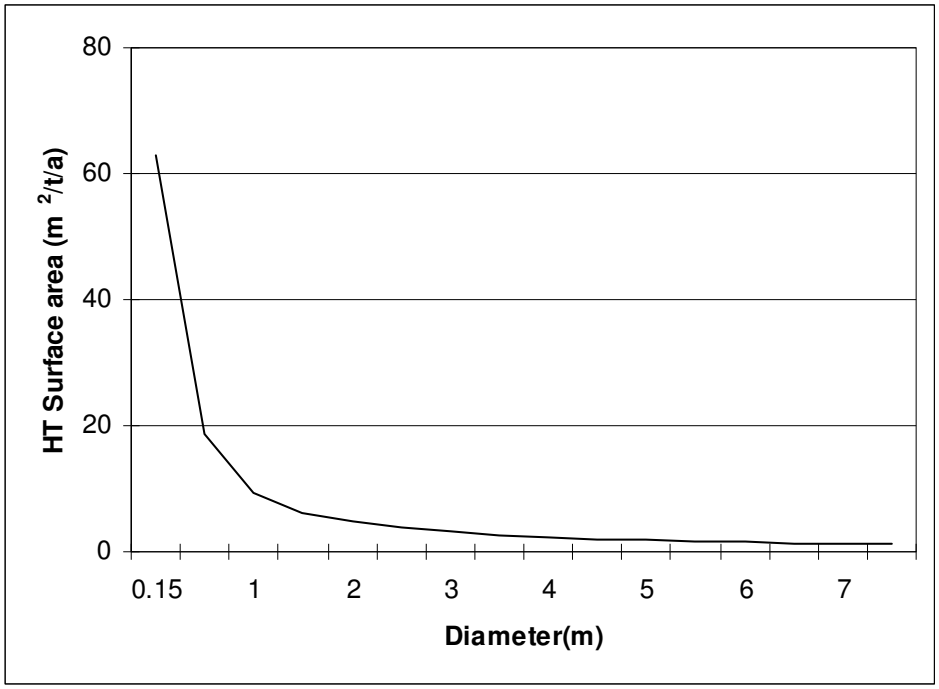

Figure 5.3.9: Specific Heat Transfer area vs. Shaft diameter

It is clear that the specific heat loss area for the pilot plant is approximately two orders of magnitude more than that of a production size plant (70 vs. 1.92m^2/t/d for a 500 000t/a shaft).

The calculated heat loss from the from the reduction shaft is 5300kJ using a heat transfer coefficient of 60W/m^2K inside and a heat transfer coefficient of 10W/m^2K on the outside. This correlates almost exactly to the heat consumption at which metallization approximates zero as determined in the computational thermo-chemistry simulation determined above for a production rate of 1kg DRI/hr.

To compensate for the high heat loss a gas heated annulus was created within the steel shell of the shaft by removing the inner of the two insulation layers and installing a LPG gas combustion ring pipe in its place. This unfortunately did not improve the metallization to any degree. An analysis indicated that with the heated annulus the heat loss from the shaft reduced only marginally. This was due to the fact that whilst the temperature of the combusted gas was much higher than ambient air, the overall heat transfer coefficient was in also substantially higher for the reason that the there now was no insulation layer around the refractory lining, and the heat transfer coefficient on the outside increased from 10 W/m^2K (natural convection) to 21 W/m^2K (forced convection). See table 5.3.2 for detail

Aspect	Unit	Original	With gas heating
Inside temperature	ºC	806	806
Inside heat transfer Coefficient	W/m2K	60	60
Refractory lining thickness	mm	25	25
Insulation layer thickness	mm	50	0
Steel shell thickness	mm	8	0
Outside heat transfer Coefficient	W/m2K	10	100
Overall heat transfer coefficient	W/m2K	3.38	20.95
Outside temperature	ºC	20	600
Heat loss	kJ/h	5261	4637

Table 5.3.2: Selected detail of conditions with and without gas heating ring

Unsteady state conditions

Figure 5.3.10 is an indication of the development of the bustle temperature averaged over the course of all tests performed on the pilot plant. Two distinct periods may be discerned. The trend firstly consists of a period of rapid temperature increase as hot gas from the combustion zone passes through the bed and heats the burden. Secondly, a period of moderate temperature increase, when, in all probability, the char temperature had increased to a sufficient level for gasification to commence.

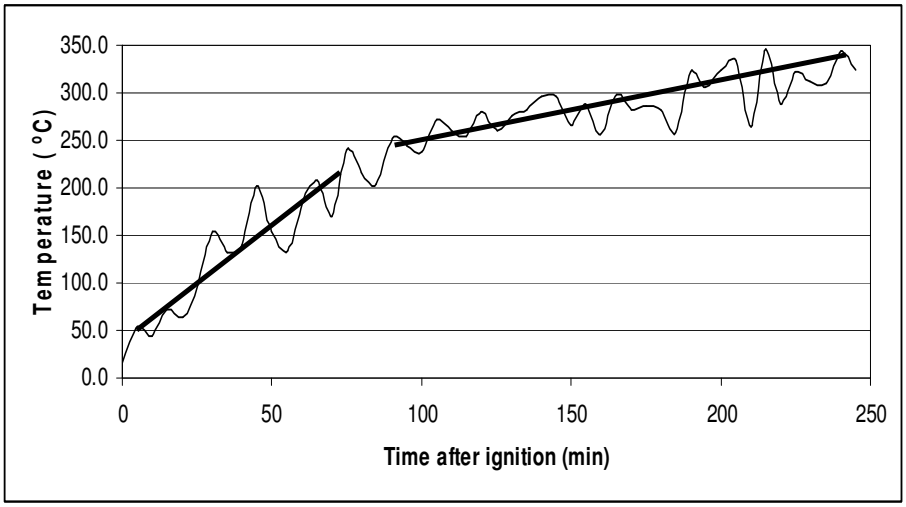

Figure 5.3.10: Average bustle temperature over all tests

The temperature tendency at the end of all the trials is still increasing, suggesting that the system had not reached steady state conditions when the trials were terminated, adding to the heat demand on the reduction shaft.

The Time the Iron Ore Particles spent in the Reducing Conditions

The designed retention time for iron ore in the reduction shaft was 4 hours, assuming that all coal is consumed in the first half of the shaft. Gasification of the carbonaceous material occurs by oxidation followed by gasification. Oxidation and gasification each consumes approximately 50% of mass of the carbonaceous material. From work done by Reed & Das (1998) it is evident that oxidation and gasification of biomass in a stratified downdraft gasifier (SDG) is completed approximately 200mm below the burden level.

When the carbonaceous material is consumed it creates a void which is filled by the iron ore moving down to fill the void, therefore the lower the bulk density of the carbonaceous material the larger the void will be that is created, and consequently the faster the ore will move down the shaft. The design of the shaft assumes that the coal is consumed fully in the top half of the shaft, after which only iron ore and ash are left which is contacted by the gas produced in the top half. Four hour retention was allowed for in the design.

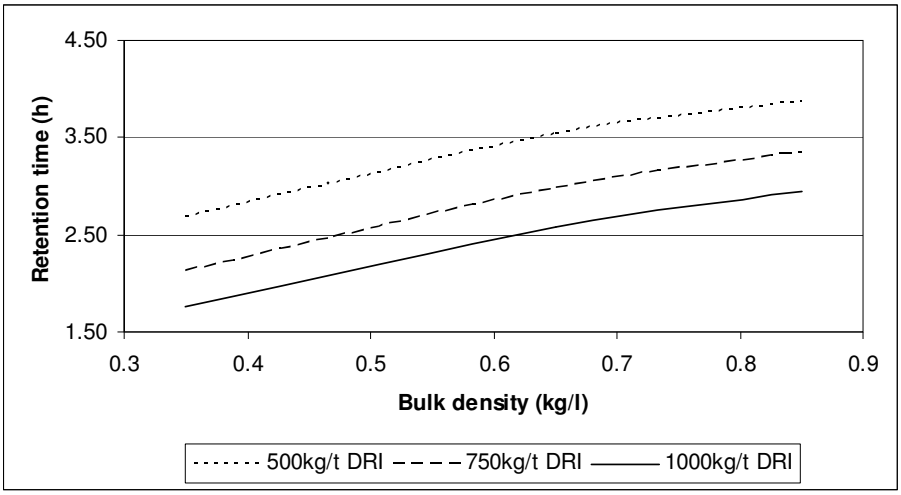

Figure 5.3.11: Retention time of iron ore vs. bulk density of the carbonaceous material for coal rates varying between 500 and 1000kg/t DRI.

Figure 5.3.11 indicates the retention times of the iron ore using varying coal rates of between 500 and 1000kg/t DRI for carbonaceous materials of different bulk densities. From this it is evident that when using charcoal, the retention time is substantially shorter than when using coal for instance. It was therefore deduced that due to the very low bulk density of specifically the charcoal, the retention time of the iron ore is decreased to such an extent that the iron ore is not metallized properly.

Charcoal as carbonaceous source was therefore replaced by anthracite which was readily available. However, this lead to the formation of accretions against the wall of the reduction shaft and its use was

discontinued in favour of the use of coal. Using coal in stead of charcoal increased did produce a better degree of metallization. It was therefore decided to use electrode chips, which has an even higher bulk density than coal. Unfortunately the use electrode chips did not improve the degree of metallization, possibly due to the fact that the advantage of the increased retention time was overshadowed by the disadvantage of the lower hydrogen content in the reduction gas.

Rate of gasification

Reed & Das (1998) performed gas analysis inside a SDG operating on biomass. Gas samples were taken at four different levels inside the gasifier and analysed. The gas analysis is shown in Figure 5.3.12.

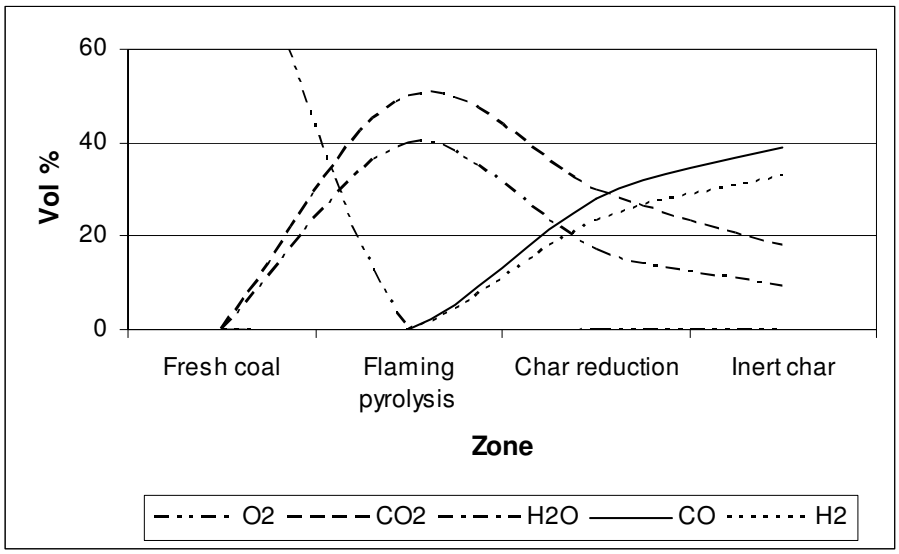

Figure 5.3.12: Gas analysis inside a stratified downdraft gasifier (Reed & Das 1998)

Gas temperature and analyses measurements were performed during trial # 21. Gas samples were taken at a level roughly 600mm below the flange of the shaft inlet. The bed level at the time was approximately 300mm below that level. It has to be kept in mind that the bed level fluctuates somewhat between fillings, explaining the difference in measured bed temperature.

The gas analysis, indicated in Figure 5.2.13, although being somewhat unexpected due to the high nitrogen and low carbon monoxide content, is in line with calculated values since the carbon source in this trial was electrode chips which contains approximately 99% carbon. The analysis corresponds with the figures reported by Reed & Das for a position between the flaming pyrolysis and the char reduction.

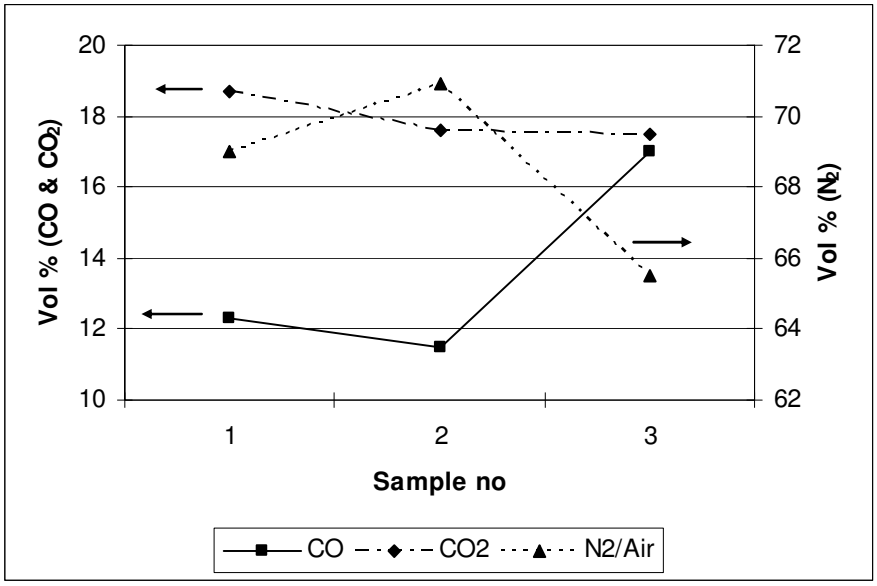

Figure 5.3.13: gas analysis 300mm below the burden level.

When the CO/(CO+CO2) ratio of the gas analyses are graphed against the temperature of the sample Figure 5.2.14 is obtained. It is clear that these values are far removed from the Bouduard equilibrium. However, the fact that the gas analysis at the lower temperature was closer to the equilibrium than the analyses at the higher temperature, indicates that the process of gasification, through which the gas analysis approaches equilibrium, was still in progress.

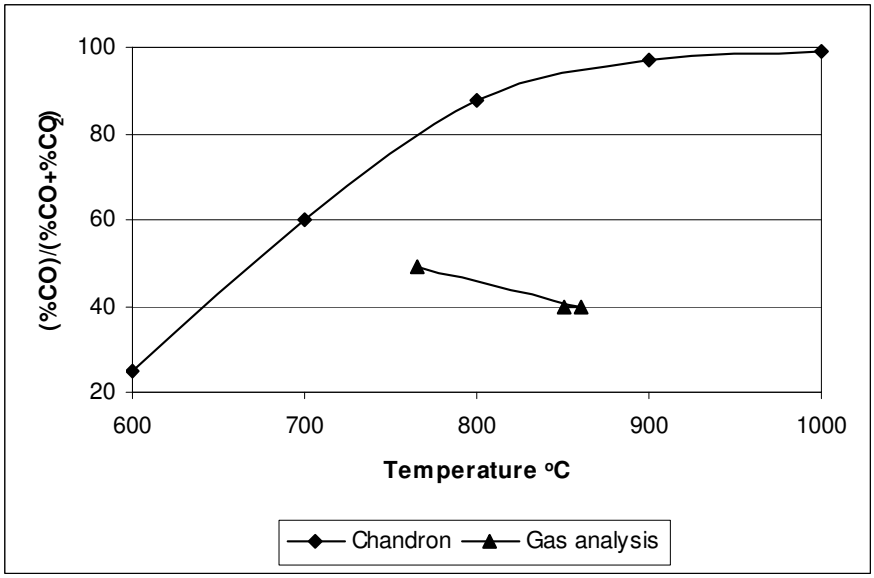

Figure 5.3.14: Gas CO/(CO+CO2) ratio vs Temperature

This however raises the question of how deep down the shaft would equilibrium have been reached. Reed & Das (1998) reports that the development of the bed in a stratified downdraft gasifier is dependent on the characteristics of the biomass, but that for a 150mm diameter stratified downdraft gasifier the end of the char reduction zone is approximately 180mm below the start of the flaming pyrolysis zone. It was found that the start of the flaming pyrolysis zone fluctuates between zero and 100mm below the top of the bed, depending on when last the bed was topped up. An average figure of 50mm may be assumed, which would place the gas analysis point 250mm below the start of the flaming pyrolysis zone. This indicates that the achievement of equilibrium is somewhat slower than in the SDG operated by Reed & Das.

Two factors influence the rate of gasification, namely temperature and reactivity of the char. It has been shown that the temperature in the gasifier, especially in the lower part was lower than that measured by Reed and Das (1998). It has been shown by Fruehan (1977) that the reactivity of graphitized electrode is lower than that of char freshly formed by the pyrolysis of either biomass or coal.

It would seem therefore that due to the lower level of temperatures in the shaft, and the fact that electrode chips was used in some trials which has a lower reactivity than char, gasification was slower than originally anticipated. This had the effect that the time that the iron ore spent in reducing conditions were shorter, explaining the lower metallization index in trial performed with electrode chips

Chapter 6

CONCLUSIONS

The following conclusions were arrived at

1. The process as conceptualized is proven to be thermodynamically viable.
2. It was possible to produce highly metallised DRI in a small scale pilot plant employing a simplified process route of the process despite the obvious shortcomings of such an approach.
3. Downdraft gasification proved to be an efficient method of gasification with the major advantage that no tars are generated which have to be treated in a subsequent processing step. It is also simple to start, stop and control.
4. The process is conceptually a viable alternative for small scale EAF operators.
5. The cause for not achieving the required metallization in some trials was a combination of thermodynamic and kinetic factors. These include:
    - The heat loss from the pilot plant was higher than anticipated. This was a consequence of two contributing factors namely
        - An exceptionally large specific heat transfer area inherent to the size of the plant, and
        - The heat transfer through the shaft walls were higher than expected.
    - The retention time that the iron ore particles spent in reducing conditions was lower than the designed retention time. This was due to either the coal rate in some tests being too high or the bulk density of some carbon sources being lower than projected.

Chapter 7

RECOMMENDATIONS

It is recommended that

1. A pilot plant be designed and erected that embodies the full flowsheet intended in the envisaged process, namely pre-heating of the ore followed by gasification and reduction.
2. That trials be performed on the pilot plant to determine the effects of raw material analysis and consumption rates as well as process operating conditions on process performance. Experiments should be planned and results analysed using experimental design techniques.
3. That the diameter of the plant, if at all possible, be larger than 1m to reduce the specific heat transfer area of the plant to the level where further increases in diameter reduces the specific heat loss area only marginally.
4. That careful attention be paid to the refractory design to further limit the heat loss
5. That the height of the reduction shaft be such that the iron ore spends at least 4 hours in the reduction shaft after the end of the char gasification zone. The effect the increase in height on the corresponding increase in the specific heat transfer area should be investigated.
6. That the effect of superficial velocity of the gasifier on the gasification efficiency be investigated in more detail.

8 REFERENCES

Ahlbrandt, Roger. S, Richard J. Fruehan, Frank Giarratani, 1996, The Renaissance of American Steel – Lessons for Managers in Competitive Industries, Oxford University Press.

Aylen, Jonathan and Kevin Anderson, 2006, Markets in ferrous scrap for steelmaking, Ironmaking and Steelmaking 33, 3 203 - 212

Battelle-Institut e.V Frankfurt, 1973, Reduction processes outside the Blast Furnace and their effect on future iron and steel production in the world.

Beeton, T.B. 1965, The measurement of the reducibility of iron ores and sinter and the correlation of these values with blast furnace performance, P.hD Thesis, University of Witwatersrand

Berry, Bryan, 1999, A Retrospective of Twentieth-Century Steel, New Steel, Nov 1999

Bianchi Ferri, Mauro and Francesco Memoli, 2007, EAF integration into the blast furnace route at Wheeling-Pittsburgh, Millenium Steel

Böhm, C, A. Eberle, 2002, Global Development of Primary Side Technologies, VAITech presentation at IPIS Meeting July 2002.

Bonalde, A, A. Henriquez, M. Manrique, 2005, Kinetic Analysis of the Iron Oxide Reduction Using Hydrogen–Carbon Monoxide Mixtures as Reducing Agent, ISIJ International, 45, 9, 1255 – 1260

Bornman, S.J, J.P. Ackerman, 1993, World's largest Coal-based Direct Reduction Plant – Nine Years Later, Steel Time International, March, 18 – 22

Brent, Allon, D, 1999, The Port Hedland Finmet Project – Fluid Bed Production of High Quality Virgin Iron for the 21st Century, International Conference on the Alternatives Routes of Iron and Steelmaking (ICARISM '99) Perth WA.
Brunner, Lincoln, 2002, What now? Every facet of steel industry watches, waits as change sweeps in. www.thefabricator.com

Burns, Stewart, 2009, Testing Times for Steel Mills, www.agmetalminer.com

Coudurier, L, D.W. Hopkins, I. Wilkomirsky, 1978, Fundamentals of Metallurgical Processes, Pergamon, Oxford.

Coulson, J.M, J.F. Richardson, 1997, Chemical Engineering, Particle Technology & Separation Processes, 4th Ed, Butterworth-Heinemann.

Creamer, Terence, 2007, Long ambition – Mittal plans to spend R2bn/y on capex, Mulls long-product opportunities, Engineering News Apr 13-19, 20 – 22

Delport H.M.W, P.J. Hollaschke, Ed, 1990, Corex Simposium 1990, SAIMM Special Purblication Series SP4,

Delport H.M.W, 1992, The COREX Process, Ironmaking and Steelmaking 19 3, 183 – 189

DME (Department Minerals and Energy RSA), 2009, Operating and Developing Coal Mines in the Republic of South Africa, http://dme.gov.za/pdfs/minerals/D2%202009%20part%202.pdf Accessed 28/11/2009

Di Blasi, Columba, 2000, Dynamic Behaviour of Stratified Downdraft Gasifiers, Chemical Engineering Science, 55, 2931 – 2944

Dippenaar, R.J, M.A. Barcza, R.T. Jones, 1988, Energy Considerations for the Melting of DRI as a Funstion of the Degree of Pre-Reduction, Proceedings: 7th Process Thecnology Conference, Totonto, Ontario, Canada April 1988

Dressel, G.L. 1998, Use of DRI in EAFs Part I, Iron & Steelmaker, October 1998, 121 – 122.

Dressel, G.L. 1998, Use of DRI in EAFs Part II, Iron & Steelmaker, November 1998, 61 – 62.

Dressel, G.L. 1998, Use of DRI in EAFs Part III, Iron & Steelmaker, December 1998, 47 – 48.

Dressel, G.L. 1999, Use of DRI in EAFs Part IV, Iron & Steelmaker, January 1999, 53 – 55.

Duarte, Pablo, E, Klaus Knop, Peter Masloch, 2002, The HYL mini-module concept: The optimum integration of a DR plant in minimills, MPT International 25, 4/2002 74-81

Energiron, 2009, The Innovative Direct Reduction Technology, http://www.energiron.com/media/news/Downloads/Energiron Brochure 2007.pdf, Accessed 22/10/09

Fenton, Michael D, 2005, Mineral Commodity Profiles – Iron and Steel, USGS Open-File Report 2005 -1254, US Geological Survey, Reston Virginia.

Finkers, H.J, A.C. Hoffmann, 1998, Structural Ratio for Predicting the Voidage of Binary Particle Mixtures, AIChE Journal Feb, 495 – 498.

Formanek, Lothar, Fritz, Rose, 2009, Uhlmann's Encyclopedia of Industrial Chemistry 5th Ed, Wiley-VCH Verlag, GmbH, Weinheim

Friede, H.M, A.A. Heija, A. Koursaris, 1982, Archaeo-metallurgical studies of iron smelting slag from prehistoric sites in Southern Africa, JSAIMM, Feb, 38 – 48

Fruehan, R.J. 1977, The Rate of Reduction of Iron Oxides by Carbon, Metallurgical Transaction B, 8B, June, 279 – 286

Geldenhuis, P.J, 1984, Coal Based Direct Reduction in South Africa – Some Results Already Achieved and Anticipated. IISI 16th Annual Meeting of the Committee on Technology, Johannesburg March 1984.

Gojić, M, 2004, Current State and Development of Steelmaking Processes, Metallurgica 43 3, 163 – 168

Gojić, M. and S. Kožuh, Development of Direct Reduction Processes and Smelting Reduction Processes for the Steel Production, Kem. Ind. 55(1) 1 - 10 2006.

Grobler, F. and R.C.A Minnitt, 1999, The increasing role of direct reduced iron in global steelmaking, JSAIMM, March/April, 111 – 116.

Hall, J, 1980, Spotlight on Highveld Steel and Vanadium Corporation Limited, JSAIMM, Sep, 323 – 326

Hamilton, Colin, 2009, A New Era for Steel – Drivers, Implications and Risks, Ironmaking and Steelmaking, 36, 4, 255 – 258.

Herman, J.C. V Leroy, 1996, Influence of Residual Elements on Steel Processing and Mechanical Properties, Metal Working and Steel Processing, Cleveland, Oct 14 – 17 1996.

Hillisch, W, J Zirngast, 2001, Status of Finmet plant operation at BHP DRI, Australia, Steel Times International, March.

Hughes, Greg, D. 1995, Increasing Productivity and Profitability with the MIDREX Process, Direct From Midrex, 1st Quarter 1995

IMBS, 2009, Finesmelt Process, http://www.imbsworld.com/process.htm, Accessed 24/11/2209

I&ST, (Iron & Steel Technology), 2009, Industry Statistics, Feb, 12 – 17

Janke, D, L. Sovow, H-J Weddige, E Schultz, 2000, Scrap-based Steel Production and Recycling of Steel, Materiali in Tehnologije, 34 6 387 - 399

Jha, Rajesh, 2009, Coal Gasification and Syngas Based DRI, International Convention on Clean, Green & Sustainable Technologies in Iron & Steel Making, Bhubaneswar, India

Jones, J.A.T, B. Bowman, P.A. Lefrank, Fruehan R.J. Editor, 1998, The Making, Shaping and Treating of Steel, 11th Edition, Steelmaking and Refining Volume, Ed. R.J. Fruehan, The AISE Steel Foundation, Pittsburgh, Pa.

Kang, Heung Won, Won Sub Chung, Takeaki Murayama, Yoichi Ono, 1998, Effect of Ore Shape on Gaseous Reduction Rate, ISIJ International, 38, 11, 1194 – 1200.

Kern, D.Q, 1950, Process Heat Transfer, McGRaw-Hill Kogakusha.

Kinsley, Robert, R, 2001, Properly Purge and Inert Storage Vessels, CEP, Feb, 57 - 61

Kneale, Clive, D, 2009, King II Report on Corporate Governance 2002, http://www.rtmc.co.za/Documents/RTMC%20Documents/Corporate%20Governace/King%20II%20REPORT%20SUMMARY%20OF%20CODE.pdf, Accessed 26/11/2009

Knoef, H.A.M. 2008, BTG Biomass Gasification, http://www.btgworld.com/uploads/documents/Gasification%20Attachment%20Website%20v2.pdf, Acessed 28/112009

Knopfle, John, Robert Hunter, 2008, Direct Reduction's Role in the World Steel Industry, Ironmaking & Steelmaking, 35, 4, 254 – 259.

Kubachefski, O, C.B. Alcock, P.J. Spencer, 1993, Materials Thermo-chemistry, 6th Edition, Pergamon Press.

Levenspiel, Octave, 1972, Chemical reaction Engineering 2nd Ed, Wiley International Edition

Löf, G.O.G, R.W. Hawley, 1948, Unsteady state Heat Transfer between Air and Loose Solids, Industrial and Engineering Chemistry, June, 1061 – 1069

Lowry, H.H. Ed, 1963, Chemistry of Coal Utilization, Supplementary Volume, John Wiley & Sons, New York.

Manamela, M.M, P.C. Pistorius, 2005, Ore size does affect direct reduction of titaniferous magnetite. JSAIMM, 105, March, 183 – 186.

Manning, C.P and R.J. Fruehan, 2001, Emerging Technologies for Iron and Steelmaking, JOM October

Mans, Peter, 1986, The use of Coal for Direct Reduction in the SL/RN Rotary Kiln Process, Sa Mining World, June, 29 – 37

Matthesius, G.A, R.M. Morris, M.J. Desai, 1987, Prediction of Volatile Matter in Coal from Proximate and Ultimate Analyses, JSAIMM, June, 157 – 161

Mayhew, Y.R, G.F.C. Rogers, 1974, Thermodynamic Properties of Fluids, Basil Blackwell, Oxford

McCabe, Warren. L, Julian C. Smith, 1976, Unit Operations of Chemical Engineering, McGraw-Hill Kogakusha.

MBM (Metal Bulletin Monthly) 2007, Alternative Ironmaking, April, 48 - 50

Midrex Corp, 2009, 2008 World Direct Reduction Statistics, http://www.midrex.com/uploads/documents/MIDREXStatsbook2008.pdf, Accessed 24/11/2009

Midrex Technologies(1), 2009, The world of Direct Reduction, http://www.midrex.com/uploads/documents/Direct Reduction Brochure1.pdf, Accessed 22/10/09

Midrex Technologies(2), 2009, Direct from MIDREX, From the Hearth: RHF Technologies, Special Report Winter 2008/2009, http://www.midrex.com/uploads/documents/DFM%20-RHFnewsletter 4Q2008.pdf, Accessed 24/11/2009

Nair, P.M, J.K. Kundoo, 2003, Ispat Industries Limited: Operation with High Percentages of Lump Ore, Direct From Midrex 1st Quarter 2003.

Ocw, 2009, Screw Conveyor, Department of Mechanical Engineering, Calos III University, http://ocw.uc3m.es/ingenieuria/transport-engineering/transparencias/Screw_conveyor.pdf Accessed 29/11/2209

Oeters, Franz, Manfred Ottow, 2009, Uhlmann's Encyclopedia of Industrial Chemistry 5th Ed, Wiley-VCH Verlag, GmbH, Weinheim.

Peacey, J.G, W.G. Davenport, 1979, The Iron Blast Furnace – Theory and Practice, Pergamon Press

Perry, Robert.H, Cecil.H. Chilton, 1973, Chemical Engineers' Handbook, 5th Edition, McGraw-Hill Kogakusha.

Palmer, Greg, Tony Howes, 1998, Heat Transfer in Rotary Kilns, Cement Industry Federation Technical Conference 1998

Pichler, H, H. Merkel, 1949, Chemical and Thermomagnetic Studies on Catalysts for the Synthesis of Hydrocarbons, Bureau of Mines Tec. Paper 718, 108pp

Plaul, F., C Böhm, J.L. Schenk, 2009, Fluidised-bed technology for the production of iron products for steelmaking, JSAIMM, 108 Feb 2009

Prnewswire 1997, Kvearner Metals Commissions Multi-Million Dollar Kiln, http://www.prnewswire.co.uk/cgi/news/release?id=13984, Accessed 24/10/2006
Reed, Thomas B, Agua Das, 1998, Handbook of Biomass Downdraft Gasifier Engine Systems, Biomass Energy Foundation Press.

Reed, Thomas, Agua Das, 1998, Handbook of Biomass Downdraft Gasifier Engine Systems 2nd Edition, The Biomass Energy Foundation Press, Colorado

A Mathematical Model for Stratified Downdraft Gasifiers, Symposium on Mathematical Modelling of Biomass Pyrolysis Phenomena, Aug 1983

Reed, Thomas, B, Benjamin Levie, Michael L. Markson, Michael S. Graboski, 1983, A Mathematical Model for Stratified Downdraft Gasifiers, Symposium on Mathematical Modelling of Biomass Pyrolysis Phenomena, Aug 1983

Reed, Thomas, Ray Desrosiers, 1979, The Equivalence Ratio: The Key to Understanding Pyrolisis, Combustion and Gasification of Fuels, Encyclopedia of Biomass Thermal Conversion, Bef Press

Reed, T.B, R Walt, S Ellis, A Das, S Deutch, 1999, Superficial Velocity – The Key to Downdraft Gasification, 4th Biomass Conference of the Americas, Oakland

Rosenquist, Terkel, 1974, Principles of Extractive Metallurgy, McGrw-Hill Kogakusha,

Schilling, H-D, B. Bonn, U. Kraus, 1985, Coal Gasification - Existing Processes and New Developments, Verlag Glückauf GmbH, Essen.

Seshadri, Varadarajan, Rodrigo Ottomi da Silva Pereira, 1986, Comparison of Formulae for Determining Heat Transfer Coefficient of Packed Beds, Transactions ISIJ, 26 604 610.

Smith, Tim, 2001, International symposium on direct reduction - The Arab Iron & Steel Union (Arab Steel), Cairo, 21 – 23 October 2001, Steel Times International, Dec/Jan 2001/2 40 - 43

Stubbles, John, 2006, The Minimill Story, AIST J Keith Brimacombe Memorial Lecture, AISTech Cleveland Ohio.

Stull, D.R., H. Prophet, 1970, JANAF Thermochemical Tables, 2nd Edition, United States Department of Commerce, Document NSRDS-NBS 37, Washington June 1971.

Sutton, David, J.R.H. Ross, Niall O'Reilly, 2009, The Future's A Gas, New Science Education Initiative, http://www.ul.ie/~childsp/CinA/Issue58/TOC14_FutureA.htm Accessed 02/06/09

Tateishi, M, H. Fujimoto, T Harada, H. Sugitatsu, 2008, Development of EAF Dust Recycling and Melting Technology Using Coal-based FASTMET Process, Direct from MIDREX, From the Hearth: RHF Technologies, Special Report Winter 2008/2009, http://www.midrex.com/uploads/documents/DFM%20-RHFnewsletter 4Q2008.pdf, Accessed 24/11/2009

Theron, J.A. 1985, M.Eng. thesis, University of Pretoria.

Thurnhofer, A, M. Schlachinger, F. Winter, M. Mali, J.L. Schenk, 2005, Iron Ore Reduction in Laboratory-scale Fluidised BGed Reactor – Effect of Pre-reduction on Final Reduction Degree, ISIJ International, 45, 2, 151 – 158

Turkdogan, E.T, R.J. Fruehan, Fruehan R.J. Editor, 1998, The Making, Shaping and Treating of Steel, 11th Edition, Steelmaking and Refining Volume, Ed. R.J. Fruehan, The AISE Steel Foundation, Pittsburgh, Pa.

Venter, J.L, A.M. Saayman, Experience with the SL/RN Process at Iscor,

Visage, S, 1982, Spotlight on Coal-based Direct Reduction at Iscor, JSAIMM, June, 165 - 167

WSA(1), (Worldsteel Association), 2009, World Steel figures in 2009, http://www.worldsteel.org/pictures/publicationfiles/WSIF09.pdf, Accessed 1/12 2009

WSA(2), (Worldsteel Association), 2009,Steel and You The Life of Steel, http://www.worldsteel.org/index.php?action=publicationdetail&id=71, Accessed 1/12 2009

Appendix 1: Mass Balance over EAF

		Inputs					Outputs			
Material	**Scrap**	**DRI**	**Dol**	**Lime**	**Coke**	**O2**	**Steel**	**Slag**	**Dust**	**Gas**
t/heat	22.85	22.85	0.0	4.9	0.4	2.86	40.1	9.4	0.9	1.3
Nm3/heat						2000				1048.3
Fe	96.16	84.39	0.00	0.00	0.00	0.00	99.88		15.00	
C	0.03	0.68	0.00	0.00	0.00	0.00	0.40			
Mn	0.80	0.00	0.00	0.00	0.00	0.00	0.46			
Cu+Ni	0.20	0.00	0.00	0.00	0.00	0.00	0.11			
S	0.05	0.06	0.00	0.00	0.00	0.00	0.039	0.101		
P	0.03	0.11	0.00	0.00	0.00	0.00	0.08			
SiO2	2.00	4.45	1.90	1.80	45.00	0.00	0.00	16.97		
Al2O3	0.50	2.18	0.90	0.90	25.00	0.00	0.00	7.18		
MgO	0.00	0.00	40.60	2.10	5.00	0.00	0.00	1.13		
CaO	0.00	0.00	56.50	95.20	15.00	0.00	0.00	49.73		
FeO	0.00	8.17	0.00	0.00	0.00	0.00	0.00	25.00		
O	0.00	1.82	0.00	0.00	0.00	0.00	0.00			
C/CO2/O	0.00	0.00	0.00	0.00	85.00	0.00	0.00			
Ash	2.50	0.00	0.00	0.00	15.00	0.00	0.00			
B2								3.00		
B4	0.00	0.00	0.00	0.00	0.00	0.00	0.00	2.11		
Total	99.8	100.0	99.9	100.0	175.0	0.0	101.0	100.0		
Yield							87.7	%		
Energy use							603.3	kWu/t		

Enthalpy required to melt an EAF charge

Component	Mr	Units	Steel	Units	Slag	Units
Fe	55.85	kg/kmol	99.9	%	0.0	%
FeO	68.9	kg/kmol	0.0	%	25.0	%
C	12	kg/kmol	0.0	%	0.0	%
SiO2	60.1	kg/kmol	0.0	%	17.0	%
Al2O3	102	kg/kmol	0.0	%	7.2	%
MgO	40.3	kg/kmol	0.0	%	1.1	%
CaO	56.1	kg/kmol	0.0	%	49.7	%
Volume			40.1	t	9.4	t
					233	kg slag/t
dH_{298-T}						
Tapping Te	1620	°C	1893	°K	1923	°K
Fe			55561449	kJ	0	kJ
FeO			0	kJ	3172192	kJ
C			0	kJ	0	kJ
SiO2			0	kJ	3007346	kJ
Al2O3			0	kJ	1310084	kJ
MgO			0	kJ	218459	kJ
CaO			0	kJ	7096352	kJ
Total			55563342	kJ	6181460	kJ
			385	kWu/t	43	kWu/t
					428	kWu/t LS
dH_f						
FeO			6886871	kJ	-8631230	kJ
			48	kWu/t	-60	kWu/t
CO			-3230000	kJ		
			-22	kWu/t		
				kWu/t	-34	kWu/t
Secondary						
Tap to tap time			60	mins		
Suck time	20	mins				
Air flow	19000	Nm3/h	22379060	kJ		kJ
Air temp	1650	°C	155	kWu/t LS		kWu/t LS
Water flow	380	m3/h	7921586	kJ		kJ
Water dT	5	°C	55	kWu/t LS		kWu/t LS
Total					603	kWu/t LS

Data Source: Peacy & Davenport

dH in kJ/kmole	m*T		C	
[Ht-H298] Fe	44		-5800	kJ/kmol
[Ht-H298] FeO	61.1		-24100	kJ/kmol
[Ht-H298] C	23.5		-11800	kJ/kmol
[Ht-H298] SiO2	72.8		-26200	kJ/kmol
[Ht-H298] Al2O3	132		-55000	kJ/kmol
[Ht-H298] MgO	55		-22300	kJ/kmol
[Ht-H298] CaO	55.5		-21200	kJ/kmol
[Ht-H298] N2	34.4		13000	kJ/kmol
[Ht-H298] O2	36.2		13500	kJ/kmol
[Ht-H298] CO	35.3		14000	kJ/kmol
$dHf_{FeO\ 1300K}$			-265000	kJ/kmol
$dHf_{CO\ 1300K}$			-114000	kJ/kmol

Scrap analyses

Name	HMS#1	HMS#2	Shred	Bales	Turnings	Pig Iron	Pool	Hecketts	Scrap mix	DRI	Used to calculate DRI	
											Ore	DRI*
ISRI #												93
t/heat	27.2	27.2							54.4	10.0		
Fe	96.167	96.157	96.950	94.390	94.380	94.960	89.910	61.940	96.162	84.391	66.500	61.845
C	0.025	0.030				4.300	4.300		0.028	0.682		0.500
Mn	0.800	0.800				0.500	0.500		0.800			
Cu+Ni	0.200	0.200				0.000	0.000		0.200			
S	0.033	0.035	0.030	0.040	0.060	0.050	0.050	0.020	0.034	0.014		0.010
P	0.025	0.028	0.020	0.020	0.020	0.090	0.090	0.010	0.027	0.109		0.080
SiO2	2.000	2.000	1.000	4.000	1.000	0.000	0.010	5.000	2.000	4.448	3.260	3.260
Al2O3	0.500	0.500	1.000	1.500	0.500	0.100	0.010	3.000	0.500	2.183	1.600	1.600
MgO	0.000	0.000	0.000	0.010	0.010	0.000	0.010	10.000	0.000	0.000		
CaO	0.000	0.000	0.000	0.010	0.010	0.000	0.010	20.000	0.000	0.000		
FeO	0.000	0.000	0.000	0.010	0.010	0.000	0.010	0.010	0.000	8.172		5.989
O	0.000	0.000	0.000	0.010	0.010	0.000	0.800	0.010	0.000	1.820	28.577	1.334
C/CO2	0.250	0.250	1.000	0.010	4.000	0.000	4.300	0.010	0.000			
Ash	2.500	2.500	2.000	5.520	1.520	0.000	0.040	38.000	2.500			
B2												
B4	0.000	0.000	0.000	0.004	0.013	0.000	1.000	3.750	0.000	0.000		
Total	100.0	100.0	100.0	100.0	100.0	100.0	100.0	100.0	99.8	100.0	99.9	73.3

Sulfur Distribution in EAF Slags

Source: Making, Shaping &Treating of Steel, Fig 2.116

%SiO2	(S)/[S]*(FeO)
10	145
15	80
20	50

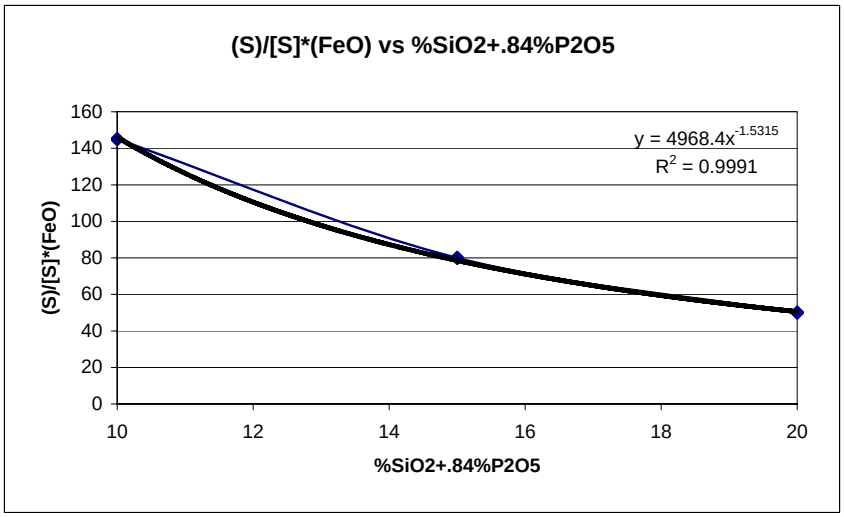

Maximum cost of DRI

Assumptions

Lime	800	R/t
Electricity	0.25	R/kWu
Electrode	40000	R/t

Material	Scrap	DRI	% DRI	Lime	Coke	O2	Steel	Slag	Dust	Gas	Yield	Power	El cons
t/heat	22.85	22.85	50.0	4.9	0.4	2.86	40.1	9.4	0.9	1.3	87.73	603.28995	2.14
	42	0	0.0	2.82	0.4	2.86	39.95	5.23	0.84	0.96	95.12	564.27	2.0

Scrap price	1500	2000	2500	3000	3500	4000	4500	5000	5500	6000
50% DRI										
Scrap	34275	45700	57125	68550	79975	91400	102825	114250	125675	137100
Lime	3904	3904	3904	3904	3904	3904	3904	3904	3904	3904
Electricity	150.8225	150.82249	150.8225	150.82249	150.8225	150.82249	150.822488	150.82249	150.82249	150.82249
Electrode	85.53	85.53	85.53	85.53	85.53	85.53	85.53	85.53	85.53	85.53
Total	38415.35	49840.35	61265.35	72690.35	84115.35	95540.35	106965.35	118390.35	129815.35	141240.35
DRI=	1184.32	1603.36	2022.39	2441.43	2860.47	3279.51	3698.54	4117.58	4536.62	4955.65
%	78.95	80.17	80.90	81.38	81.73	81.99	82.19	82.35	82.48	82.59
100% scrap										
Scrap	63000	84000	105000	126000	147000	168000	189000	210000	231000	252000
Lime	2256	2256	2256	2256	2256	2256	2256	2256	2256	2256
Electricity	141.07	141.07	141.07	141.07	141.07	141.07	141.07	141.07	141.07	141.07
Electrode	80	80	80	80	80	80	80	80	80	80
Total	65477.07	86477.069	107477.1	128477.07	149477.1	170477.07	191477.069	212477.07	233477.07	254477.07

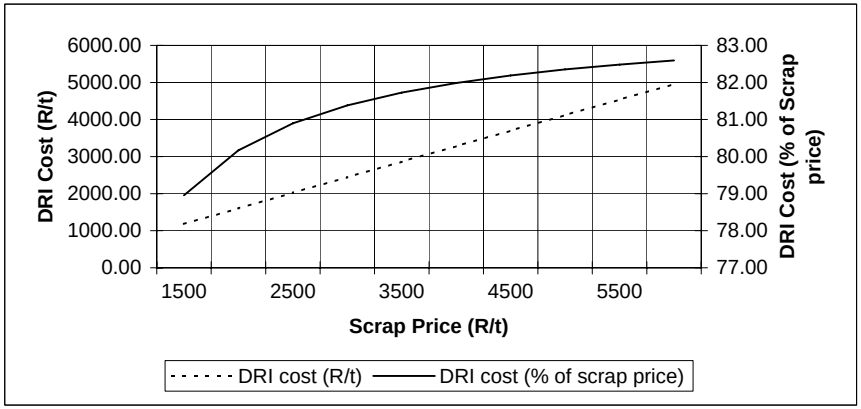

Appendix 2: Prediction of volatiles composition

Source: Matthesius, Morris & Desai SAIMM June 1987

X											Y		Anal
0.9632	0.7500	0.8000	0.4286	0.2727	0.8342	0.0000	0.0000	0.0000	0.0000		Coke		C
0.0059	0.2500	0.2000	0.0000	0.0000	0.0679	1.0000	0.1111	0.1765	0.0588		CH4		H
0.0036	0.0000	0.0000	0.5714	0.7273	0.0652	0.0000	0.8889	0.0000	0.0000		C2H6		O
0.0129	0.0000	0.0000	0.0000	0.0000	0.0197	0.0000	0.0000	0.8235	0.0000		CO		N
0.0144	0.0000	0.0000	0.0000	0.0000	0.0130	0.0000	0.0000	0.0000	0.9412	**X**	CO2	=	S
1.0000	0.0000	0.0000	0.0000	0.0000	0.0000	0.0000	0.0000	0.0000	0.0000		Tar		1-V
0.0000	1.0000	0.0000	0.0000	0.0000	0.0000	0.0000	0.0000	0.0000	0.0000		H2		.82H
0.0000	0.0000	1.0000	0.0000	0.0000	0.0000	0.0000	0.0000	0.0000	0.0000		H2O		.15H
0.0000	0.0000	0.0000	1.0000	0.0000	0.0000	0.0000	0.0000	0.0000	0.0000		NH3		.59O
0.0000	0.0000	0.0000	0.0000	1.0000	0.0000	0.0000	0.0000	0.0000	0.0000		H2S		.31O

X x Y = B

=> B x X^{-1} = Y

	Anal		Gus 8		X^{-1}										Gus 8	Y
	C		85.64		0	0	0	0	0	1	0	0	0	0	81.60	Coke
	H		4.01		0	0	0	0	0	0	1	0	0	0	3.29	CH4
	O		5.98		0	0	0	0	0	0	0	1	0	0	0.60	C2H6
	N		2.29		0	0	0	0	0	0	0	0	1	0	3.53	CO
	S		2.08	**X**	0	0	0	0	0	0	0	0	0	1	1.85	CO2
	1-V		81.6		1.198753	0	0	0	0	-1.154639	-0.899065	-0.959003	-0.513786	-0.3269	2.49	Tar
x H		0.82	3.2882		-0.065592	1	-0.124986	-0.214329	-0.062473	0.061392	-0.200806	-0.147527	0.09953	0.108789	1.84	H2
		0.15	0.6015		-0.087927	0	1.124986	0	0	0.080642	0.065946	0.070342	-0.605131	-0.794224	2.43	H2O
x O		0.59	3.5282		-0.028677	0	0	1.214329	0	0.011957	0.021508	0.022942	0.012291	0.00782	1.44	NH3
		0.31	1.8538		-0.016557	0	0	0	1.062473	0.000648	0.012418	0.013246	0.007096	0.004515	0.93	H2S
															100	

Leeupan DR

Source: DME 2007

Proximate (Air dry)	Moist	3.9	3.9	3.90
	Ash	12.4	12.4	
	Volatiles	22.2		
	S	0.78		
	C Fix	60.72		
		100		
Ultimate (DAF)	C	84.24	70.51	
	H	4.06	3.40	
	O	8.84	7.40	
	N	1.92	1.61	
	S	0.93	0.78	
		99.99		
Volatiles	Coke	77.80		65.12
	CH4	3.33		2.79
	C2H6	0.61		0.51
	CO	5.22		4.37
	CO2	2.74		2.29
	Tar	4.00		3.35
	H2	1.80		1.50
	H2O	3.74		3.13
	NH3	1.02		0.85
	H2S	-0.26		0.00
		99.99		
Ash	SiO2	47.1		5.84
	Al2O3	38.9		4.82
	Fe2O3	2.83		0.35
	P2O5	0.46		0.06
	TiO2	1.89		0.23
	CaO	2.45		0.30
	MgO	1.07		0.13
	K2O	0.93		0.12
	Na2O	1.51		0.19
	SO3	2.65		0.33
		99.79		
Total			99.99	100.18

CV 27.65 MJ/kg

Prediction of volatiles composition of Leeupan DR

Source: Matthesius, Morris & Desai SAIMM June 1987

X											Y		Anal
0.9632	0.7500	0.8000	0.4286	0.2727	0.8342	0.0000	0.0000	0.0000	0.0000		Coke		C
0.0059	0.2500	0.2000	0.0000	0.0000	0.0679	1.0000	0.1111	0.1765	0.0588		CH4		H
0.0036	0.0000	0.0000	0.5714	0.7273	0.0652	0.0000	0.8889	0.0000	0.0000		C2H6		O
0.0129	0.0000	0.0000	0.0000	0.0000	0.0197	0.0000	0.0000	0.8235	0.0000		CO		N
0.0144	0.0000	0.0000	0.0000	0.0000	0.0130	0.0000	0.0000	0.0000	0.9412	**X**	CO2	=	S
1.0000	0.0000	0.0000	0.0000	0.0000	0.0000	0.0000	0.0000	0.0000	0.0000		Tar		1-V
0.0000	1.0000	0.0000	0.0000	0.0000	0.0000	0.0000	0.0000	0.0000	0.0000		H2		.82H
0.0000	0.0000	1.0000	0.0000	0.0000	0.0000	0.0000	0.0000	0.0000	0.0000		H2O		.15H
0.0000	0.0000	0.0000	1.0000	0.0000	0.0000	0.0000	0.0000	0.0000	0.0000		NH3		.59O
0.0000	0.0000	0.0000	0.0000	1.0000	0.0000	0.0000	0.0000	0.0000	0.0000		H2S		.31O

X x Y = B

=> B x X^{-1} = Y

	Anal		Leupan		X^{-1}										Volatiles	Y
	C		84.24		0	0	0	0	0	1	0	0	0	0	77.80	Coke
	H		4.06		0	0	0	0	0	0	1	0	0	0	3.33	CH4
	O		8.84		0	0	0	0	0	0	0	1	0	0	0.61	C2H6
	N		1.92		0	0	0	0	0	0	0	0	1	0	5.22	CO
	S		0.93	**X**	0	0	0	0	0	0	0	0	0	1	2.74	CO2
	1-V		77.8		1.198753	0	0	0	0	-1.154639	-0.899065	-0.959003	-0.513786	-0.3269	4.00	Tar
x H		0.82	3.3292		-0.065592	1	-0.124986	-0.214329	-0.062473	0.061392	-0.200806	-0.147527	0.09953	0.108789	1.80	H2
		0.15	0.609		-0.087927	0	1.124986	0	0	0.080642	0.065946	0.070342	-0.605131	-0.794224	3.74	H2O
x O		0.59	5.2156		-0.028677	0	0	1.214329	0	0.011957	0.021508	0.022942	0.012291	0.00782	1.02	NH3
		0.31	2.7404		-0.016557	0	0	0	1.062473	0.000648	0.012418	0.013246	0.007096	0.004515	-0.26	H2S
															99.99	

Appendix 3: Process Mass & Enthalpy Balance

Assumptions

Metallisation	**93** %			
Oxide	**Fe2O3**	O/Fe =	1.5	
Coal	Leeupan DR Fraction			
CO	**67.00**	**33.00**	CO_2	
H_2	**67.00**	**33.00**	H_2O	
Combustion	CO, H2 react in ratio present			

Comments

1. Coal proximate anal on air-dry basis
2. Coal ultimate anal on air-dry basis
3. Kilomoles of Gas.Air is only the required O2

Bold cells are independent cells

Sulphur dist 100.00 % in DRI

		Pre-heat Shaft					Reduction Shaft					
	Unit	**Ore**	**C Gas**	**C Air**	**Top Gas**	**Oxide**	**Coal**	**Steam**	**Gas. Air**	**DRI**	**Red Gas**	
Moist	%	1.50					3.90					
B.D.	t/m3	2.55				2.55	0.65					
Fe	%	65.82				65.81	0.00			90.11		
SiO2	% (in ash)	3.50				3.50	47.10			4.79		
Al2O3	% (in ash)	1.40				1.40	38.90			1.92		
CaO	% (in ash)	0.06				0.06	2.45			0.08		
MgO	% (in ash)	0.04				0.04	1.07			0.05		
Other	% (in ash)	0.90				0.90	10.27			1.23		
S	%	0.01				0.01	0.78			0.01		
Ash	%						12.40					
C	%						70.51					
H	%						3.40					
O	%	28.28		23.30		28.28	7.40		23.30	1.81		
N	%			76.70			1.61		76.70			
CO	Vol %		26.5		0.0						26.5	67.0
CO2	Vol %		13.0		23.8						13.0	
H2	Vol %		8.6		0.0						8.6	
H2O	Vol %		4.3		7.8			100.00			4.3	
N2	Vol %		47.6		68.4						47.6	
Mr	kg/m3		27.4		31.0			18	28.84		27.4	
Kmoles	Kmoles(O_2)		**0.71**	0.12	1.2	0.34	0.91	0.00	0.22	0.34	1.78	
	Kmoles std			0.6		0.002	0.01		1.07	0.00	0.01	
Mass	Rate (t/h)	0.03	0.02	0.02	0.04	0.03	**0.01**	**0.00**	0.03	**0.02**	0.049	
Vol	Vol (Nm3/h)		16	13	26			0.0	24		40	40
Temp	Temp (°C)	25	35	25	200	1200	25		25	850	850	35
Press	Press (kPa)											
CV	CV (MJ/kg)				0.00		27.58				4.28	
Gas velocity	m/s		20	20	20				20		20	20
Diam	mm		18	16	28				21		54	28
Coal Rate	kg Coal/t DR	1369	553	815	0	1369	571		1464	1000	1390	
Ret Time	h	700	2000	68.3	h	1000	3000			114.9	h	

Mass Balance Check

Pre-heat shaft			
In		**Out**	
Ore	**0.03**	Oxide	0.03
Comb gas	0.02	Top gas	0.04
Comb air	0.02		
	0.065		**0.065**
Red shaft			
In		**Out**	
Oxide	0.03	DRI	0.02
Coal	0.01	Red gas	0.05
Gasif air	0.03	Ash+S	0.00
	0.071		**0.071**
Overall			
In		**Out**	
Ore	0.03	DRI	0.02
Coal	0.01	Top gas	0.04
Gasif air	0.03	Ash+S	0.00
Comb air	0.02	Extra gas	0.03
	0.089		**0.089**

Reduction shaft

Enthalpy Demand	201,935	kJ/h
Enthalpy Supply	-202,000	kJ/h

Pre-heat shaft

Enthalpy Demand	67,365	kJ/h
Enthalpy Supply	-68,139	kJ/h

Ore	28.8	kg/h
Reductant	12.0	kg/h

Kmoles Check

Fe					0.339				0.339		
C						0.705				0.705	
H2						0.230				0.230	
O2					0.254	0.041		0.224	0.012	0.507	0.507
N2						0.007		0.842		0.849	0.849

Mass & Enthalpy balance

Reduction Shaft

Sensible Heat in Reagents						
Specie	**A*T**	**B**	**Temp C**	**Enthalpy kJ/kmole**	**Kmoles**	**Enthalpy kJ**
Fe2O3	144	-43000	1200	169112	0.169	28649
FeO	52.2	-15600	0	-1349	0.000	0
Fe	30.8	-9200	0	-792	0.000	0
C	15.3	-4600	25	-41	0.705	-29
CO	30.2	-9100	0	-855	0.000	0
CO2	45.6	-14100	0	-1651	0.000	0
H2	29.3	-8800	27.3	-1	0.204	0
H2O	35.8	-10800	28	-24	0.026	-1
O2	31.6	-9600	25	-183	0.224	-41
N2	30	-9000	25	-60	0.842	-51
						28528
Heat of Reaction						
C + O2 <=> CO2			-394000	1	0.233	-91,670
C + ½O2 <=> CO			-111000	1	0.472	-52,434
CO + ½O2 <=> CO2			-283000	0	0.000	0
H2 + ½O2 <=> H2O			-242000	1	0.050	-12,075
Diss. Of coal			-1441	kJ/kg		-17,292
Fe2O3 <=> 2Fe + 1½O2			826000	1	0.000	0
Fe2O3 <=> 2FeO + ½O2			294000	1	0.169	49,807
FeO <=> Fe + ½O2			266000	1	0.315	83,817
						-39,847
Sensible Heat in Products						
Fe2O3	135	-40200	0	-3345	0.000	0
FeO	52.2	-15600	0	-1349	0.000	0
Fe	38.4	-11400	1200	45163	0.339	15,302
C	15.3	-4600	0	-423	0.000	0
CO	35.3	-14000	850	25642	0.472	12,113
CO2	58.6	-26000	850	39808	0.233	9,262
H2	32.5	-12200	850	24298	0.154	3,744
H2O	47.4	-22200	850	31030	0.076	2,355
O2	36.2	-13500	850	27153	0.000	0
N2	34.4	-13000	850	25631	0.849	21,756
						64,531
Summary						
Reduce oxide						133,624
Heat DRI						15,302
Heat Gas						49,229
Heat loss						3,779
Total Enthalpy Demand						**201,935**
Oxidise reductant, including diss of coal						-173,471
Sens Heat in Oxide						-28,649
Sens Heat in Reductant						29
Sens Heat in Air						92
Total Enthalpy Supply						**-202,000**

Pre-heat shaft Shaft

Sensible Heat in Reagents						
Specie	**A*T**	**B**	**Temp C**	**Enthalpy kJ/kmole**	**Kmoles**	**Enthalpy kJ**
Fe2O3	135	-40200	25	30	0.169	5
FeO	52.2	-15600	0	-1349	0.000	0
Fe	30.8	-9200	0	-792	0.000	0
C	15.3	-4600	25	-41	0.000	0
CO	30.2	-9100	35	202	0.188	38
CO2	45.6	-14100	35	-55	0.093	-5
H2	29.3	-8800	35	224	0.061	14
H2O	35.8	-10800	35	226	0.030	7
N2	30	-9000	35	240	0.338	81
O2	31.6	-9600	25	-183	0.125	-23
N2	30	-9000	25	-60	0.469	-28
						89
Heat of Reaction						
C + O2 <=> CO2			-394000	1	0.000	0
C + ½O2 <=> CO			-111000	1	0.000	0
CO + ½O2 <=> CO2			-283000	1	0.188	-53,208
H2 + ½O2 <=> H2O			-242000	1	0.061	-14,842
Diss. Of coal			-1441 kJ/kg			0
Fe2O3 <=> 2Fe + 1½O2			826000	0	0.000	0
Fe2O3 <=> 2FeO + ½O2			294000	0	0.000	0
FeO <=> Fe + ½O2			266000	0	0.000	0
						-68,050
Sensible Heat in Products						
Fe2O3	144	-43000	1200	169112	0.169	28,649
FeO	52.2	-15600	0	-1349	0.000	0
Fe	38.4	-11400	850	31723	0.000	0
C	15.3	-4600	0	-423	0.000	0
CO	30.2	-9100	200	5185	0.000	0
CO2	45.6	-14100	200	7469	0.281	2,096
H2	29.3	-8800	200	5059	0.000	0
H2O	35.8	-10800	200	6133	0.092	561
O2	31.6	-9600	200	5347	0.000	0
N2	30	-9000	200	5190	0.807	4,188
						35,494
Summary						
Reduce oxide						0
Heat Ore						28,649
Heat Gas						6,845
Heat loss						31,870
Total Enthalpy Demand						**67,365**
Oxidise reductant, including diss of coal						-68,050
Sens Heat in Oxide						-5
Sens Heat in Reductant						-134
Sens Heat in Air						51
Total Enthalpy Supply						**-68,139**

Heat Transfer Through Shaft Wall

Theory (Holman)

$q = hAdT$
$q = kA/dx.dT$
$q = hAdT = kA/dx.dT = kA/dx.dT = kA/dx.dT = hAdT$
$q = (T_{in} - T_{out}) / (1/h_{in} + dx/k + dx/k + dx/k + 1/h_{out})$

Reduction shaft

T in:

Bed temps

mm below	Temp	dT
0	30	
100	1350	
200	950	400
300	850	100
400	850	0
500	850	0
T in	**806**	

h inner	112	W/m2'C				1/h	0.01
k working lir	1.1	W/m'C	Thickness	75	mm	dx/k	0.07
k insulating	0.32	W/m'C	Thickness	75	mm	dx/k	0.23
k steel shell	50	W/m'C	Thickness	8	mm	dx/k	0.00
h outer	10	W/m2'C				1/h	0.10
							0.41 **2.43**
T outer	20	'C					
q=	**1909**	W/m2					
T1	789	'C					
T2	659	'C					
T3	211	'C					
T4	211	'C					

Shaft dimensions:

Steel diam	350	mm
Height	500	mm
Circumf	1.10	m
Area	0.55	m2
Heat loss	1050	W
	3779112	J/h
	3779	**kJ/h**

Pre-heat shaft

T in:

Bed temps

mm below	Temp
0	200
100	200
200	400
300	800
400	1200
500	1400
T in	**600**

h inner	112	W/m2'C				1/h	0.01
k working lir	1.1	W/m'C	Thickness	75	mm	dx/k	0.07
k insulating	0.32	W/m'C	Thickness	75	mm	dx/k	0.23
k steel shell	50	W/m'C	Thickness	8	mm	dx/k	0.00
h outer	10	W/m2'C				1/h	0.10
							0.41 **2.43**
T outer	20	'C					
q=	**1409**	W/m2					
T1	583	'C					
T2	453	'C					
T3	5	'C					
T4	5	'C					

Shaft dimensions:

Steel diam	1000	mm
Height	2000	mm
Circumf	3.14	m
Area	6.28	m2
Heat loss	8853	W
	31870370	J/h
	31870	**kJ/h**

Calculation of Bustle Gas Temp

Assumption

Assume cooling gas enters cooling zone at 35 C
Assume gas leaves cooling zone at 235 C

Cooling Gas analysis

CO	Vol %	26.5
CO2	Vol %	13.0
H2	Vol %	8.6
H2O	Vol %	4.3
N2	Vol %	47.6

Reduction Gas analysis

CO	Vol %	26.5
CO2	Vol %	13.0
H2	Vol %	8.6
H2O	Vol %	4.3
N2	Vol %	47.6

Top Gas analysis

CO	Vol %	0.0
CO2	Vol %	23.8
H2	Vol %	0.0
H2O	Vol %	7.8
N2	Vol %	68.4

Sensible Heat to be extracted

Specie	A*T	B	Temp C	Enthalpy kJ/kmole	Kmoles	Enthalpy kJ
Fe2O3	135	-40200	0	-3345	0	0
FeO	52.2	-15600	0	-1349	0	0
Fe	38.4	-11400	850	31723	0.339	10748
C	15.3	-4600	0	-423	0	0

Cooling Gas

Specie	A*T	B	Temp C	Enthalpy kJ/kmole	Kmoles per Nm3	Enthalpy kJ
CO	30.2	-9100	235	6241.6	0.012	74
CO2	45.6	-14100	235	9064.8	0.006	53
H2	29.3	-8800	235	6084.4	0.004	23
H2O	35.8	-10800	235	7386.4	0.002	14
N2	30	-9000	235	6240	0.021	133
					0.045	297

Specie	A*T	B	Temp C	Enthalpy kJ/kmole	Kmoles per Nm3	Enthalpy kJ
CO	30.2	-9100	35	201.6	0.012	2
CO2	45.6	-14100	35	-55.2	0.006	0
H2	29.3	-8800	35	224.4	0.004	1
H2O	35.8	-10800	35	226.4	0.002	0
N2	30	-9000	35	240	0.021	5
					0.045	8

Reduction Gas

Specie	A*T	B	Temp C	Enthalpy kJ/kmole	Kmoles per Nm3	Enthalpy kJ
CO	35.3	-14000	850	25641.9	0.012	303
CO2	58.6	-26000	850	39807.8	0.006	232
H2	32.5	-12200	850	24297.5	0.004	94
H2O	47.4	-22200	850	31030.2	0.002	59
N2	34.4	-13000	850	25631.2	0.021	544
					0.045	1232

Specie	A*T	B	Temp C	Enthalpy kJ/kmole	Kmoles per Nm3	Enthalpy kJ
CO	30.2	-9100	35	201.6	0.012	2
CO2	45.6	-14100	35	-55.2	0.006	0
H2	29.3	-8800	35	224.4	0.004	1
H2O	35.8	-10800	35	226.4	0.002	0
N2	30	-9000	35	240	0.021	5
					0.045	8

Top Gas

Specie	A*T	B	Temp C	Enthalpy kJ/kmole	Kmoles per Nm3	Enthalpy kJ
CO	30.2	-9100	200	5184.6	0.000	0
CO2	45.6	-14100	200	7468.8	0.011	79
H2	29.3	-8800	200	5058.9	0.000	0
H2O	35.8	-10800	200	6133.4	0.003	21
N2	30	-9000	200	5190	0.031	159
					0.045	259

Specie	A*T	B	Temp C	Enthalpy kJ/kmole	Kmoles per Nm3	Enthalpy kJ
CO	30.2	-9100	35	201.6	0.000	0
CO2	45.6	-14100	35	-55.2	0.011	-1
H2	29.3	-8800	35	224.4	0.000	0
H2O	35.8	-10800	35	226.4	0.003	1
N2	30	-9000	35	240	0.031	7
					0.045	8

Increase in kJ/Nm3 288
Nm3/hr required 37.30

Reduction gas 39.96 Nm^3/h @ 850 ºC
Cooling gas 37.30 Nm^3/h @ 235 ºC
Total fan flow 77.26 Nm^3/h @ 35 ºC

Water Required

Assume water dT 10 ºC
Water cp 4.178 kJ/kgK

Theory

McCabe & Smith p704 & p696

$j_H = h/c_pG * (c_p\mu/k)^{2/3}$

Seshadri et al: Modified Ranz-Marshall

Modified Ranz-Marshall

$h = k/d_p[2+0.6(Re/e)^{.5}.(Pr)^{.33}]$

Wall HT coeff McCabe&Smith

$Nu = hd/k = 1.94Re^{0.5}Pr^{033}$

$Re = Gdp/\mu$

Figure 22-6

$j_H(\varepsilon/f)$	N_{Re}		$j_H(\varepsilon/f)$ (Calc'd)
0.21	20		0.205
0.11	100		0.102
0.048	500		0.051
0.034	1000		0.038
0.018	5000		0.019
0.016	10000		0.014

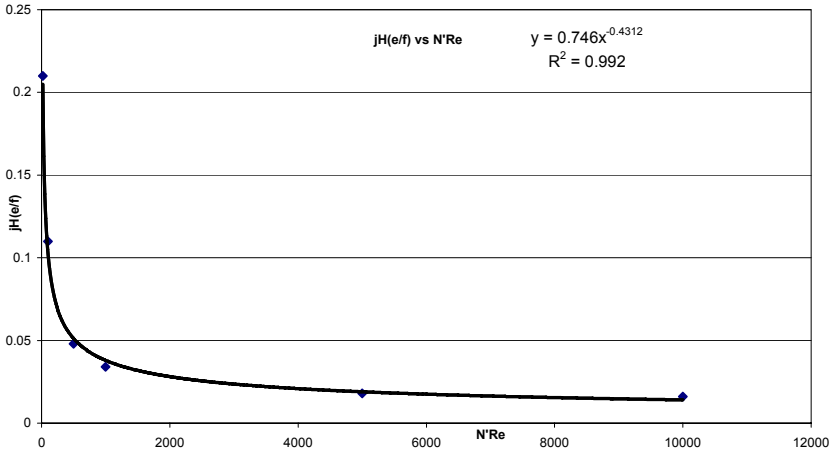

$j_H(e/f) = 0.746\ Re^{-0.4312}$

$Re = \sqrt{A}\ G/\mu$

A = Total surface area of a individual Particle m^2

G = Mass Velocity kg/m^2s

Q = hAdT

Particle			**Bed**	
Diameter	12	mm		
Volume	9.05E-07	m^3		
Matl density	5220	kg/m^3	2550	kg/m^3
Mass	0.0047	kg/particle	539917	particles/m^3
Surface Area	0.00045	m^2/particle	244	m^2/m^3
$\sqrt{A}$	0.0213	m^2		

Gas	**CO_2**	**N_2**	**Mix**	
Mr	44	28	29.63	
Comp (Vol)	23.8	68.4		
Comp (Mass)	35.3	64.7		
Temp	1000	1000		C
Cp	1.6421	1.1817	1.344	kJ/kgK
μ	0.00005292	0.000039	0.000039	kg/ms
k	0.09314	0.0617	0.06439221	W/mK
$c_p\mu/k$	9.33E-01	7.47E-01	8.20E-01	

Gas rate 26 Nm3/h

0.010 kg/s

Shaft

Diameter 0.15 m

Area 0.018 m^2

G 0.549 kg/m^2s

Re	297	Rep	2.96
$j_H(e/f)$	0.0640	Nu	3.13E+00
e	0.4		
f	0.83		

j_H	0.133			
h	102.72	W/m^2C	92.91	16.79
hv	30814.6		27872.2	
Q	$mcpdT = hAdT_{lm}$			

$(H^o_{1200}-H^o_{25)Fe2O3}$	169112	kJ/kmol	
kmol	0.000	kmol/s	
	8	kJ/s	0.0059 kg/s gas req'd
	7958	W	

dTlm

	Gas	Ore	Th2-Tc2	Th1-Tc1
In	1400	25	175	
Out	200	1200		200
			187	187

A required	0.41	m^2		
Vol required	0.00	m^3	0.00	0.00
H of shaft	0.10	m	0.08	0.09

Dp (mm)	H (m)
10	0.06
15	0.11
20	0.16
25	0.22
30	0.28

Orifice calculation

Theory (Perry 5th Ed 5-11)

$w = KYA_2\sqrt{(2(p_1-p_2)\rho_1)}$ (kg/s)

K = f(β, Position of downstream tap)) (no dimens)

β = Diam ratio (no dimens)

$Y = 1 - (1-r)/k\ (0.41 + 0.35\beta^4)$ (no dimens)

$r = p_2/p_1$ (no dimens)

$k = c_p/c_v$ (no dimens)

A_2 = cross sectional area of throat (m2)

u_{ave}/u_{max} = f(Re*) * u = u_{max} (no dimens)

β	K
0.224	0.618
0.316	0.63
0.388	0.64
0.447	0.66
0.5	0.675
0.548	0.71
0.594	0.755
0.635	0.79
0.672	0.84
0.704	0.905

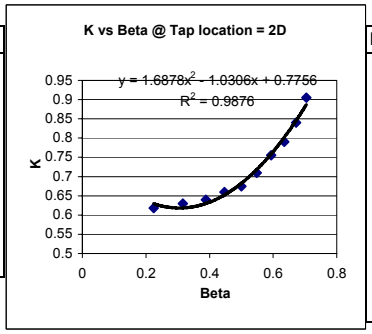

Re (u_{max})	v_{ave}/v_{max}
0.5	3.00E+03
0.74	4.00E+03
0.75	5.00E+03
0.755	6.00E+03
0.76	7.00E+03
0.765	8.00E+03
0.77	9.00E+03
0.775	1.00E+04
0.79	2.00E+04
0.8	3.00E+04
0.81	4.00E+04
0.82	5.00E+04

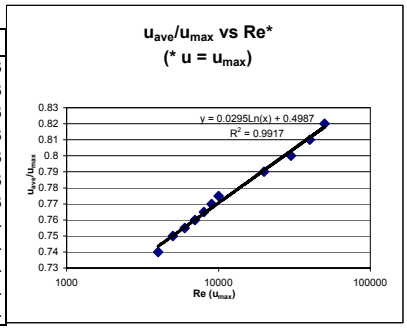

K = 1.6878 β^2 − 1.0306 β + 0.7756

u_{ave}/u_{max} = 0.0295 ln(Re*) + 0.4987

Gas:

Comp	Vol %	Mr	μ @ 35ºC	$y_i\mu_i M_i^{½}$	$y_i M_i^{½}$	cp/cv
CO	26.5	28	0.0185	0.025923	7.414697	1.4
CO2	13.0	44	0.015	0.012978	5.73888	1.3
H2	8.6	2	0.009	0.001099	0.17276	1.4
H2O	4.3	18	0.01	0.001805	0.765815	1.4
N2	47.6	28	0.018	0.045322	13.32338	1.4
Mix	100.0	27.42		0.087127	27.41554	1.4
					0.003178	cP
					3.18E-06	Ns.m2

Calculation

V =	39.96	Nm^3/hr	V =	37.30	Nm^3/hr
w =	0.0136	kg/s	w =	0.0114	kg/s
ρ_1 =	1.101	kg/m3	ρ_1 =	1.101	kg/m3
k (c_p/c_v) =	1.4		k (c_p/c_v) =	1.4	
μ =	3.18E-06		μ =	3.18E-06	
q_1 =	44.4	m^3/h	q_1 =	37.3	m^3/h
D	200	mm	D	150	mm
u =	0.39	m/s	u =	0.59	m/s
Re =	2.72E+04		Re =	3.05E+04	
D2	**110**	mm	D2	**91**	mm
A_2 =	0.00950	m2	A_2 =	0.00650	m2
Gues p2	1.5	kPa	Gues p2	1.5	kPa
	153	mm H2O		153	mm H2O
β =	0.550		β =	0.607	
Y =	0.869		Y =	0.865	
K =	0.719		K =	0.772	
p_1-p_2 =	2	Pa	p_1-p_2 =	3	Pa
	0	mm H2O		**0**	mm H2O
u_{ave}/u_{max} =	0.80		u_{ave}/u_{max} =	0.00	
u_{max} =	0.49		u_{max} =	0.73	

Orifice calibration

V =	15.90	Nm^3/hr
w =	0.0054	kg/s
ρ_1 =	1.101	kg/m3
k (c_p/c_v) =	1.4	
μ =	3.18E-06	
q_1 =	17.7	m^3/h
D	100	mm
u =	0.63	m/s
Re =	2.17E+04	
D2	**70**	mm
A_2 =	0.00385	m2
Gues p2	1.5	kPa
	153	mm H2O
β =	0.550	
Y =	0.869	
K =	0.719	
p_1-p_2 =	2	Pa
	0	mm H2O
u_{ave}/u_{max} =	0.00	
u_{max} =	0.79	
U measure	0.6	
	0.7	

OK

Appendix 4. Description of TGA Analysis Procedure

Introduction

This is a description of the procedure followed in the TGA tests of the discreet Iron Ore particles reduced with CO.

Apparatus

1. **Tube Furnace:** Carbolite STF1500 with Carbolite Controller
2. **Furnace Tube:** 1200mmx 69mm ID/81mm OD Al2O3
3. **Gas inlet:** 100mm of 75x3mm Aluminium tube sealing on the furnace tube by two flanges compressing a 10mm o-ring
4. **Chemical Balance:** Sartorius TE214S, 210g max, 0.1mg accuracy (Draft cover removed)
5. **Scale enclosure:** Rectangular box 300x400x150mm made from 6mm Perspex sealing in a 10mm wide X 15mm deep water seal machined into a 30mm Polypropylene Base
6. **Seal between scale enclosure and aluminium tube:** Two concentric Perspex tubes, 100mm high X 60 OD and 90mm high X 84 ID x 4mm thick mounted on the scale enclosure and filled with water.
7. **Radiation shield:** 85mm OD x 60mm ID x 25mm thick CB96 Cerablanket disk.
8. **Sample support rod:** 700mm x 6mm Al_2O_3 tube fixed to 70mm OD chipboard disk
9. **Connection:** RS232 to USB cable and driver
10. **Data Logging:** Laptop running Eltima RS232 Logger to capture scale readings at a frequency of 23 readings/8.5s

Procedure

1. A sample of the iron ore was prepared by selecting a number of spherical -12+10mm particles from the bulk sample.
2. The Tube Furnace was turned on, the controller setpoint was set to the required temperature and the furnace temperature allowed to reach and stabilise at this temperature (30 minutes)
3. The scale was turned on and allowed to stabilise for at least 30 minutes
4. The Iron particle was weighed and the mass noted accurately.
5. The sample holding disk was placed on the scale pan.
6. The scale enclosure was closed and it was ensured that the water seal was filled with water
7. 5l/min UHP Argon was opened and purged into the scale enclosure and into the Aluminium tube inlet for 10 min
8. After approximately 10 mins the gas inlet to the scale enclosure was closed whilst the Argon purging was maintained.
9. The sample support rod, crucible holder and crucible were placed onto the sample support holding disk.
10. The sample was placed into the crucible.
11. The furnace was lowered until the Aluminium tube protruded at least 3mm into the water seal, ensuring a tight gas seal.
12. The Argon flow was closed and the CO opened at 5l/min
13. The mass change was logged on the laptop. It was ensured that logging happened by opening the text file every now and then.

14. When the test was completed which could be due to either of the following conditions being reached:
    - The sample has reached 95% of maximum possible mass loss,
    - The mass loss is slower than .1mg/min,
    - The time allowed for the test has elapsed

    the CO flow was closed and Argon was opened @ 5l/min
15. The tube furnace was turned off.
16. The furnace was raised until the crucible was directly opposite the Argon inlet in the Al tube. Argon was purged with the sample in this position for 10 minutes.
17. The furnace was raised fully, the crucible removed and the reduced iron oxide inserted into a glass sample holder previously purged with Argon
18. When the sample has cooled down sufficiently, the sample was weighed.

Data Processing

1. Plot the mass vs. time
2. From the analysis of the iron ore, the maximum possible mass was determined if all the hematite is reduced to iron
3. The Reduction % was plot as Mass loss/Maximum possible mass loss expressed as a percentage
4. From the difference between the sample mass loss, and the maximum of the continuous mass loss, the scale drift was determined and removed from the mass loss trend, assuming a constant rate of drift.

Appendix 5. Pilot Plant Test Procedure

Safety

1. A **H**azard **I**dentification & **R**isk **A**ssessment (HIRA) was performed before testing commenced. From this only CO Poisoning was identified as a real and potent danger to any person working on the pilot plant and to other persons in the vicinity. To combat this threat two actions were taken:
    1.1. Care was taken to ensure that as much of the CO formed during the gasification of the coal and not consumed (oxidised to CO2) in the process, was combusted to CO2. A LP-gas fired flare was designed and manufactured for the pilot plant set-up and experimented with until CO levels in the vicinity there-of remained below 25ppm for the duration of the test.
    1.2. A CO monitor was acquired and it was ensured that this was calibrated as specified for by the manufacturer, that it was turned on properly and kept close to where to where persons spent most of their time for the duration of all the tests. The CO monitor reading was also verified with another CO monitor.
2. A CO and/or H_2 Gas explosion was identified as another possible threat, but since a CO monitor with an alarm level of 25ppm CO was used to monitor CO levels, and the H_2 concentration of the gas was typically half of the CO concentration, the H_2 concentration when the CO alarm is activated (at a level of 25ppm) would be 13ppm which is substantially below the lower explosive limit of H_2 (4% in air). This threat was deemed sufficiently addressed during normal operation.
3. During a power outage, the procedure is to bank the furnace by closing:
    - The Top Gas valve,
    - Burden Charging valve,
    - Gasification Air valve and
    - The DRI Outlet valves immediately.

    The CO monitor and the pilot flame are also kept running for at least 30 minutes.
4. Once power returns, the burden temperature in the top part of the bed is determined first, and only when above 700'C is the ID fan re-started. If not the normal commissioning procedure is followed.

Preparation

5. A specific objective of each trial was determined before preparations for the trial started
6. Once the specific objective is known a detailed Mass and Enthalpy calculation was performed to determine:
    - The required DRI production rate that will satisfy the trial objectives, i.e. retention time etc
    - The coal rate anticipated
    - The amount of raw materials required.
    - The top gas flow anticipated and the pressure difference across the orifice plate (u-tube deviation) anticipated
7. A crucial requirement for each trial was to ensure that enough pilot flame gas (LP gas) was available to last the duration of the test. (0.5kg per hour)
8. Enough sample of the correct sieve grade analysis of both the iron oxide and the reductant was prepared to last the duration of the test.

9. In the trials during which the heat loss compensation system was operated, enough LP gas to heat the heat loss annulus to last the duration of the test had to be ensured.
10. During the initial trials, and whenever modifications were made to the plant, a pressure test was performed on the gas circuit of the plant by closing the Top Gas valve, disconnecting the ID Fan inlet pipe and blocking off the scrubber gas outlet with a plug. When the ID fan is started in this condition the gas circuit is placed under pressure, and checking for leaks with soapy water could be performed.

Test Procedure

1. The shaft below the reduction zone was charged with a suitable filler material, such as crushed charcoal or crushed electrode. Since this material was below the reduction gas outlet, it did not participate in any heat exchange or reaction but served only fill the bottom cone. Care had to be taken to ensure that material did not enter the reduction gas outlet.
2. For purposes of heating up the reduction zone rapidly, a high reactivity, low ash pre-heat combustible material was charged above the filler material. (Charcoal)
3. When the Heat Loss compensation system was used, it was ignited as a first pre-heat step. Care had to be taken to ensure that the flames were spread evenly.
4. When the shell pre-heat temperature reached the required level, the water system was started and left to stabilise ensure. This was evident from the fact that the scrubber supply water pressure stabilised at approximately 50kPa. (See separate manual)
5. At this stage the pilot flame was ignited and left for a few minutes to ensure it burned properly.
6. After this, the ID fan was started and the Top Gas valve was opened and adjusted until the Top Gas Flow Indicator indicated the required flow.
7. Once all these preparations had been done a piece of Firelighter (Blitz) was lighted and placed on top of the pre-heat combustible.
8. The top of the burden was observed, and if it did not ignite within 1 – 2minutes, or if the Firelighter burned out, more lighted Firelighters were placed on top of the burden.
9. Once the burden ignited it had to be ensured that the top gas was combusted properly by varying the pilot flame size and/or position. It was crucial to ensure that the pilot flame was combusting the gas efficiently, as a poorly burning pilot flame quickly resulted in a CO alarm.
10. The bustle gas temperature was observed and when it reached 250'C, charging the pre-mixed Ore/Reductant blend was started.
11. Since a gearbox with a high enough reduction ratio could not be obtained within the financial means available, the DRI screw had to be turned by hand. This was done by rotating the screw a through a specific rotation angle at pre-determined times (e.g. 45º every 9 minutes). If the screw outlet became filled with material, the DRI outlet valve was opened and the material extracted after which the valve was closed again.
12. The Bustle Gas temperature was noted at pre-determined intervals.
13. It was also found necessary to ensure that no part of the plant overheated by touching different parts of the plant by hand during the test. Smells indicating high temperature was also be aware of obvious. (Overheating of the DRI Cooling cone immediately above the DRI screw was found to be overheating on one occasion due to air sucked in through a left open DRI Discharge valve.)
14. When a CO alarm was registered, the procedure followed included the following:

- The pilot flame was inspected. It was also ensured that the top gas was being combusted properly. If no obvious fault was detected here,
- The plant was inspected for a CO leak. The top gas and cooling gas circuits for were inspected for obvious signs of leaks. The CO monitor was also used to locate possible leaks
- If a leak was found it was attempted to fix it. However if the leak could not be fixed within 5 minutes, the test was stopped.
- If no fault was detected, and the CO alarm persisted, the test was also stopped, after which the gas leak was investigated by performing a pressure test. This obviously meant repeating the trial.

15. After the test was completed, which could be due to two reasons
    - no more raw material left or
    - desired time elapsed

    the furnace was banked by using the banking procedure.
16. After banking the furnace, the flare and heat loss annulus were shut down.
17. The furnace was left overnight in the banked condition.

Furnace loading out procedure

18. When the burden had cooled sufficiently, the furnace was load out by:
    - Opening the DRI Outlet valve
    - Rotating the DRI screw until all filler material was removed and reduction shaft burden started appearing.
    - Sampling was done as required
19. Analyses of samples usually started directly after the loading out operation.